



# ONE-POT SYNTHESIS OF PYRANO[2,3-*c*]PYRAZOLES USING LEMON PEEL POWDER AS A GREEN AND NATURAL CATALYST

Swati S. Ghodke<sup>[a]</sup>, Sunil U. Tekale<sup>[a]</sup>, Rashmi D. Pathrikar<sup>[b]</sup>, Priya M. Khandare<sup>[a]</sup>, László Kótai<sup>[c]</sup> and Rajendra P. Pawar<sup>[a]\*</sup>

**Keywords:** Pyranopyrazoles; lemon peel powder; one-pot synthesis; natural catalyst

A simple one-pot four-component synthesis of pyrano[2,3-*c*]pyrazoles has been achieved by the condensation of aldehydes, malononitrile, ethyl acetoacetate and hydrazine hydrate using lemon peel powder as a natural catalyst in ethanol under reflux condition. The advantages of this reaction are less reaction time, high yield, easy availability of the catalyst and green nature of the protocol.

**\* Corresponding Author's**

E-mail: [rppawar@yahoo.com](mailto:rppawar@yahoo.com)

- [a] Department of Chemistry, Deogiri College, Station Road, Aurangabad-431005, Maharashtra, India  
 [b] Department of Chemistry, Rajeshree Shau Arts Commerce and Science College, Pathri, Maharashtra, India  
 [c] Research Centre for Natural Sciences, Budapest, Hungary

**General procedure for the synthesis of substituted pyranopyrazoles**

In a 25 mL round bottom flask aldehyde (1 mmol), malononitrile (1 mmol), hydrazine hydrate (1 mmol), ethyl acetoacetate (1 mmol) and lemon peel powder (10 wt%) was taken in 5 mL ethanol solvent. The resulting reaction mixture was refluxed for a period as indicated in Table 1. The progress of reaction was monitored by using TLC plates in ethyl acetate / n-hexane (7:3). After completion of reaction, the reaction mass was diluted with hot ethanol and filtered off to separate lemon peel powder catalyst as the residue. The residue was washed with hot ethanol (3 x 5 mL), the combined filtrates were concentrated and recrystallized from ethanol to afford the corresponding pure product. All the products were confirmed by comparison of their melting points with the literature values and analysis of IR, <sup>1</sup>H NMR and mass spectral data.

## INTRODUCTION

Pyranopyrazole derivatives are an interesting class of nitrogen and oxygen-containing heterocyclic compounds.<sup>1</sup> Multi-component reactions are known to be selective, effective, atom-economical, time-saving and easy to perform.<sup>2</sup> Pyranopyrazole based heterocyclic compounds have attracted a significant attention due to their pharmaceutical and biological activities.<sup>3</sup> Pyranopyrazoles are the fused heterocyclic compounds which show various biological activities such as fungicidal,<sup>4</sup> anti-inflammatory,<sup>5</sup> anticancer,<sup>6</sup> antimicrobial,<sup>7</sup> antioxidant<sup>8</sup> and bactericidal.<sup>9</sup> Considering the importance of pyranopyrazoles, researchers have reported several methods for their synthesis by using different catalysts such as nano-ZnO,<sup>10</sup> triethanolamine,<sup>11</sup> sodium benzoate,<sup>12</sup> L-tyrosine,<sup>13</sup> NMPyTs,<sup>14</sup> phenylboronic acid,<sup>15</sup> etc.

In continuation of our efforts to the clean synthetic protocol for the synthesis of heterocyclic compounds; herein we wish to report one-pot four-component synthesis of pyranopyrazoles by the reaction of aromatic aldehydes, malononitrile, hydrazine hydrate and ethyl acetoacetate using lemon peel powder as a catalyst under reflux condition.

## EXPERIMENTAL

All the reagents and chemicals were used without further purification. Melting points were recorded in open capillaries and were uncorrected. Progress of the reaction was monitored by TLC plates using ethyl acetate:n-hexane (7:3). FTIR spectra were recorded on a Shimadzu IR Affinity-1S spectrophotometer. <sup>1</sup>H NMR spectra were recorded on a 400 MHz spectrophotometer and chemical shifts were expressed in δ ppm relative to Me<sub>4</sub>Si as the internal standard.

**6-Amino-3-methyl-4-(4-nitro-phenyl)-1,4-dihydropyrano[2,3-*c*]pyrazole-5-carbonitrile (1)**

<sup>1</sup>H NMR (400 MHz, CDCl<sub>3</sub>): δ ppm 2.74 (s, 3H, CH<sub>3</sub>), 4.75 (s, 1H, CH), 7.30 (d, 1H, Ar-H), 7.31 (d, 1H, Ar-H), 7.65 (s, 2H, NH<sub>2</sub>), 7.79 (d, 2H, Ar-H), 11.04 (s, 1H, NH); ESI-MS: 298.06 (M+1)<sup>+</sup>.

**6-Amino-3-methyl-4-(4-hydroxyphenyl)-1,4-dihydropyrano[2,3-*c*]pyrazole-5-carbonitrile (2)**

<sup>1</sup>H NMR (400 MHz, CDCl<sub>3</sub>): δ ppm 2.75 (s, 3H, CH<sub>3</sub>), 4.45 (s, 1H, CH), 6.52 (d, 1H, Ar-H), 6.53 (dd, 1H, Ar-H), 6.54 (dd, 1H, Ar-H), 6.62 (d, 1H, Ar-H), 7.50 (s, 2H, NH<sub>2</sub>), 13.4 (s, 1H, NH); ESI-MS: 269 (M+1)<sup>+</sup>.

**6-Amino-3-methyl-4-(4-chlorophenyl)-1,4-dihydropyrano[2,3-*c*]pyrazole-5-carbonitrile (3)**

<sup>1</sup>H NMR (400 MHz, CDCl<sub>3</sub>): δ ppm 2.31 (s, 2H, NH<sub>2</sub>), 2.89 (s, 3H, CH<sub>3</sub>), 4.76 (s, 1H, CH), 7.01 (d, 2H, Ar-H), 7.15 (d, 2H, Ar-H), 12.03 (s, 1H, NH); ESI-MS: 287 (M+1)<sup>+</sup>.

**6-Amino-3-methyl-4-(4-fluorophenyl)-1,4-dihydropyrano[2,3-c]pyrazole-5-carbonitrile (4)**

<sup>1</sup>H NMR (400 MHz, CDCl<sub>3</sub>): δ ppm 2.10 (s, 2H, NH<sub>2</sub>), 2.73 (s, 3H, CH<sub>3</sub>), 4.74 (s, 1H, CH), 6.75 (d, 2H, Ar-H), 7.01 (d, 2H, Ar-H), 11.07 (s, 1H, NH); ESI-MS: 271.09 (M+1)<sup>+</sup>.

**6-Amino-3-methyl-4-(4-bromophenyl)-1,4-dihydropyrano[2,3-c]pyrazole-5-carbonitrile (5)**

<sup>1</sup>H NMR (400 MHz, CDCl<sub>3</sub>): δ ppm 2.50 (s, 2H, NH<sub>2</sub>), 2.69 (s, 3H, CH<sub>3</sub>), 4.71 (s, 1H, CH), 6.92 (d, 2H, Ar-H), 7.21 (d, 2H, Ar-H), 10.21 (s, 1H, NH); ESI-MS: 331.02 (M+1)<sup>+</sup>.

**6-Amino-4-(3,4-dimethoxyphenyl)-3-methyl-1,4-dihydropyrano[2,3-c]pyrazole-5-carbonitrile (6)**

<sup>1</sup>H NMR (400 MHz, CDCl<sub>3</sub>): δ ppm 1.80 (s, 3H, CH<sub>3</sub>), 3.85 (s, 6H, CH<sub>3</sub>), 4.55 (s, 1H, CH), 6.56 (s, 1H, CH), 6.61 (d, 1H, CH), 6.65 (d, 1H, CH), 7.60 (s, 2H, NH<sub>2</sub>), 13.2 (s, 1H, NH); ESI-MS: 313 (M+1)<sup>+</sup>.

**6-Amino-4-(2-chlorophenyl)-3-methyl-1,4-dihydropyrano[2,3-c]pyrazole-5-carbonitrile (7)**

<sup>1</sup>H NMR (400 MHz, CDCl<sub>3</sub>): δ ppm 2.00 (s, 2H, NH<sub>2</sub>), 2.70 (s, 3H, CH<sub>3</sub>), 4.54 (s, 1H, CH), 6.65 (d, 1H, Ar-H), 6.66 (dd, 1H, Ar-H), 6.67 (dd, 1H, Ar-H), 6.75 (d, 1H, Ar-H), 13.7 (s, 1H, NH); ESI-MS: 287 (M+1)<sup>+</sup>.

**6-Amino-4-(2-hydroxyphenyl)-3-methyl-1,4-dihydropyrano[2,3-c]pyrazole-5-carbonitrile (8)**

<sup>1</sup>H NMR (400 MHz, CDCl<sub>3</sub>): δ ppm 2.75 (s, 3H, CH<sub>3</sub>), 4.45 (s, 1H, CH), 6.52 (d, 1H, Ar-H), 6.53 (dd, 1H, Ar-H), 6.54 (dd, 1H, Ar-H), 6.62 (d, 1H, Ar-H), 7.50 (s, 2H, NH<sub>2</sub>), 12.04 (s, 1H, NH); ESI-MS: 269 (M+1)<sup>+</sup>.

**6-Amino-4-furan-2-yl-3-methyl-1,4-dihydropyrano[2,3-c]pyrazole-5-carbonitrile (9)**

<sup>1</sup>H NMR (400 MHz, CDCl<sub>3</sub>): δ ppm 2.40 (s, 2H, NH<sub>2</sub>), 2.67 (s, 3H, CH<sub>3</sub>), 4.94 (s, 1H, CH), 5.77 (d, 1H, Ar-H), 6.01 (dd, 1H, CH), 7.10 (d, 1H, Ar-H), 13.01 (s, 1H, NH); ESI-MS: 243.05 (M+1)<sup>+</sup>.

**6-Amino-3-methyl-4-(3-nitrophenyl)-1,4-dihydropyrano[2,3-c]pyrazole-5-carbonitrile (10)**

<sup>1</sup>H NMR (400 MHz, CDCl<sub>3</sub>): δ ppm 0.97 (s, 3H, CH<sub>3</sub>), 4.05 (s, 1H, NH), 6.23 (s, 2H, NH<sub>2</sub>), 6.67-6.87 (m, 2H, Ar-H), 7.19 (t, 1H, CH), 7.30 (d, 1H, Ar-H), 11.38 (s, 1H, NH); ESI-MS: 299.23 (M+2)<sup>+</sup>.

**6-Amino-4-(4-dimethylaminophenyl)-3-methyl-1,4-dihydropyrano[2,3-c]pyrazole-5-carbonitrile (11)**

<sup>1</sup>H NMR (400 MHz, CDCl<sub>3</sub>): δ ppm 2.50 (s, 2H, NH<sub>2</sub>), 2.74 (s, 3H, Ar-H), 2.89 (s, 6H, CH<sub>3</sub>), 4.45 (s, 1H, CH), 6.43 (d,

2H, Ar-H), 6.84 (d, 2H, Ar-H), 12.40 (s, 1H, NH); ESI-MS: 296.12 (M+1)<sup>+</sup>.

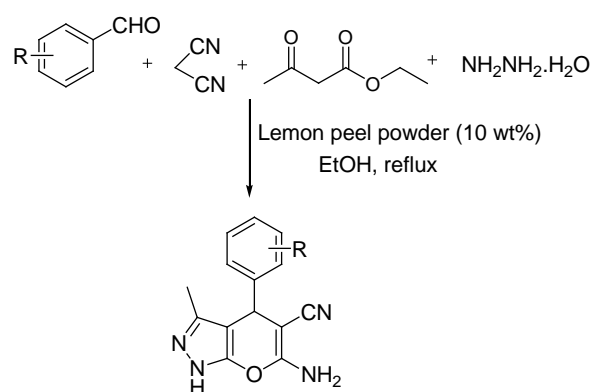
**RESULT AND DISCUSSION**

In the present work, we have synthesized pyranopyrazole derivatives using variously substituted aromatic aldehydes. A model four component condensation reaction was performed on 4-hydroxybenzaldehyde, malononitrile, ethyl acetoacetate and hydrazine hydrate using lemon peel powder as a catalyst in water solvent or without water or ethanol solvents at room temperature, reflux condition and by using ultrasound irradiation.

To follow the principles of green chemistry, initially a model reaction was carried on 4-hydroxybenzaldehyde in the absence of solvent or without solvent at room temperature, reflux condition and ultrasonic irradiation. But the corresponding product was obtained in a less amount (52 %, 45 %). Then we carried out the same reaction in the presence of water, ethanol solvent under room temperature, reflux condition and ultrasonic irradiation. We observed that the reaction required a long reaction time in water with lesser yield as compared to ethanol. Excellent yield was obtained in ethanol solvent under reflux conditions as compared to room temperature and ultrasonic irradiation. The results obtained are presented in Table 2.

Next, we optimized the amount of catalyst concentration on the same reaction by using 5, 10, 20 and 30 wt.% of the catalyst and observed 50, 90, 90, and 91 % of the product, respectively, in case of the model condensation reaction.

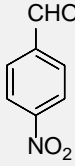
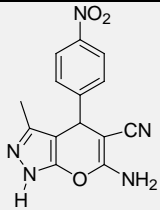
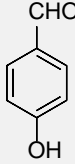
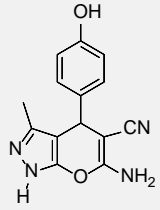
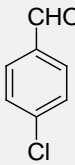
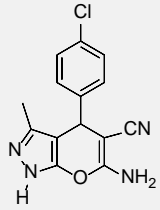
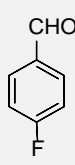
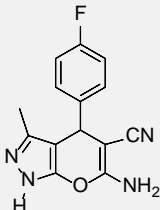
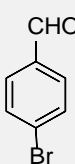
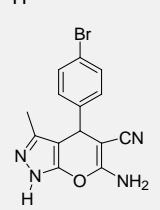
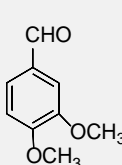
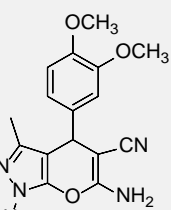
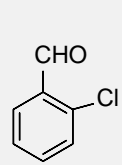
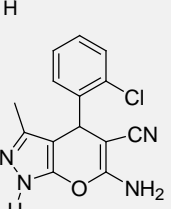
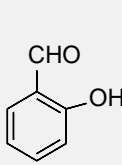
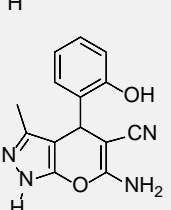
We also carried out the same reaction under solvent-free condition, but the product was obtained in a very less amount (10%). In conclusion, the best result was obtained with 10 wt % of lemon peel powder in ethanol under reflux condition (Table 3). Further increasing the amount of catalyst does not affect yield of the product to a greater extent.



**Scheme 1.** General reaction for the synthesis of pyranopyrazoles

After completion of reaction, the reaction mass was diluted with hot ethanol and filtered off to separate lemon peel powder catalyst as the residue. The residue catalyst was washed with hot ethanol (3 x 5 mL), combined filtrates were concentrated and recrystallized from ethanol to afford the corresponding pure pyranopyrazole product.

**Table 1.** Synthesis of pyranopyrazols derivative

Entry	Benzaldehyde	Product	Time, min	Yield, %	M.P., °C (Found)	M.P. °C (lit.)
1			120	84	246-248	248-250 <sup>17</sup>
2			130	92	222-224	220-222 <sup>17</sup>
3			80	80	226	228 <sup>16</sup>
4			82	82	240-242	242-244 <sup>17</sup>
5			85	71	176-178	178 <sup>18</sup>
6			120	58	160-162	161-163 <sup>17</sup>
7			120	68	246-247	245 <sup>16</sup>
8			130	62	210-212	208-210 <sup>18</sup>

9			80	65	218	219 <sup>18</sup>
10			120	74	188-190	190-192 <sup>18</sup>
11			90	76	222-224	224-225 <sup>18</sup>

**Table 2.** Effect of various solvent on the model reaction

Entry	Solvent	Temperature	Time, min	Yield, %
1	H <sub>2</sub> O	Reflux	180	52
2	Solvent-free	Reflux	300	45
3	Ethanol	Reflux	120	91

**Table 3.** Effect of catalyst on the synthesis of pyranopyrazoles under reflux condition

Entry	Amount of catalyst, wt%	Yield, %
1	No catalyst	10
2	5	50
3	10	90
4	20	90

## CONCLUSION

In conclusion, we report the synthesis of pyranopyrazoles by using one pot four-component procedure with excellent yield. Easy handling, clean method and atom economical transformation are some of the important advantages of the present method.

## ACKNOWLEDGMENT

The authors are thankful to the Principal, Deogiri College, Aurangabad, for providing necessary laboratory facilities.

## REFERENCES

- <sup>1</sup>Suryavanshi, A. W., Copper ferrite super magnetic nano- catalyzed synthesis of 6-amino-3-methyl-4-(substituted-phenyl)-2,4-dihydropyranopyrazolo[2,3-c]pyrazole-5-carbonitrile. *Int. Res. J. Sci. Eng.*, **2018**, 123-126.
- <sup>2</sup>Patil, R. M., and Rajput, A. P., Synthesis of 6-amino-2,4-dihydropyranopyrazolo[2,3-c]pyrazole-5-carbonitriles catalyzed by cerium(IV)carboxymethylcellulose under solvent-free conditions. *J. Applic. Chem.*, **2018**, 7(3), 553-558.
- <sup>3</sup>Patil, D. C., Balaskar, R. S., Thakare, M. S., Dipke, S. S., Solvent-free synthesis of 1,4-dihydropyranopyrazolo[2,3-c]pyrazole derivatives. *Int. J. Innov. Res. Sci., Eng. Technol.*, **2016**, 4(5), 18268-18272. <https://doi.org/10.15680/IJRSET.2016.0510144>.
- <sup>4</sup>Zolfigol, M. A., Tavasoli, M., Moosavi-Zare, A. R., Moosavi, P., Kruger, H. G., Shiri, M. and Khakyzadeh, V., Synthesis of pyranopyrazoles using isonicotinic acid as a dual and biological organocatalyst. *RSC Adv.*, **2013**, 3, 25681-25685. <https://doi.org/10.1039/c3ra45289a>.
- <sup>5</sup>Al-Amiery, A. A., Al-Bayati, R. I., Saed, F. M., Ali, W. B., Kadhum, A. A. H., Mohamad, A. B., Novel pyranopyrazoles: Synthesis and theoretical studies. *Molecules*, **2012**, 17, 10377-10389. <https://doi.org/10.3390/molecules170910377>.
- <sup>6</sup>Chavan, H. V., Babar, S. B., Hoval, R. U., and Bandgar, B. P., Rapid one-pot four-component synthesis of pyranopyrazoles using heteropolyacid under solvent-free condition. *Bull. Korean Chem. Soc.*, **2011**, 32(11), 3963-3966. <https://dx.doi.org/10.5012/bkcs.2011.32.11.3963>.
- <sup>7</sup>Ardiansah, B., Current progress on the synthesis methods of pyranopyrazoles. *Int. J. Chem. Tech. Res.*, **2019**, 12(5), 273-280. <http://dx.doi.org/10.20902/IJCTR.2019.120531>.
- <sup>8</sup>Kaur, M. and Sohal, H. S., Synthesis of new pyranopyrazoles based benzoxazole derivatives, *Int. J. Curr. Res.*, **2017**, 9(10), 59725-59728.
- <sup>9</sup>Davarpanah, J., Khoram, R., Synthesis of pyranopyrazoles compound using heterogeneous base catalyst based on 1, 3, 5-triazine-2, 4, 6-triamine modified. *J. Nanoanalysis*, **2017**, 4(1), 20-30.
- <sup>10</sup>Tekale, S. U., Kauthale, S. S., Jadhav, K. M., and Pawar, R. P., Nano-ZnO catalyzed green and efficient one-pot four-

- component synthesis of pyranopyrazols. *J. Chem.*, **2013**, *8*, <https://dx.doi.org/10.1155/2013/840954>.
- <sup>11</sup>Sonar, J. P., Pardeshi, S. D., Dokhe, S. A., Zine, A. M., Pawar, R. P. and Thore, S. N, An efficient protocol for the one-pot synthesis of pyranopyrazols in aqueous medium using triethanolamine as a catalyst. *Arch. Org. Inorg. Chem. Sci.*, **2018**, *3(1)*, 314-317, <https://doi:10.32474/AOICS.2018.03.000155>.
- <sup>12</sup>Kiyania, H., Samimib, H. A., Ghorbania, F. and Esmailia, S., One-pot four-component synthesis of pyrano[2,3-*c*]pyrazoles catalyzed by sodium benzoate in aqueous medium. *Curr. Chem. Lett.*, **2013**, *2*, 197-206. <https://doi:10.5267/jcc12013.07.002>.
- <sup>13</sup>Rupnar, B. D., Pagore, V. P., Tekale, S. U., Shisodia, S. U., and Pawar, R. P., L-tyrosine catalyzed mild and efficient synthesis of dihydropyrano[2,3-*c*]pyrazole under microwave irradiation. *Der Chem. Sin.*, **2017**, *8(2)*, 229-234.
- <sup>14</sup>Kamble, V. T., Bondle, G. M., Atkore, S. T., N-methyl pyridinium p-toluene sulfonate (NMPyTs) catalyzed synthesis of pyrano[2,3-*c*]pyrazoles. *Iranian Chem. Comm.*, **2017**, *5*, 268-277.
- <sup>15</sup>Imene, A. K., Wassima, G., Raouf, B., Taous, B. and Abdelmadjid, D., Phenylboronic acid-catalyzed a four-component synthesis of pyrano[2,3-*c*]pyrazole derivatives in aqueous media: an eco-friendly method, *Der Pharma Chemica*, **2015**, *7(8)*, 175-180.
- <sup>16</sup>Chine, S. S., Patil, S. S., Laterite catalyzed ultrasound-assisted greener protocol for the synthesis of pyranopyrazols. *Int. J. Res. Anal. Rev.* **2018**, *5*, 1786-1789.
- <sup>17</sup>Pagore, V. P., Rupnar, B. D., Tekale, S. U and Pawar, R. P., Green and efficient synthesis of pyranopyrazols catalyzed by ammonium chloride in water. *Der Pharma Chemica*, **2015**, *7(6)*, 312-317.
- <sup>18</sup>Khandare, P. M., Ingle, R. D., Taware, A. S., Shisodia, S. U., Pawar, S. S., Kotai, L., Pawar, R. P., One-pot synthesis and biological evaluation of pyranopyrazols in aqueous medium. *Eur. Chem. Bull.*, **2017**, *6(9)*, 410-414. <https://doi:10.17628/ecb.2017.6.410-414>.

Received: 06.01.2020.

Accepted: 06.02.2020.



# DETERMINATION OF HEAVY METAL CONTENTS IN WATER OF LLAPI RIVER (KOSOVO). A CASE STUDY OF CORRELATIONS COEFFICIENTS

Fatbardh Gashi,<sup>[a]</sup> Elida Dreshaj,<sup>\*[a]</sup> Naser Troni,<sup>[b]</sup> Albert Maxhuni<sup>[b]</sup> and Fisnik Laha<sup>[c]</sup>

**Keywords:** Water; heavy metals; atomic absorption spectroscopy; correlation coefficients; Llapi river.

Atomic absorption spectroscopy has been used to analyses and assesses the heavy metal content in water of the Llapi river, Kosovo. In this study, the assessment of heavy metals in water was realized in the summer period. Statistical studies have been carried out by calculating basic statistical parameters, anomalies (extremes and outliers) and correlation coefficients between different pairs of variables. The concentration of Cr, Ni, Zn, Cu and Fe in all sample stations were found to be under WHO recommended norms. But the concentration of Cd and Pb in all sample stations and concentrations of Mn at several stations were found to be above WHO recommended norms originated from mineral sources (ores) in this area. The statistical regression analysis has been found a highly significant positive relationship of Cd with Ni, Mn, Fe and Pb originated mainly of sulphide ores in this area.

## \*Corresponding Authors

E-Mail: elida.dreshaj@hotmail.com

- [a] The College of Medical Sciences "Rezonanca", 10000 Prishtina, Kosovo  
[b] Department of Chemistry, Faculty of Mathematics and Natural Sciences, University of Prishtina "Hasan Prishtina" Kosovo  
[c] UBT - Higher Education Institution, Prishtina, Kosovo

in the world are those with the densest population. It should, therefore, be the foremost goal of environmentalists to prevent such pollution, and to educate the community towards proper management of ecosystems.<sup>8</sup> Heavy metal ions can exist in several different forms.<sup>9</sup> The factors which determine the form of the metal ion are the extent of complexation and the oxidation state. In many samples, metal ions are present in their hydrated forms. Hydrated metal ions are usually written without the water ligands included in the chemical formula.

## INTRODUCTION

The quality of water is an issue of significant interest for the residents of the EU.<sup>1</sup> In peat bogs, water flows freely in the active layer of water or acrotelm. Water storage is critical to the balance of water in peat swamps and in surrounding areas. Logging activity, agriculture, peat extraction and destruction of peat swamp drainage activity also have an adverse effect and has an unfavorable implication on the hydrology.<sup>2</sup>

The sources of physico-chemical contamination are numerous and include the land disposal of sewage effluents, sludge and solid waste, septic tank effluent, urban runoff and agricultural, mining and industrial practices.<sup>3,4</sup> Chemical contamination of drinking water is often considered a lower priority than microbial contamination by regulators because adverse health effects from chemical impurities are generally associated with long-term exposures. In contrast, the results from microbial contamination are usually immediate practices.<sup>5</sup> The decomposition of organic matter and pollution due to anthropogenic activity are the primary sources of pollution of water.<sup>6</sup> As reported by Brils,<sup>7</sup> adequate water quality in Europe is one of the most critical concerns for the future.

Proper management of natural and environmental waters will give results if leading institutions continuously monitor information about the ecological situation. Therefore, seeing it as a challenge for environmental chemists, our goal is to determine the amount and nature of pollutants in the environment. One could claim that the most polluted areas

Determination of the concentrations of trace heavy elements in aqua systems is difficult and the results obtained often vary according to the chosen analytical technique. Atomic absorption spectroscopy (AAS) is a frequently used instrumental technique for the determination of trace heavy metal ions because of its low cost and short analysis time.<sup>10</sup>

Waters of Kosovo have been poorly investigated. Gashi et al.<sup>11</sup> performed the first step with the investigation of the rivers Drini i Bardhë, Morava e Binçës, Lepenc and Sitnica, which was of supra-regional interest. They conducted studies of mineralogical and geochemical composition and contamination status of stream sediments of mentioned rivers of Kosovo. By comparing the concentrations of toxic elements with the existing criteria for sediment quality, in that study was found that sample points in Fushë Kosova and Mitrovica of Sitnica River are significantly polluted, caused by Zn and Pb processing by flotation and Zn electrolysis factory. In Morava e Binçës River, also two sites were found to be contaminated with Cd. As Drenica River is the most important tributary of Sitnica River,<sup>12</sup> the next paper presents the detailed investigation and monitoring of the Sitnica river watershed, which is the most polluted river in Kosovo. Gashi et al.<sup>13-15</sup> performed research of ecotoxic metals: copper, lead, cadmium, zinc and manganese in waters of four main rivers (Drini i Bardhë, Morava e Binçës, Lepenc and Sitnica) of Kosovo and suggested to authorities concerned a monitoring network on main rivers of Kosovo. Also, the authors highlighted two locations in Sitnica River as very polluted with ecotoxic elements.

## Study area and sampling

The Llapi is a river in the north-eastern part of Kosovo and the 82.7 km long right tributary to the Sitnica river,<sup>16</sup> which runs through the middle of Podujevo. The source of Llapi river is considered to be the Pollata village in the Albanik Mt., where the rivers of Murgulla and Sllatina are joined. This river is wide from 9 to 12 meters and deep up to 1.2 meters. The river brings an average of  $4.9 \text{ m}^3 \text{ s}^{-1}$ , however, there are considerable variations with the maximum going up to  $25 \text{ m}^3 \text{ s}^{-1}$ . The Llapi river originates from Albaniku Mountain in the Prishtina region. Near the village of Stanovci i Poshtëm, the Llapi river splits and empties into the Sitnica river. The sampling process of river water was performed on August 12, 2015, to cover the river spatially, taking into account anthropogenic pressures, the different habitats, and the hydro morphological conditions of the river.



**Figure 1.** Study area with sampling stations.

At each sampling location, water samples were collected in polyethylene bottles. Before taking water samples, the bottles were rinsed three times with the river's water to be collected. Water samples were collected for analysis according to the recommended procedures, near the river bank at a depth of 15 cm, put into  $1 \text{ dm}^3$  bottles stored at  $4^\circ \text{C}$ .<sup>17,18</sup>

**Table 1.** Sampling stations (summer period) with a detailed description

Sample	Locality	Possible pollution sources
S <sub>1</sub>	Marincë	Low probability
S <sub>2</sub>	Sllatinë	Low probability
S <sub>3</sub>	Pollatë	Settlement, traffic and agriculture
S <sub>4</sub>	Bajqinë	Settlement, traffic and agriculture
S <sub>5</sub>	Podujevë (exit)	The settlement, wastewater from Podujeva city, traffic and agriculture
S <sub>6</sub>	Gllamnikë	The settlement, agriculture wastewater from "ABB" meat and juice factory
S <sub>7</sub>	Llozhan	Settlement, wastewater, traffic and agriculture
S <sub>8</sub>	Milloshëvë	Settlement, wastewater, traffic and agriculture
S <sub>9</sub>	Lummadh	Settlement, wastewater, traffic and agriculture

Preservation and experimental procedure for the water samples are carried out according to the standard methods for the examination of water Samples are preserved in refrigerator after treatment.<sup>19-21</sup> GPS device Extras measured geographic coordinates, "GARMIN, 12 channel," and locations were well described. The levels of heavy metals in water were compared with WHO standards for drinking water.<sup>22</sup> The study area with the sampling locations is shown in Figure 1 and the details about all sampling sites were presented in Table 1.

## MATERIALS AND METHODS

Twice distilled water was used in all experiments. All instruments are calibrated according to the manufacturer's recommendations. All tests were performed at least three times to calculate the average value. Determination of the concentrations of trace heavy metals: Cr, Cd, Ni, Zn, Mn, Cu, Fe and Pb in environmental samples is difficult and the results obtained often vary according to the chosen analytical technique. Atomic absorption spectroscopy (AAS) is an important instrumental technique for the determination of trace/heavy metal ions because of its low cost and short analysis time. Determination of Zn (213.89 nm), Fe (371.99 nm), Mn (403.08 nm), Ni (341.48 nm), Cr (425.44 nm), Cu (327.40 nm), Cd (326.11 nm) and Pb (405.78 nm) were performed using atomic absorption spectrometer model "PERKIN ELMER 400 ANALYST".

The detection limit for analyzed heavy metals is presented in Table 2. Program statistic 6.0<sup>23</sup> was used for the statistical calculations in this work, such as descriptive statistics, Pearson's correlation factor and two-dimensional box plot diagrams for determination of anomalies (extremes and outliers) for solution data. Relationships between the observed variables were tested using correlation analysis, and the level of significance was set at  $p < 0.05$  for all statistical analyses.

## RESULTS AND DISCUSSION

The concentration of 8 heavy metals was presented in Table 2 and basic statistical parameters for 6 variables in 9 water samples are shown in Table 3. Using experimental data and box plot approach of Tukey,<sup>24</sup> extreme and outlier values were determined for the whole region. Two dimensional scatter box with plots diagrams are presented in Figure 2. Anomalous values (outliers and extremes) of 6 variables are shown in Table 4. The matrix of correlation coefficients ( $r$ ) of the selected six variables was presented in Table 5.

The concentration of Cr, Ni, Zn, Cu and Fe in all sample stations were found to be under WHO recommended norms. Cadmium concentrations in unpolluted natural waters are usually below  $1 \mu\text{g dm}^{-3}$ .<sup>25</sup> It is chemically similar to zinc and occurs naturally with zinc and lead in sulphide ores. The concentration of Cd in all sample stations was found to be above-recommended norms (WHO the highest desirable limit  $0.005 \text{ mg dm}^{-3}$ ), as a possible sign of natural pollutions originated from cadmium sulphide ores in this area.

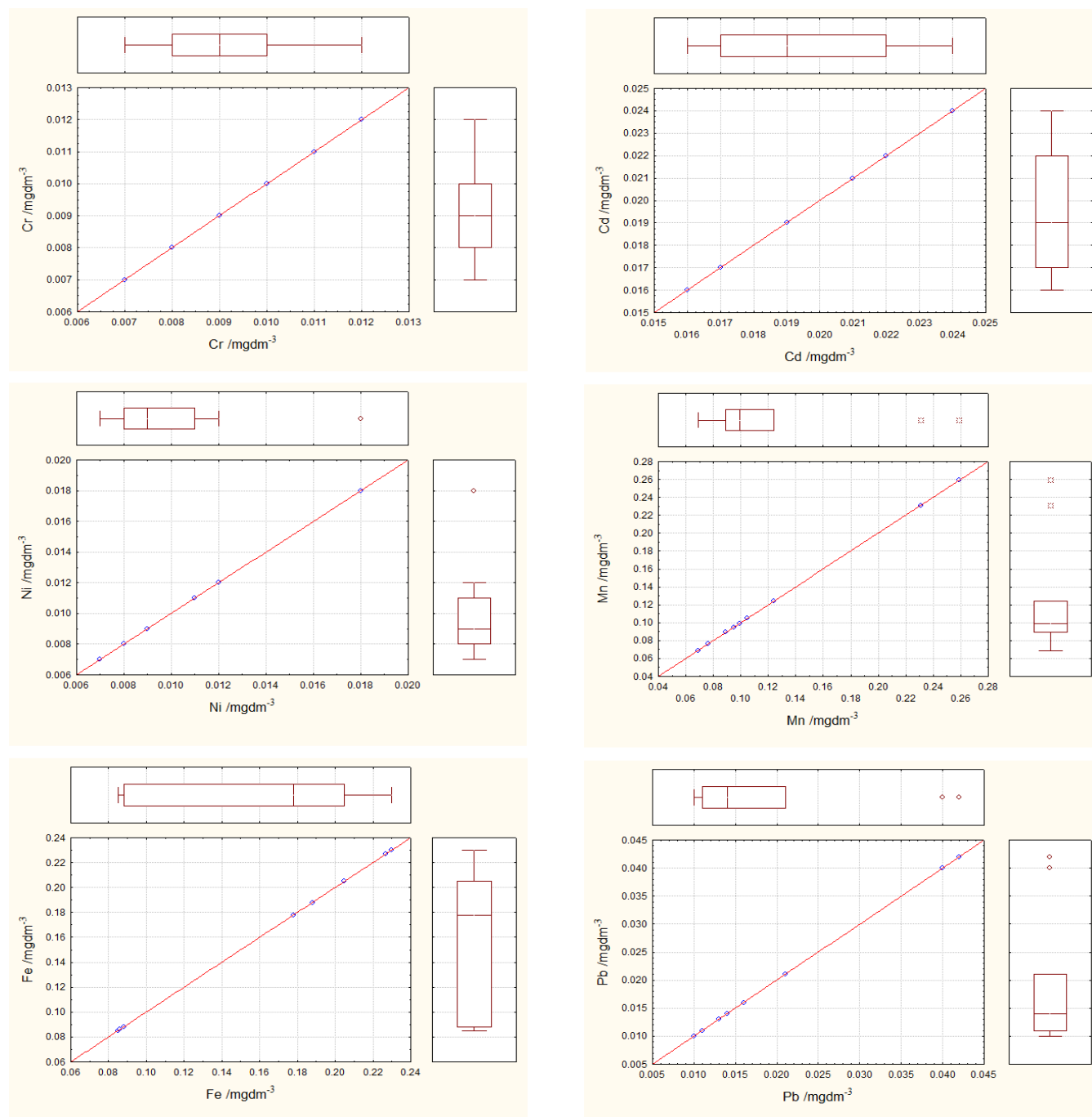


**Figure 2.** Scatter box plot diagrams of some selected heavy metals.

**Table 2.** The concentration of some metals in water sample stations

Heavy metal	Detection limit, mg dm <sup>-3</sup>	WHO standard, mg dm <sup>-3</sup>	S <sub>1</sub>	S <sub>2</sub>	S <sub>3</sub>	S <sub>4</sub>	S <sub>5</sub>	S <sub>6</sub>	S <sub>7</sub>	S <sub>8</sub>	S <sub>9</sub>
Cr	0.003	0.05	0.008	0.007	0.007	0.008	0.009	0.010	0.010	0.012	0.011
Cd	0.0008	0.005	0.022	0.019	0.019	0.021	0.024	0.022	0.017	0.016	0.017
Ni	0.006	0.07	0.009	0.008	0.008	0.012	0.018	0.011	0.011	0.009	0.007
Zn	0.0015	5	nd*	nd							
Mn	0.0015	0.1	0.099	0.105	0.095	0.124	0.259	0.231	0.089	0.076	0.069
Cu	0.0015	2	0.005	0.004	0.004	0.004	0.005	0.006	0.005	0.005	nd
Fe	0.005	0.3	0.205	0.178	0.178	0.188	0.227	0.230	0.088	0.085	0.086
Pb	0.010	0.01	0.011	0.010	0.010	0.021	0.040	0.042	0.016	0.014	0.013

\*not detected

**Table 3.** Descriptive statistics of 6 variables in 9 cases

Variable, mg dm <sup>-3</sup>	Descriptive statistics						
	Mean	Geometric	Median	Minimum	Maximum	Variance	Std. dev.
Cr	0.0091	0.0090	0.0090	0.0070	0.0120	0.00	0.0018
Cd	0.0197	0.0195	0.0190	0.0160	0.0240	0.00	0.0027
Ni	0.0103	0.0099	0.0090	0.0070	0.0180	0.00	0.0033
Mn	0.1274	0.1146	0.0990	0.0690	0.2590	0.00	0.0689
Fe	0.1628	0.1511	0.1780	0.0850	0.2300	0.00	0.0603
Pb	0.0197	0.0169	0.0140	0.0100	0.0420	0.00	0.0126

**Table 4.** Anomalous values (extremes and outliers) of 6 metals in 9 water samples

Sample	Extremes of parameters (x)	Outliers of parameters (o)
S <sub>1</sub>	No reg.	No reg.
S <sub>2</sub>	No reg.	No reg.
S <sub>3</sub>	No reg.	No reg.
S <sub>4</sub>	No reg.	No reg.
S <sub>5</sub>	Mn (0.259 mgdm <sup>-3</sup> )	Ni (0.018 mgdm <sup>-3</sup> ), Pb (0.04 mgdm <sup>-3</sup> )
S <sub>6</sub>	Mn (0.231 mgdm <sup>-3</sup> )	Pb (0.042 mgdm <sup>-3</sup> )
S <sub>7</sub>	No reg.	No reg.
S <sub>8</sub>	No reg.	No reg.
S <sub>9</sub>	No reg.	No reg.

**Table 5.** Matrix of correlation coefficients (r) of selected six variables

	Correlations, marked correlations are significant at $p < 0.05000$					
	Cr	Cd	Ni	Mn	Fe	Pb
Cr	1.00					
Cd	-0.46	1.00				
Ni	-0.01	0.67	1.00			
Mn	-0.07	0.81	0.81	1.00		
Fe	-0.61	0.94	0.48	0.74	1.00	
Pb	0.19	0.66	0.77	0.95	0.56	1.00

Concentrations of Mn at stations S<sub>2</sub>, S<sub>4</sub>, S<sub>5</sub> and S<sub>6</sub> were found to be above-recommended norms (WHO the highest desirable limit 0.1 mg dm<sup>-3</sup>) as a possible sign of natural pollutions originated from manganese ores in this area and uncontrolled use of fertilizers, varnish and fungicides in this area. Pb in all sample stations were found to be above WHO recommended norms from 0.01 mg dm<sup>-3</sup>, originated (possible) from lead sulphide ores in this area.<sup>26</sup>

Basic statistical parameters (Mean, Geometric mean, Median, Minimum, Maximum, Variance and Standard deviation) for six parameters analyzed in water samples are presented in Table 3. Based on the two-dimensional scatter box plot diagrams (Fig. 2) from 6 experimental data were constructed and anomalous values (Table 4). In the sample station, S<sub>5</sub> and S<sub>6</sub> extreme values of Mn (0.259 and 0.231 mgdm<sup>-3</sup>, respectively) were registered. The sample S<sub>5</sub> and S<sub>6</sub>, the outlier value of Pb (0.040 and 0.042 mgdm<sup>-3</sup>, respectively) was recorded.

Also, the outlier value of Ni at the sample station S<sub>5</sub> was registered. The statistical regression analysis has been found a highly useful technique for the linear correlating between various water parameters, and the correlation coefficient (Table 5) indicates a positive and negative significant correlation of variables with each other. A positive correlation means one parameter increase with other parameters and negative correlation means one parameter increase with other parameters decreases. In this study summer period (see Table 5). Cd showed a highly significant positive relationship with Ni, Mn, Fe and Pb originated mainly of sulphide ores in this area.<sup>26</sup> Ni showed a highly significant positive relationship with Mn and Pb. Manganese showed a highly significant positive correlation with Fe and Pb.

## CONCLUSIONS

The concentration of heavy metals - Cr, Ni, Zn, Cu and Fe - in all sample stations were found to be under WHO recommended norms. The concentration of Cd in all sample stations were found to be above-recommended standards as a possible sign of natural pollutions originated from cadmium sulphide ores in this area. Concentrations of Mn at stations S<sub>2</sub>, S<sub>4</sub>, S<sub>5</sub> and S<sub>6</sub> were found to be above-recommended norms as a possible sign of natural pollutions originated from Manganese ores in this area and uncontrolled use of fertilizers, varnish and fungicides in this area. Pb in all sample stations was found to be above WHO recommended norms originated (possible) from Lead sulphide ores in this area.

Based on the two-dimensional scatter box plot diagrams in sample stations, S<sub>5</sub> and S<sub>6</sub> anomalies values of Mn and Pb were registered. Also, the outlier value of Ni at the sample station S<sub>5</sub> was registered. The statistical regression analysis has been found a highly significant positive relationship of Cd with Ni, Mn, Fe and Pb originated mainly of sulphide ores in this area. Ni showed a highly significant positive correlation with Mn and Pb. Manganese showed a highly significant positive relationship with Fe and Pb.

From the results, it was found out that river water quality did not fulfill the criteria set by the WHO and the distribution of pollutants (heavy metals) indicated natural pollutions and anthropogenic sources as the influence of wastewaters from the settlement, agriculture impact and wastewater from meat and juice factory.

## REFERENCES

- <sup>1</sup>Chirila, E., Bari, T., and Barbes, L., Drinking water quality assessment in Constanta town. *Ovidius Univ. Ann. Chem.*, **2010**, *21*, 87-90.
- <sup>2</sup>Hamilton, L. S., *Food and Agriculture Organization of the United Nations*, 1<sup>st</sup> Ed., Rome, **2008**, 78.
- <sup>3</sup>Close, M., Dann, R., Ball, A., Pirie, R., Savill, M. and Smith, Z., Microbial groundwater quality and its health implications for a border-strip irrigated dairy farm catchment, New Zealand, *J. Water Health*, **2008**, *6(1)*, 83-98. <https://doi.org/10.2166/wh.2007.020>
- <sup>4</sup>Keswick, B. H., *Groundwater Pollution Microbiology*. New York, John Wiley and Sons. **1984**, 39-64.
- <sup>5</sup>Thompson, T., Fawell, J., Kunikane, S., Jackson, D., Appleyard, S., Callan, P., Bartram, J. and Kingston, P., *Chemical safety of drinking-water: Assessing priorities for risk management*, World Health Organization. Geneva, **2007**.
- <sup>6</sup>Montgomery, J. M., *Water Treatment, Principles and Design*. John Wiley & Sons, New York, **1996**, 474.
- <sup>7</sup>Brils, J., Sediment monitoring and the European water framework directive. *Ann. Inst. Superiore Sanita*, **2008**, *44*, 218-223.
- <sup>8</sup>Šajn, R., Bidovec, M., Andjelov, M., Piric, S. and Gosar, M., *Geochemical atlas of Ljubljana and surround. Geološki Zavod Slovenije (Geological Survey of Slovenia)*, Ljubljana, **1998**, 670.
- <sup>9</sup>Kim, H. T., *Soil sampling, preparation and analysis*, Marcel Dekker, New York. **1995**, 408.
- <sup>10</sup>Mohamed, R. A., Abdel-Lateefa, A. M., Mahmouda, H. H. and Helalal, A. I., Determination of trace elements in water and sediment samples from Ismaelia Canal using ion chromatography and atomic absorption spectroscopy. *Chem. Spec. Bioavail.*, **2012**, *24(1)*, 31-38. <https://doi.org/10.3184/095422912X13257005726800>
- <sup>11</sup>Gashi, F., Franciskovic-Bilinski S. and Bilinski, H., Analysis of sediments of the four main rivers (Drini i bardhë, Morava e Binces, Lepenc and Sitnica) in Kosovo. *Fresenius Environ. Bull.*, **2009**, *18*, 1462-1471.
- <sup>12</sup>Gashi, F., Stanislav Frančičković-Bilinski, S., Bilinski, H. and Kika, L., Assessment of the effects of urban and industrial development on water and sediment quality of the Drenica River in Kosovo. *Environ. Earth Sci.*, **2016**, *75(9)*, article number 801. <https://doi.org/10.1007/s12665-016-5612-7>
- <sup>13</sup>Gashi, F., Frančičković-Bilinski, S., Bilinski, H., Troni, N., Bacaj, M. and Jusufi, F., Establishing of monitoring network on Kosovo rivers: preliminary measurements on the four main rivers (Drini i Bardhë, Morava e Binçës, Lepenc and Sitnica). *Environ. Monit. and Assess.*, **2011**, *175*, 279-289. <https://doi.org/10.1007/s10661-010-1511-7>
- <sup>14</sup>Gashi, F., Troni, N., Faiku, F., Laha, F., Haziri, A., Kastrati, I., Beshtica, E. and Behrami, M., Chemical and statistical analyses of elements in river water of Morava e Binçës. *Am. J. Environ. Sci.*, **2013**, *9(2)*, 142-155. <https://doi.org/10.3844/ajessp.2013.142.155>
- <sup>15</sup>Gashi, F., Troni, N., Hoti, R., Faiku, F., Ibrahim, R., Laha, F., Kurteshi, K., Osmani S. and Hoti, F., Chemical determination of some elements in water of Sitnica (Kosovo) by ICP-MS technique. *Fresenius Environ. Bull.*, **2014**, *23(1)*, 91-97.
- <sup>16</sup>Wikipedia.org/wiki/Lab\_river
- <sup>17</sup>WHO, Guideline for drinking water quality 3rd ed. Vol.1 recommendations WHO, Geneva, **2004**, 189.
- <sup>18</sup>WHO, Chemical safety of drinking-water: Assessing priorities for risk management. *Int. J. Environ.*, **2007**.
- <sup>19</sup>APHA, Standard methods for the examination of water and wastewater. American Public Health Association, 20<sup>th</sup> ed. DC, NY. **1998**, 100-138.
- <sup>20</sup>Baba, A., Kaya, A., Birsoy, Y. K., The effect of Yatagan thermal power plant (Mugla, Turkey) on the quality of surface and ground waters. *Water Air Soil Pollute.*, **2003**, *149*, 93-111. <https://doi.org/10.1023/A:1025660629875>
- <sup>21</sup>Dalmacija B., *Water Quality Control in Towards of Quality Management*, (in Serbian), Textbook. **2000**.
- <sup>22</sup>World Health Organization., *Guidelines for Drinking-water Quality*, 4<sup>th</sup> ed. Geneva, **2011**.
- <sup>23</sup>Stat Soft, Inc. STATISTICA (data analysis software system), ver. 6. **2001**. <http://www.statsoft.com>.
- <sup>24</sup>Tukey, J. W., *Exploratory data analysis*. Addison-Wesley. **1977**.
- <sup>25</sup>Friberg, L., Nordberg, G. F. and Vouk, V. B., *Handbook of the toxicology of metals*. Vol. II. Amsterdam, Elsevier, **1986**, 130-184.
- <sup>26</sup>Feraud, J., Maliqi, G. and Meha, V. Famous mineral localities: The Trepeca mine. *The Mineral Record*, **2007**, *38(4)*, 337-368.

Received: 10.01.2020

Accepted: 07.02.2020



# IMPACT OF HEAVY METALS ON *OREOCHROMIS NILOTICUS* FISH AND USING ELECTROPHORESIS AS BIO-INDICATOR FOR ENVIRONMENTAL POLLUTION OF ROSETTA BRANCH, RIVER NILE, EGYPT

Magda F. Mohamed<sup>[a, b]\*</sup>, Nasr M. Ahmed<sup>[c]</sup>, Yasmien M. Fathy<sup>[d]</sup> and Ismail A. Abdelhamid<sup>[d]</sup>

**Keywords:** use the Keywords style for the list of keywords, separating with a comma each items.

In the present work, samples of water and fish were collected from the river Nile at El- Qanater El- Khyria as non-polluted site and from downstream of El-Rahawy drain (El-Qatta) as a polluted drain during different seasons of 2016. The concentration of metals (Fe, Zn, Cu, Pb, Mn and Cd) in water and their accumulations in fish muscles were measured. Electrophoresis pattern of *Oreochromis niloticus* including protein pattern, calcium pattern and  $\beta$ -esterase have been determined. In the present study, results revealed increased concentrations of studied metals in water and fish samples mainly during the winter season. The values of Fe, Cu, Pb, Mn, Zn and Cd were higher than the permissible limits in water, while Fe, Pb and Zn exceeded the permissible limits in fish muscles, especially those of El-Qatta station. Results of electrophoretic protein pattern showed similarities in arrangement of the bands in liver and muscles tissues in fishes taken from both locations (A and B). The cumulative risk impacts have been discussed.

\* Corresponding Authors

E-Mail: magdafikry85@yahoo.com

- [a] Department of Chemistry (Biochemistry Branch), Faculty of Science, Cairo University, Giza, Egypt  
[b] Department of Chemistry, Faculty of Science and Arts, Khulais, University of Jeddah, Saudi Arabia  
[c] National Institute of Oceanography and Fisheries, Cairo, Egypt  
[d] Department of Chemistry, Faculty of Science, Cairo University, 12613 Giza, Egypt

bioindicator for detecting metals contaminating the freshwater ecosystems.

The heavy metals contamination is a very serious threat due to their toxicity, bioaccumulation and biomagnifications in the food web.<sup>4</sup> Also, metals are regarded as dangerous pollutants of the aquatic ecosystem due to their toxicity impact on living organisms.<sup>5,6</sup> While, the essential metals such as Cu, Zn and Fe have normal physiological regulatory functions.<sup>7</sup> They may accumulate and reach toxic levels in living organisms. Furthermore, the non-essential metals are usually strong toxic chemicals and their accumulation in organism's tissues may lead to intoxication, infertility, tissue damage and dysfunction of a variety of organs.<sup>8</sup> Concern about the impact of anthropogenic pollution on aquatic ecosystems is growing, where metals from man-made pollution sources are continuously released into both aquatic and terrestrial ecosystems. Heavy metals may accumulate in fish tissues from the surrounding water and/or food to be a very serious threat for fish and human health.<sup>3,9,10</sup>

## INTRODUCTION

The river Nile is one of the longest rivers in the world (its mainstream is about 6,740 km in length). The total area of its basin is about 2.9 million km<sup>2</sup>. 22 % of the Nile's course runs through Egypt. At the north of Cairo, the Nile divides into two branches, the Rosetta branch to the west and the Damietta to the east.<sup>1</sup> Rosetta branch represents the area of investigation and its length is about 225 km. The width of the branch varies from 150 to 200 m and its average depth varies from 2 to 3.5 m. Nowadays, Rosetta branch suffers from several environmental problems. It receives pollutants from three main sources, the first source is El-Rahawy drain which receives domestic and agriculture wastes from Giza city and pours more than 1,900,000 m<sup>3</sup> day<sup>-1</sup> of its effluents into Rosetta branch. The second source results from Kafr El-Zayat industrial area and the third source of pollution is several small agricultural drains that discharge their wastes into the branch in addition to sewage discharged from several cities.<sup>2</sup>

An electrophoretic method has been described for distinguishing between fish slices according to their protein constituent. Reproducible electrophoretic patterns were obtained for different samples and sizes of the same fish type, but small differences were shown for fish of widely different origin.<sup>11</sup> A comparative study of fish species correspondence was accomplished using three different electrophoretic methods. Sarcoplasmic proteins were extracted from three related fish species and exposed to gel isoelectrofocusing, two-dimensional polyacrylamide gel electrophoresis and capillary zone electrophoresis.<sup>12</sup>

Metals are non-biodegradable and once discharged into water, they precipitated on sediment particles and accumulated in the living aquatic organisms. So, fishes absorb these metals from the surrounding water, sediment and food, which may accumulate in their tissues in significant amounts,<sup>3</sup> therefore, fish can be used as a

The present work was conducted to explore the effect of water pollutants of the river Nile (Rosetta branch) from El-Qanater El-Khyria to El-Rahawy drain (El-Qatta) on fish organs and estimate the amount of heavy metals in water and fish muscles.



**Figure 1.** Map of northern Egypt showing the area of study and sampling stations on the Rosetta branch.

Furthermore, the study was concerned with revealing the adverse effect of these heavy metals on the biomacromolecules (proteins and calcium pattern and enzymes  $\beta$ -esterase) that were separated and identified electrophoretically and use of electrophoresis as an effective tool in revealing the adverse effect of heavy metals which accumulate in different fish organs when exposed to toxic concentrations.

## EXPERIMENTAL

The studied area is located at the beginning of Rosetta Branch, about 25 km downstream of Cairo. Seasonal sampling of water and fish was performed from winter 2016 to autumn 2016. Two stations were chosen for this study. The first was El-Qanater El-Khyria city, while the second was El-Qatta (after El-Rahawy drain 7 Km). El-Rahawy drain is a huge drain, which receives domestic and agricultural wastes from Giza city and pours its effluents into the Rosetta branch (Figure 1).

### Heavy metals in water

20 mL of conc. nitric acid were added to 500 mL of water sample in a beaker and boiled on a hotplate until complete digestion of suspended material. The remaining volume was made up to 100 mL with deionized distilled water. A portion of this solution was used for the quantitative determination of heavy metals (iron, copper, lead, manganese, zinc and cadmium) using atomic absorption model (Perkin Elmer 3110, USA) with graphite atomizer HGA-600, according to the reported method.<sup>13</sup> The results are expressed in  $\text{mg L}^{-1}$ .

### Heavy metals in fish

Fish samples were transferred to weighing beakers and placed overnight in a drying oven thermostatically regulated at 105 °C. Dried samples (1 g) were taken and digested,<sup>14</sup> where 5 mL each of conc. perchloric and nitric acids were

used. The digested solutions were cooled and made up to 25 mL using deionized water, the concentration of trace elements (Fe, Cu, Pb, Mn, Zn and Cd) in solution were determined using atomic absorption model (Perkin Elmer 3110, USA) with graphite atomizer HGA-600, according to the reported method.<sup>13</sup> The results are expressed in  $\text{mg kg}^{-1}$  of dry weight and then converted to  $\text{mg kg}^{-1}$  of wet weight basis.

### Electrophoretic study

#### Preparation of the tissue homogenates

Liver and muscle tissues were excised from fishes (*O. niloticus*) caught from the two different areas. The tissues were washed with cold phosphate buffered saline, frozen rapidly with liquid nitrogen, ground then homogenized in 0.05 M Tris-HCl buffer (pH 7.4). The homogenates were left in refrigerator overnight and shaken using vortex for 15 sec and then centrifuged at 10,000 rpm at 4°C for 15 min. The supernatants including water-soluble proteins were transferred to Eppendorf tubes and stored at the deepfreezer until electrophoretic analysis.

#### Electrophoretic protein and calcium patterns

The native electrophoretic patterns were carried out through vertical slab polyacrylamide Gel Electrophoresis using Mini-gel electrophoresis (Biorad, USA) according to a reported method<sup>15</sup> and its recent modification<sup>16</sup> The resolving gel was prepared at the concentration 8 % from stock solution consisting of acrylamide: bis-acrylamide (30 % T, 2.67 % C) (acrylamide/bis = 29.2:0.8) and 10 % glycerol.

After the electrophoretic run, the native bands were stained by Commassie Brilliant Blue G-250 for visualization. The relative mobility (*RF*) and band percent (*B*, %) of the isolated proteins were determined in addition to the molecular weights (MWs) that estimated in comparison to marker of standard molecular weights (ranging from 6.458

to 195.755 KDa). Moreover, lipid and calcium moieties of the native proteins were stained by mean of isoelectrophoresis using Sudan Black B and Alizarin Red S respectively as suggested earlier.<sup>17,18</sup>

#### Electrophoretic localization of in-gel enzyme activity:

The electrophoretic  $\beta$ -esterase in the native gel was stained using benzidine stain prepared as per a reported method.<sup>19</sup> After developing the colored bands of enzyme activity, the gel was fixed in 7 % glacial acetic acid for 30 min, then it was preserved in 5 % acetic acid prepared in 10 % methanol.

## RESULTS AND DISCUSSION

### Heavy metals in water

Heavy metals concentrations in the water samples at the two localities of the River Nile, at El- Qanater El- Khyria as non-polluted site and from downstream of El-Rahawy drain (El-Qatta) as a polluted site, during the period of study are presented in Figures 2 to 7.

The concentration of iron in the water at the two stations varied from the maximum value of 0.760 mg L<sup>-1</sup> at El-Qatta during winter to a minimum value of 0.126 mg L<sup>-1</sup> at El-Qanater El-Khyria during spring. The concentration at El-Qatta station is higher than the permissible level of 0.5 mg L<sup>-1</sup>, according to the Egyptian Organization for Standardization,<sup>20</sup> (Figure 2). The low iron content in spring is possibly due to the consumption of iron by phytoplankton<sup>21</sup> and oxidation of Fe<sup>2+</sup> to Fe<sup>3+</sup> and subsequent precipitation as hydroxide at high dissolved oxygen content,<sup>22</sup> whereas, the high value of iron concentration at station II during winter may be ascribed to the breakdown of organic matter and dead microorganisms that releases the metal into water.<sup>23</sup> Finally, the increasing of iron may be due to the small water level during the drought period and discharge of effluent from El-Rahawy drain which is loaded with agriculture and domestic sewage.<sup>24</sup>

Copper values in the investigated area varied in the range of 0.016 – 0.021, 0.010-0.017, 0.009-0.018 and 0.010 -0.020 mg L<sup>-1</sup> during winter season, spring season, summer season and autumn season, respectively, (Figure 3), which are higher than the permissible level (0.010 mg L<sup>-1</sup>) according to Egyptian Standards of the Environmental Laws no. 48/1982 decree 92/2013.<sup>25</sup> Winter recorded the highest values (0.021 mg L<sup>-1</sup>) of (Cu) at El-Qatta station may be due to decrease water level in the River Nile and increase domestic sewage at El-Rahawy drain. While summer recorded the lowest values, the decrease (0.009 mg L<sup>-1</sup>) in Cu-concentration in water is probably due to its tendency to form complex with organic ligands and humic matter, which leads to lessening the penetration of free ions into water, where 90 % of (Cu) in water is complexed by dissolved organic and suspended matters.<sup>26,27</sup>

The concentrations of lead in water are 0.017-0.059, 0.017-0.052, 0.015-0.038 and 0.020-0.055 mg L<sup>-1</sup> during winter, spring, summer and autumn, respectively (Figure 4).

The increase in lead during winter (0.059 mg L<sup>-1</sup>) at El-Qatta station might be ascribed to the reduction in water discharges during drought period, whereas the highest value of Pb may be resulted from heavy metals in agricultural waste runoff containing fertilizers, agrochemicals, or pesticides at El-Rahawy drain. Thus, El-Qatta station showed a higher level of lead than the permissible value<sup>20</sup> (0.050 mg L<sup>-1</sup>) except for summer season.

The present results showed that manganese values in the investigated areas range between 0.048-0.135, 0.048-0.085, 0.030-0.055 and 0.045-0.123 mg L<sup>-1</sup> during winter, spring, summer and autumn, respectively. The low concentration of manganese may be attributed to oxidation of Mn<sup>2+</sup> to solid MnO<sub>2</sub> which precipitates to the sediment layer.<sup>23</sup> El-Qatta station showed higher value than the permissible<sup>20</sup> level (0.050 mg L<sup>-1</sup>) as observed in Figure 5. The seasonal average values of zinc concentrations in water vary between the maximum value of 0.155 mg L<sup>-1</sup> at El-Qatta during winter and a minimum value of 0.059 mg L<sup>-1</sup> at El-Qanater El-Khyria during summer. Low Zn concentration may be related to the contribution of phytoplankton, pH and dissolved oxygen concentration.<sup>2</sup> Zinc in the River Nile exceeded the permissible levels at El-Qatta station,<sup>28</sup> (Figure 6).

Cadmium concentrations of the two stations in the water range between (0.0030-0.011 mg L<sup>-1</sup>) and are higher than the permissible level (0.001 mg L<sup>-1</sup>) recommended by Egyptian Standards of the Environmental Laws no. 48/1982 decree 92/2013,<sup>25</sup> (Figure 7). The maximum concentration of cadmium during winter at El-Qatta station might be attributed to the effect of pollution sources in that sites, as sewage and domestic wastes at El-Rahawy drain.

Generally, the concentrations of heavy metals in water samples were in the of Fe > Zn > Mn > Pb > Cu > Cd. The concentration of heavy metals in water samples showed seasonal variations, elevated in winter seasons, may be due to decreased level of water during drought period which results elevation of concentration of the metals,<sup>29,24</sup> and due to increase of the amount of discharge of agricultural, sewage waste water and industrial wastes into water of the River Nile in winter season.<sup>30</sup> While decreased in summer seasons may be attributed to phytoplankton growth which can absorb large quantity of heavy metals from water and also due to increase the water level during the summer season in the River Nile.<sup>31</sup>

### Accumulation of heavy metals in muscles of *O. niloticus* fish

Metal concentrations in the muscle samples of *O. niloticus* at the two localities of the River Nile at El- Qanater El- Khyria as non-polluted site and from downstream of El-Rahawy drain (El-Qatta) as a polluted site during the study period are illustrated in (Figure 8 to 13). The annual average of metal concentrations in the muscle samples were ranked in the order of Fe > Zn > Mn > Cu > Pb > Cd.

The concentration of iron in fish muscles varies between 14.455 and 36.763 mg kg<sup>-1</sup> at El-Qanater El-Khyria during summer and El-Qatta during winter. Iron was the most abundant metal in the tissues studied.

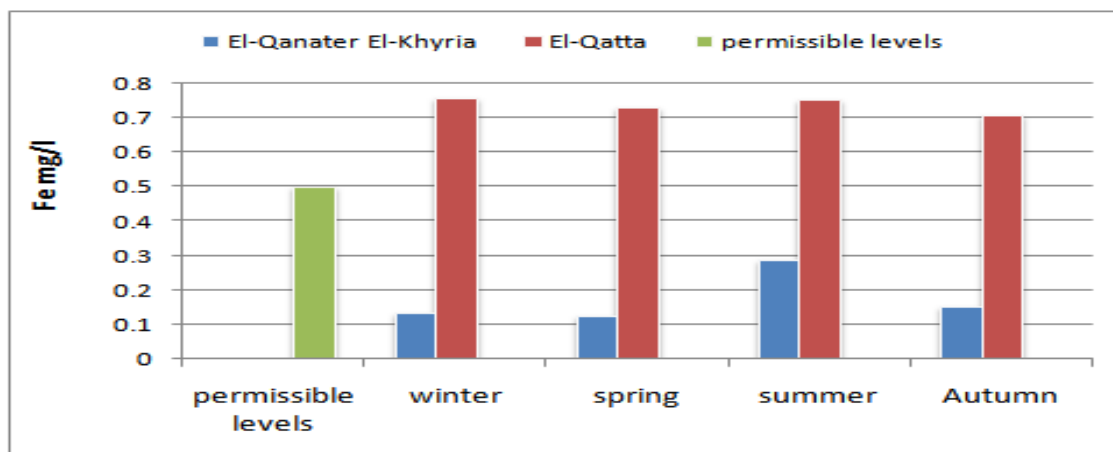


**Figure 2.** Seasonal variation of iron concentrations in water at El-Qanater El-Khyria and El-Qatta of the River Nile. Permissible limit is according to ref. 20.

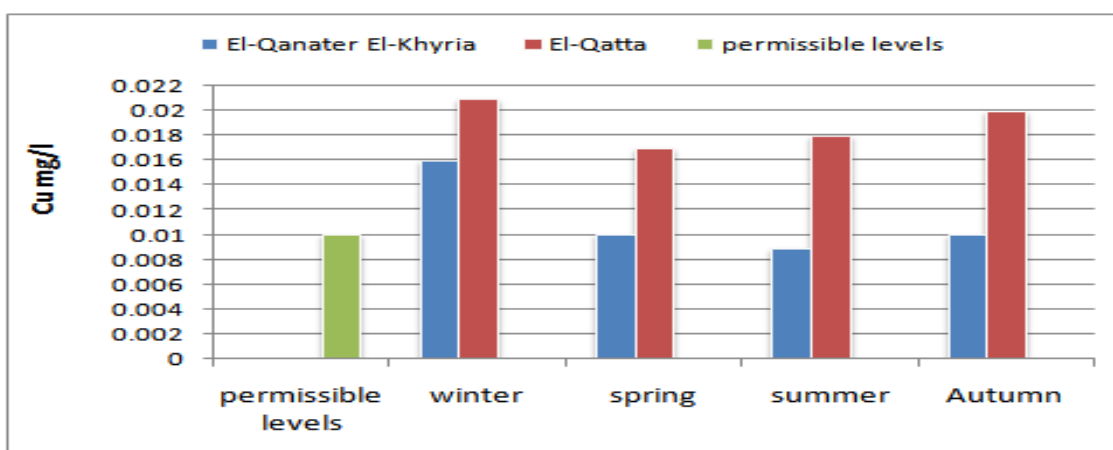


**Figure 3.** Seasonal variation of copper concentrations in water at El-Qanater El-Khyria and El-Qatta of the River Nile. Permissible limit is according to ref. 25.

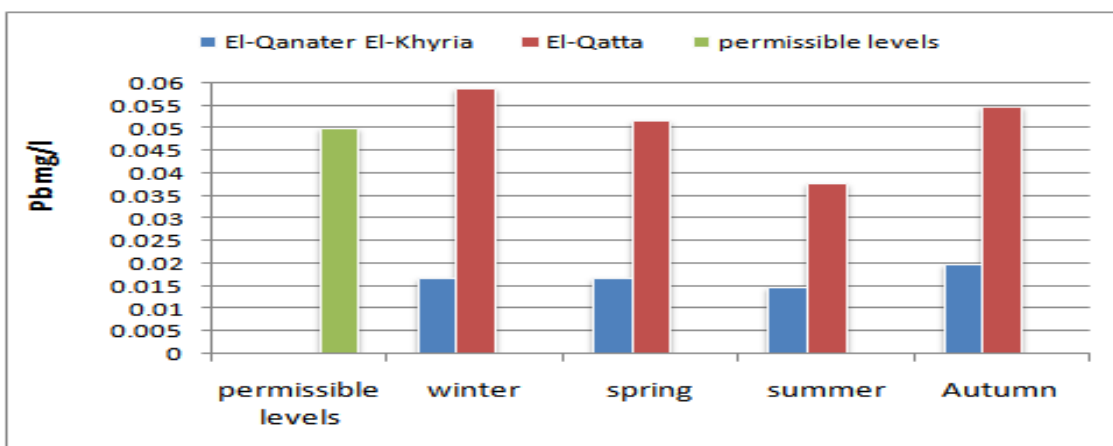


**Figure 4.** Seasonal variation of lead concentrations in water at El-Qanater El-Khyria and El-Qatta of the River Nile. Permissible limit is according to ref. 20.

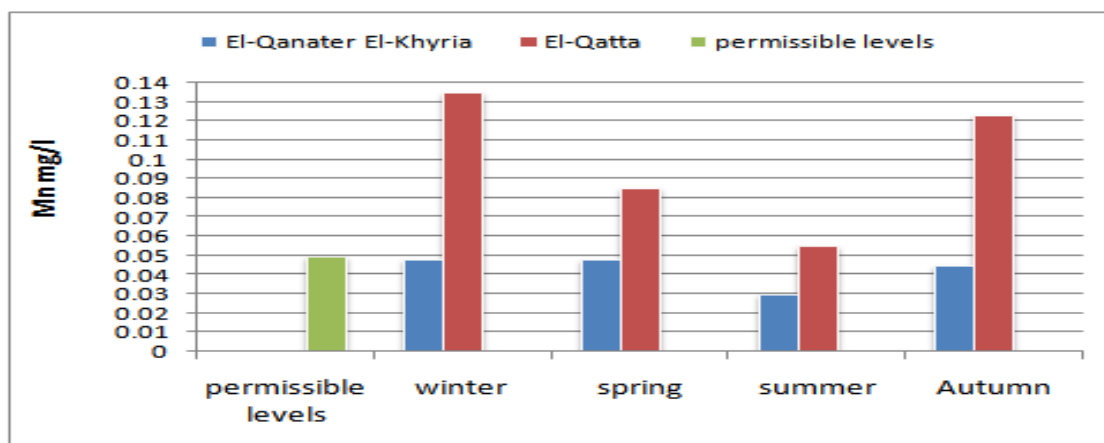


**Figure 5.** Seasonal variation of manganese concentrations in water at El-Qanater El-Khyria and El-Qatta of the River Nile. Permissible limit is according to ref. 20.

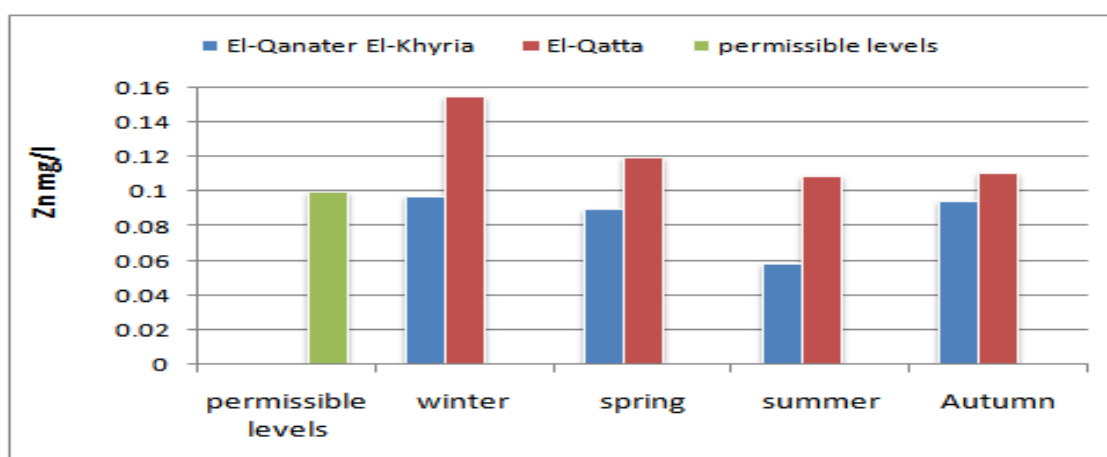


**Figure 6.** Seasonal variation of zinc concentrations in water at El-Qanater El-Khyria and El-Qatta of the River Nile. Permissible limit is according to ref. 28.

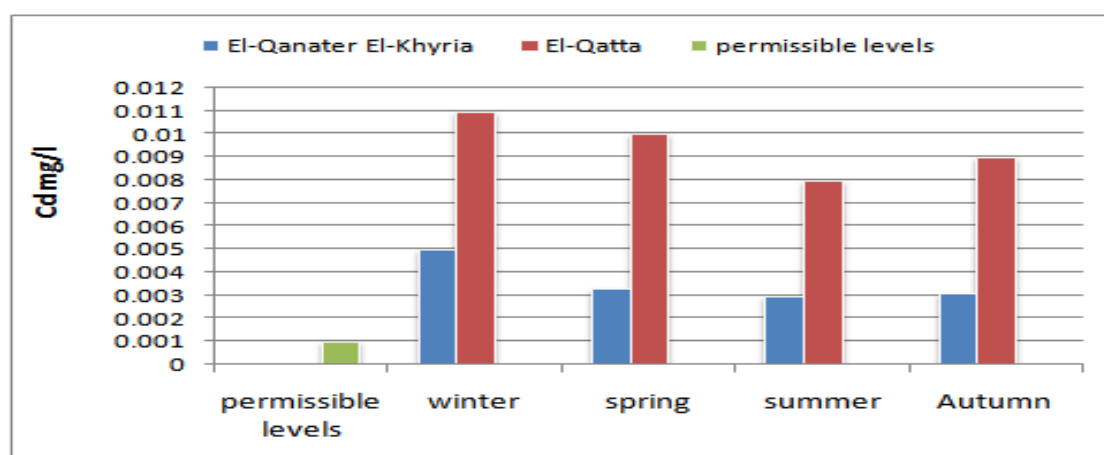


**Figure 7.** Seasonal variation of cadmium concentrations in water at El-Qanater El-Khyria and El-Qatta of the River Nile. Permissible limit is according to ref. 25.

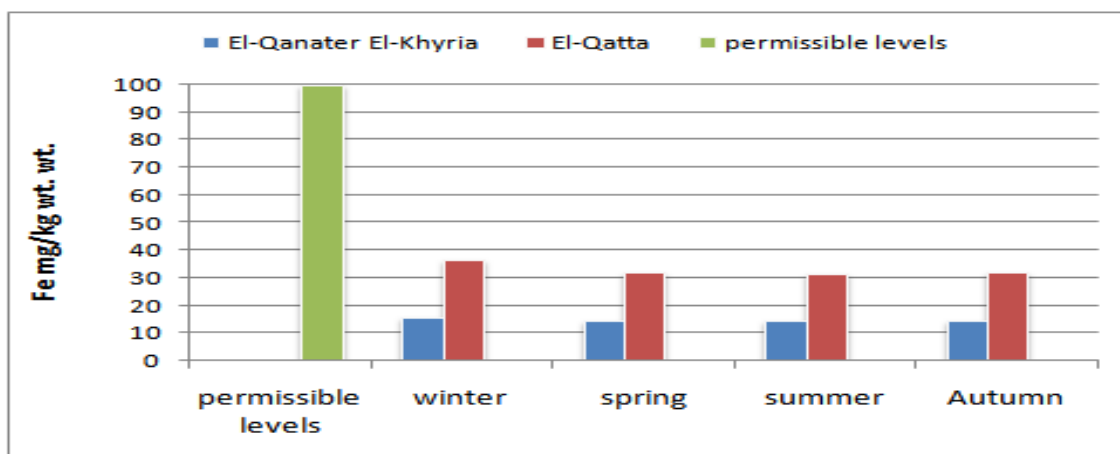


**Figure 8.** Seasonal variation of iron concentrations in the muscles of *O. niloticus* at El-Qanater El-Khyria and El-Qatta of the River Nile. Permissible limit is according to ref. 32.

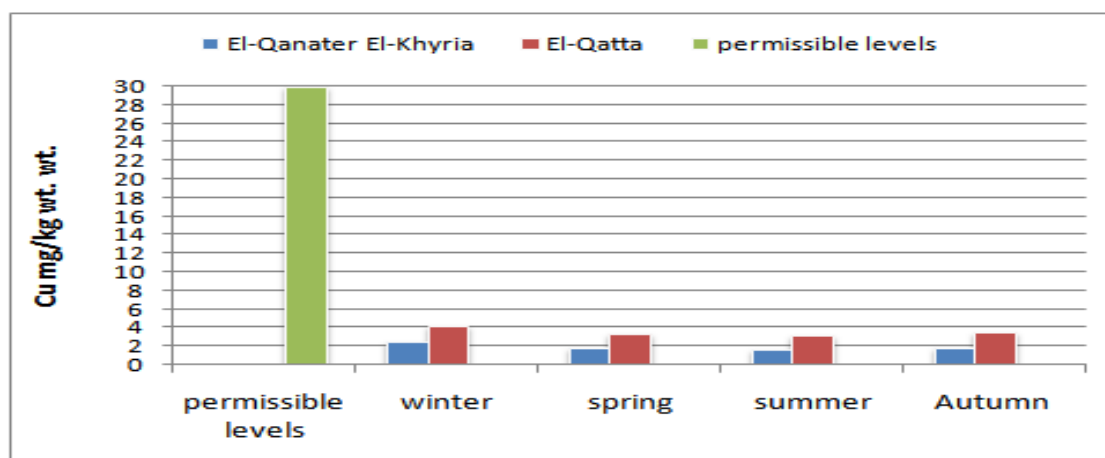


**Figure 9.** Seasonal variation of copper concentrations in the muscles of *O. niloticus* at El-Qanater El-Khyria and El-Qatta of the River Nile. Permissible limit is according to ref. 32.

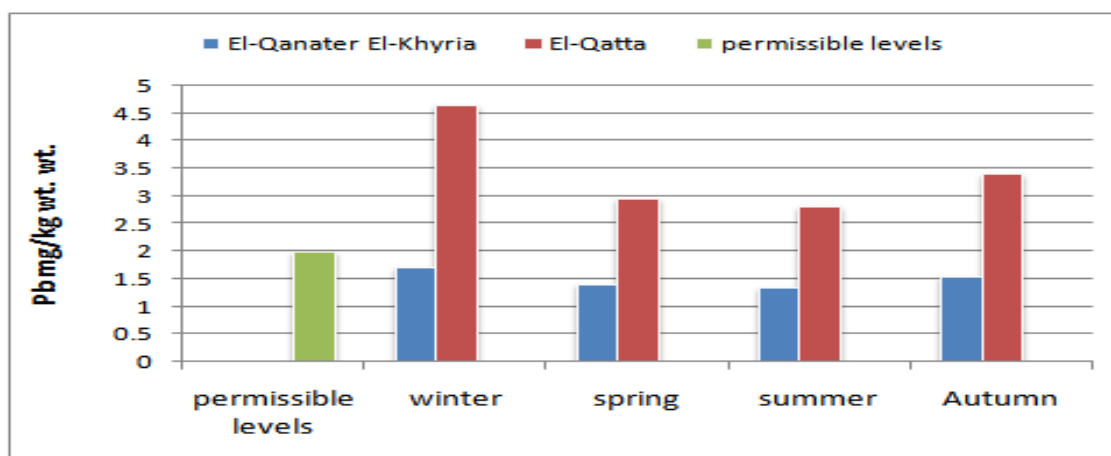


**Figure 10.** Seasonal variation of lead concentrations in the muscles of *O. niloticus* at El-Qanater El-Khyria and El-Qatta of the River Nile. Permissible limit is according to ref. 32.

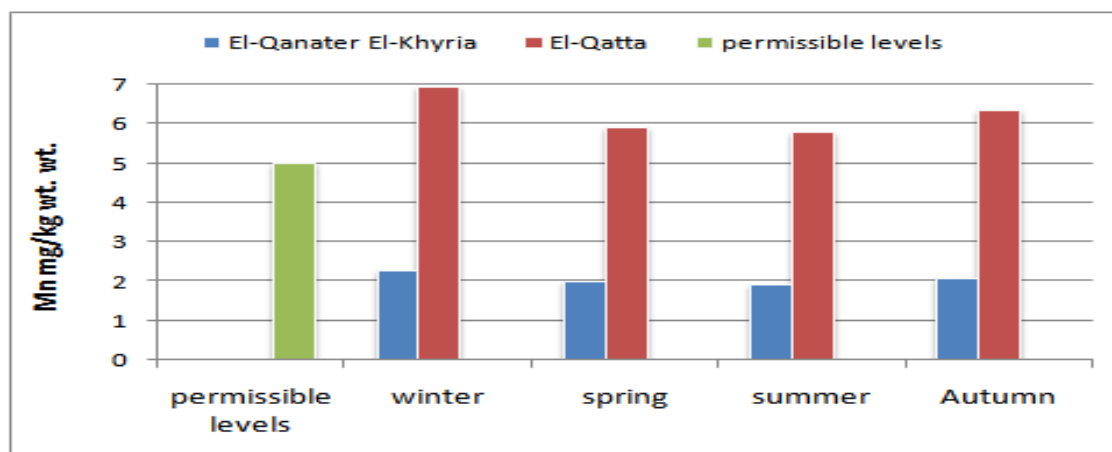


**Figure 11.** Seasonal variation of manganese concentrations in the muscles of *O. niloticus* at El-Qanater El-Khyria and El-Qatta of the River Nile. Permissible limit is according to ref. 32.

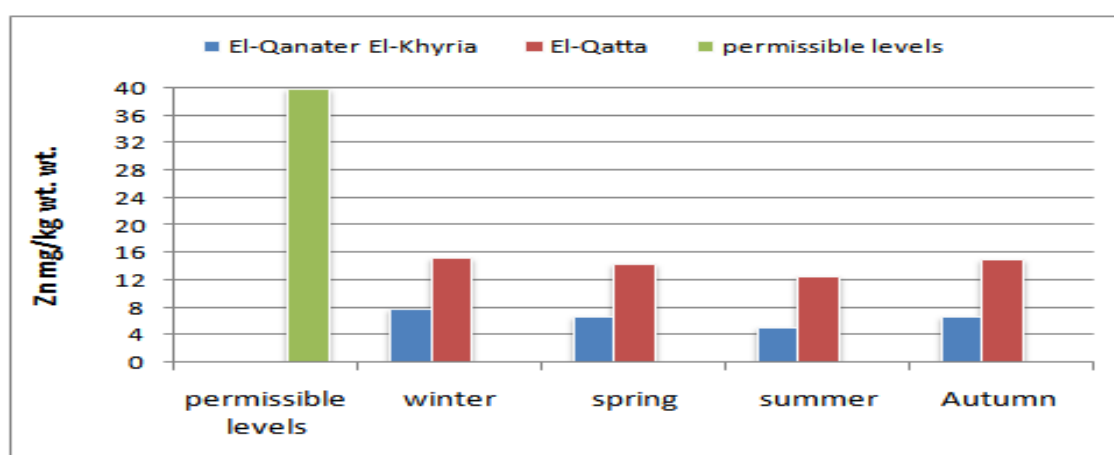


**Figure 12.** Seasonal variation of zinc concentrations in the muscles of *O. niloticus* at El-Qanater El-Khyria and El-Qatta of the River Nile. Permissible limit is according to ref. 32.

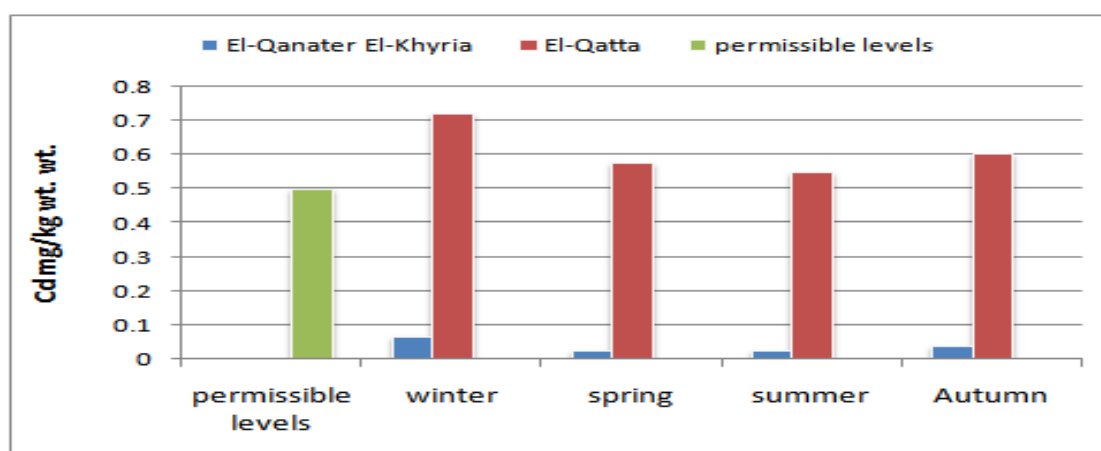


**Figure 13.** Seasonal variation of cadmium in the muscles of *O. niloticus* at El-Qanater El-Khyria and El-Qatta of the River Nile. Permissible limit is according to ref. 32.

The high accumulation of Fe in fish muscles can be attributed to the large amount of Fe detected in water. Higher Fe content in the fish muscles at El-Qatta station agrees with earlier finding.<sup>30</sup> The present data (Figure 8) showed that iron concentrations in the fish muscles were less than permissible level.<sup>32</sup> The highest accumulation of iron in fish muscles may be attributed to the large amount of iron in water of the River Nile and domestic sewage at El-Rahawy drain, however the minimum values at El-Qanater may be due to oxidation of  $\text{Fe}^{2+}$  to  $\text{Fe}^{3+}$  which remains as  $\text{Fe}(\text{OH})_3$  in the sediment of the oxygenated water.

Copper concentration of the muscles of the fish varies between 1.675 to 2.566  $\text{mg kg}^{-1}$  wt. wt. at El-Qanater El-Khyria and 3.235 to 4.226  $\text{mg kg}^{-1}$  wt. wt. at El-Qatta station during summer and winter season, respectively. Concentrations of copper (Figure 9) in the fish muscles are still less than the permissible level of 30  $\text{mg kg}^{-1}$  wt. wt.<sup>32</sup> Decreased copper concentration in the muscles of *O. niloticus* fish may well be due to the decrease in Cu concentration in water because of the decrease in water discharge during cold seasons and increase of domestic waste at El-Rahawy drain.<sup>33,24</sup> On the other hand an increase in Cu concentration in muscles of *O. niloticus* fish may be due to the increment of copper in water because in flow of large quantity of sewage waste in studied area.

The maximum value of lead (4.658  $\text{mg kg}^{-1}$  wt. wt.) was recorded during winter at El-Qatta station, while the lowest value (1.351  $\text{mg kg}^{-1}$  wt. wt.) was registered during summer at El-Qanater El-Khyria. The study revealed (Figure 10) that the lead concentration in muscles of *O. niloticus* fish of the studied area was higher than the permissible limit of 2.0  $\text{mg kg}^{-1}$  at El-Qatta station.<sup>32</sup> Figure 11 shows observed concentrations of Mn in the muscles which ranged from 1.945 to 6.954  $\text{mg kg}^{-1}$  wt. wt., these results, at El-Qatta, were higher than permissible level<sup>32</sup> of 5.0  $\text{mg kg}^{-1}$ . The highest value of zinc (Figure 12) was recorded in the fish muscles at El-Qatta station during winter (15.417  $\text{mg kg}^{-1}$  wt. wt.), while the lowest value (5.211  $\text{mg kg}^{-1}$  wt. wt.) recorded in El-Qanater El-Khyria station during summer. The values are lower than permissible level 40.0  $\text{mg kg}^{-1}$  wt. wt.<sup>32</sup>

The increase of Pb and Mn concentration in muscles of *O. niloticus* may be due to high concentration of the metal in water brought about by large amount of sewage discharged at El-Rahawy drain. The increase of zinc may be attributed

to the increase in metabolic rates which result in increased heavy metals uptake as has been previously indicated.<sup>34</sup> On the other hand, it may be due to the increase of Zn in water at El-Qatta station because of decrease in water discharge during winter season and increase domestic waste at El-Rahawy drain. The results (Figure 13) showed that cadmium values in the investigated area in the range between 0.0675-0.721, 0.027-0.578, 0.027-0.551 and 0.0405-0.605  $\text{mg kg}^{-1}$  wt. wt. during winter, spring, summer and autumn, respectively. The values were lower than permissible level<sup>32</sup> of 0.5  $\text{mg kg}^{-1}$  at El-Qanater El-Khyria station, while higher than permissible level<sup>32</sup> at El-Qatta station during all seasons. The high level of cadmium accumulation in the fish muscles may well be due to its strong binding with cystine residue of metallothionein as suggested earlier.<sup>31,35</sup> Also, the high levels of cadmium may be attributed to waste from sewage, industrial and mining operations as well as from the phosphate fertilizer at El-Rahawy drain station which accumulates most of the cadmium in the environment.<sup>36</sup>

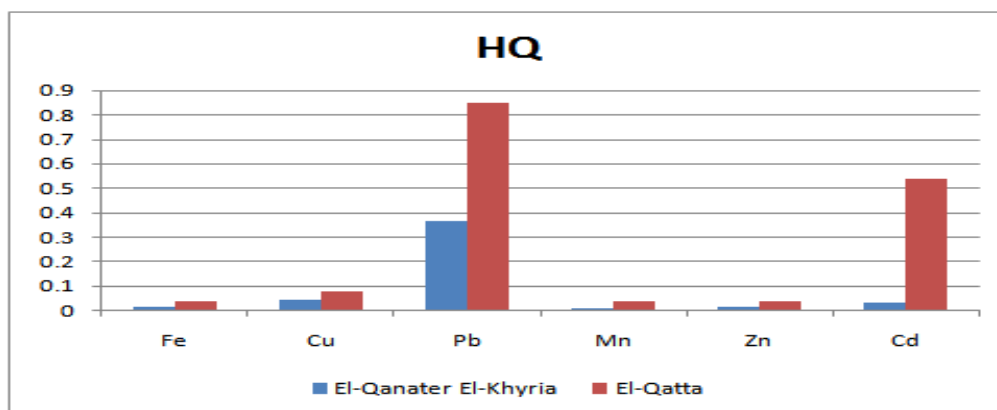
Generally, the maximum values of accumulation of metals in fish muscles of *O. niloticus* at El-Qatta station during winter season may be attributed to their increase in water of the Rosetta branch of the river Nile because of domestic sewage at El-Rahawy drain and lower level water during the drought period.

#### Hazard quotient (HQ)

The Hazard Quotient is a ratio of estimated dosage of polluted to a reference dose level.<sup>37</sup> It is calculated for the individual heavy metals using the following Eqn. (1).

$$HQ = \frac{EF \times ED \times FI \times MCf}{RfD_0 \times BW \times AT} \times 10^{-3} \quad (1)$$

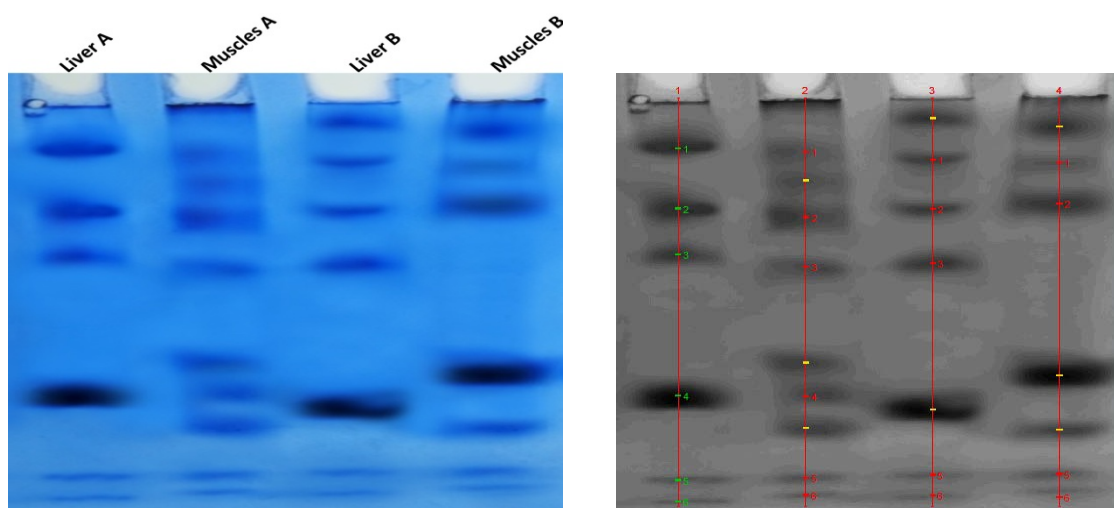
where, *EF* is the exposure amount (365 days year<sup>-1</sup>), *ED* is the life time exposure period (70 years), *FI* is mass of the fish ingested by person per day (57 mg) in Egypt,<sup>38</sup> *MCf* is the metal concentration in fish (in  $\text{mg kg}^{-1}$ ), *BW* is the body weight, a body weight of 70 kg is recommended<sup>39</sup> as a default value for the adult. *AT* is average time for non-carcinogens (365 days year<sup>-1</sup> × *ED*), *RFD<sub>0</sub>* is the reference dosage by mouth ( $\text{ppm day}^{-1}$ ).



**Figure 14.** Hazard Quotient (HQ) to humans due to individual metal through the muscles of *O. niloticus* at El-Qanater El-Khyria and El-Qatta station of the River Nile.

**Table 1.** HQ and HI to human population from metals through muscle of *O. niloticus* Rosetta branch.

Metal	CMF (mg kg <sup>-1</sup> wt. wt.) El-Qanater	CMF (mg kg <sup>-1</sup> wt. wt.) El-Qatta	RfD <sub>0</sub> (mg kg <sup>-1</sup> per day)	HQ El-Qanater	HQ El-Qatta
Fe	14.89375	33.20863	0.7	0.018684	0.04166
Cu	1.96525	3.60025	0.04	0.043144	0.079038
Pb	1.50625	3.46725	0.0036	0.367415	0.845756
Mn	2.08	6.2675	0.14	0.013047	0.039312
Zn	6.645375	14.418	0.3	0.019452	0.042203
Cd	0.0405	0.61375	0.001	0.035565	0.538957
<b>HI</b>	$\Sigma$			<b>0.497307</b>	<b>1.586926</b>

**Figure 15.** Native electrophoretic protein pattern showing the variations in number and arrangement of protein bands in liver and kidney tissues isolated from two different locations (A and B).**Table 2a.** Data of the electrophoretic protein pattern in liver of fishes living in different contaminated areas with different environmental conditions.

El-Qanater				El-Qatta			
Rf	Band intensity	B, %	Qty	Rf	Band intensity	B, %	Qty
0.125	188.258	17.478	4.457	0.051	174.669	14.636	8.221
0.272	185.678	17.239	11.202	0.152	174.693	14.638	5.296
0.385	180.856	16.791	8.011	0.274	173.965	14.577	6.245
0.730	210.465	19.540	8.679	0.406	176.846	14.819	8.324
0.937	156.804	14.558	3.592	0.765	194.946	16.336	13.064
0.990	155.039	14.394	2.013	0.925	151.675	12.710	3.267

**Table 2b.** Data of the electrophoretic protein pattern in muscles of fishes living in different contaminated areas with different environmental conditions.

El-Qanater				El-Qatta			
Rf	Band intensity	B, %	Qty	Rf	Band intensity	B, %	Qty
0.134	171.222	11.264	4.217	0.072	185.165	15.703	8.456
0.203	178.818	11.764	3.028	0.160	169.296	14.357	1.600
0.293	181.541	11.943	7.686	0.260	175.980	14.924	10.254
0.415	170.667	11.228	5.255	0.681	204.329	17.328	12.710
0.650	176.669	11.623	6.391	0.814	156.977	13.312	7.787
0.733	169.296	11.138	3.909	0.922	148.433	12.588	4.558
0.932	155.644	10.240	4.073				
0.974	146.064	9.609	3.710				

Rf = Relative Mobility, B % = Band percent, Qty = Band Quantity.

### Hazard Index (HI)

Hazard Index (HI) and Hazard Quotient (HQ) are used to estimate the health risk for humans from fish.<sup>37</sup> Eqn. (2) is used to calculate both HI and HQ.

$$HI = \sum n_i = 1HQ_i \quad (2)$$

Total HQ is expressed as the HI.<sup>40</sup> When HQ is equal to or lower than one, it signify no appreciable health risk, while if  $HQ > 1$ , then it specify a reason for health concern.<sup>39</sup> Greater is the values of HQ and HI (above 1), the greater is the level of risk associated with fish consumption. Hence,  $HI < 1$  means no hazard,  $1 > HI < 10$  means moderate hazard while greater than 10 means high hazard risk.<sup>41</sup> The HQ (Figure 14) due to intake of the studied metals through *O. niloticus* from the El Qanater and El-Qatta station are in the range for Fe (0.01868 – 0.04166), Cu (0.04314– 0.07904), Pb (0.3675 – 0.84576), Mn (0.01305 – 0.03931), Zn (0.01945 – 0.04221) and Cd (0.03556 – 0.53896).

HI values (Table 1) because of consumption of *O. niloticus* from the two stations are different.  $HI = 0.4973$  for El-Qanater El-Khyria, thus the HI of total for analyzed non-carcinogenic metals are less than the acceptable limit ( $HI = 1$ ) and thus do not have human health risk concern, while HI for the analyzed heavy metals were higher than the acceptable limit ( $HI < 1$ ) at El-Qatta station ( $HI = 1.5869$ ) and therefore, the cumulative metals risk impact is alarming particularly at high rates of fish consumption.<sup>39</sup>

### Electrophoretic study

It is well known that the rate of accumulation of metals in an organism's body vary from organ to organ. In an earlier study there was an equilibrium between concentricity of the metals in an organism's environment and its rate of ingestion and accumulation in muscles.<sup>42</sup>

The native protein pattern showed effect of aquatic toxic substances on the protein molecules totally. As recorded in Tables 2a and 2b and illustrated graphically in Figure 15, the native electrophoretic protein pattern revealed that there were four common bands noticed for both liver and muscle

tissues at Rfs 0.125, 0.272, 0.937 and 0.990 (B, %: 17.478, 17.239, 14.558 and 14.394; Quant. 4.457, 11.202, 3.592 and 2.013, respectively). There were no unique or characteristic bands. With respect to liver of fishes taken from location A, as match to the electrophoretic protein pattern in liver of fishes living at Qanater El-Kahayria water (Figure 15), elevation of the heavy metals at El-Rahawy water caused qualitative mutagenecity, it was found that there are 2 abnormal bands identified in liver of fishes taken from location B at Rfs 0.051 and 0.765 (B, %:14.363 and 16.336; Quant. 8.221 and 13.064, respectively). On the other hand, as compared to muscles of fishes taken from location A, it was noticed that there was qualitative variations represented by appearance of unique band identified at Rf 0.072 (B, %: 15.703; Quant. 8.456) with disappearance of 3 bands identified in muscles A (location A) at Rfs 0.203, 0.650 and 0.809 (B, %:11.764, 11.623 and 11.191; Quant. 3.028, 6.391 and 7.594, respectively). As revealed in Table 3, the native protein showed physiological alterations in liver and muscles of fishes living at El-Qatta water severely more than at El-Qanater El-Khyria. Results showed a significant difference arrived to 45.4 % in the liver and 48.1 % in the muscle. This might be attributed to ability of the metals to change activities of the hepatic enzymes leading to histopathology hepatic changes. Furthermore, the deleterious effects of heavy metals depend on the metal type and concentration and length of exposure.<sup>43</sup>

**Table 3.** Data of the similarity index (SI) and genetic distance (GD) of the electrophoretic pattern of protein in liver and muscle tissues of fishes living in different contaminated areas with different environmental conditions.

		Liver A	Muscles A	Liver B	Muscles B
		Similarity Index			
Liver A	Genetic distance	100	66.1	54.6	37.8
Muscles A		33.9	100	43.3	51.9
Liver B		45.4	56.7	100	37.3
Muscles B		62.2	48.1	62.7	100

The electrophoretic alterations in the native protein patterns may refer to effect of the heavy metals especially Pb and Cd, turn proteins and peptides susceptible to structural modifications in sub-cellular compartments and tissues.<sup>44</sup>

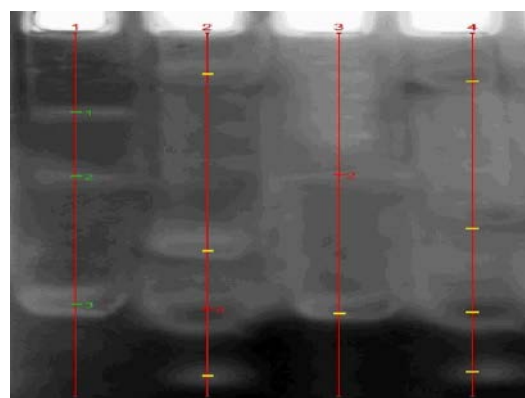
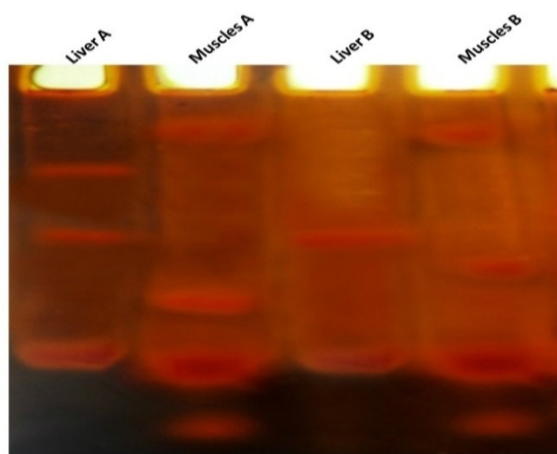


**Figure 16.** Native electrophoretic patterns of calcium moieties of native protein pattern showing the variations in number and arrangement of protein bands in liver and muscles tissues isolated from two different locations (A and B).

**Table 4a.** Data of the electrophoretic patterns of calcium in liver of fishes living in different contaminated areas with different environmental conditions.

El-Qanater				El-Qatta			
Rf	Band intensity	B, %	Qty	Rf	Band intensity	B, %	Qty
0.218	98.816	30.348	7.162	0.391	128.638	58.428	3.272
0.395	109.094	33.504	6.046	0.774	91.527	41.572	4.967
0.748	117.701	36.148	2.760				

**Table 4b.** Data of the electrophoretic pattern of calcium in muscles of fishes living in different contaminated areas with different environmental conditions.

El-Qanater				El-Qatta			
Rf	Band intensity	B, %	Qty	Rf	Band intensity	B, %	Qty
0.113	120.796	29.545	3.191	0.133	125.493	30.502	2.280
0.601	117.804	28.814	6.002	0.540	121.753	29.593	2.212
0.762	90.623	22.165	1.881	0.770	90.163	21.915	1.042
0.944	79.626	19.476	7.513	0.935	74.013	17.990	6.723

The electrophoretic calcium moieties of native protein pattern showed effect of the aquatic toxicity on the protein portion linked to calcium portion inside cells. As recorded in Table 4a and 4b and illustrated graphically in Figure 16, the native electrophoretic calcium moieties of native protein pattern presented that there was one common band in both of liver and muscle tissues identified at *Rf* 0.748 (*B*, % 117.701; Quant. 2.760). There were no unique or characteristic bands. With respect to liver of fishes taken from location A, it was found that the 1<sup>st</sup> normal band disappeared without appearance of any abnormal bands. On the other hand, as compared to muscles of fishes taken from location A, it was noticed that there was qualitative variations represented by deviation of the 2<sup>nd</sup> normal band to be appeared at *Rf* 0.540 (*B*, % 29.593, Quant. 2.212).

**Table 5.** Data of SI and GD of the electrophoretic pattern of calcium in liver and muscles tissues of fishes living in different contaminated areas with different environmental conditions.

		Liver A	Muscles A	Liver B	Muscles B
		Similarity Index			
Liver A	Genetic Distance	100	66.1	54.6	37.8
Muscles A		33.9	100	43.3	51.9
Liver B		45.4	56.7	100	37.3
Muscles B		62.2	48.1	62.7	100

Data of the similarity indices and genetic distances compiled in table 5, number and arrangement of the bands in

liver tissues in fishes taken from both locations (A and B) are similar by 33.9 %; while those in the muscle tissues are similar by 38.4 %. The similarity indices, there were similarity and physiological relationships among all the groups depending on the electrophoretic calcium moieties of native protein, results showed a significant difference arrived to 66.1 % in the liver and 61.6 % in the muscle. The native electrophoretic pattern showed physiological alterations in muscles and liver of fishes living in El-Rahawy drain water severely more than in El-Qanater El-Khyria water. Alterations in the electrophoretic calcium pattern of native protein pattern in liver and muscles tissues. This may be related to contamination with Cd that alters calcium homeostasis.<sup>45</sup>

The electrophoretic  $\beta$ -esterase showed that the aquatic toxicity exerted adverse effect leading to alterations in expression of these enzymes. As recorded in Table 6 a and 6b and illustrated graphically in Figure 17, the native electrophoretic  $\beta$ -esterase pattern revealed that  $\beta$ -esterase enzyme expressed as 2 types in liver tissue and 4 types in the muscle tissues. There were no common or characteristic bands. As compared to liver of fishes isolated from location A, there was qualitative difference represented by deviation of the 2<sup>nd</sup> band to be identified at *Rf* 0.784 (*B*, % 56.837 and Quant. 13.040). On the other hand, as compared to muscles tissues of fishes isolated from location A with those isolated from location B, it was found that there are no physiological or qualitative variations in number and arrangement of bands of native  $\beta$ -esterase pattern.

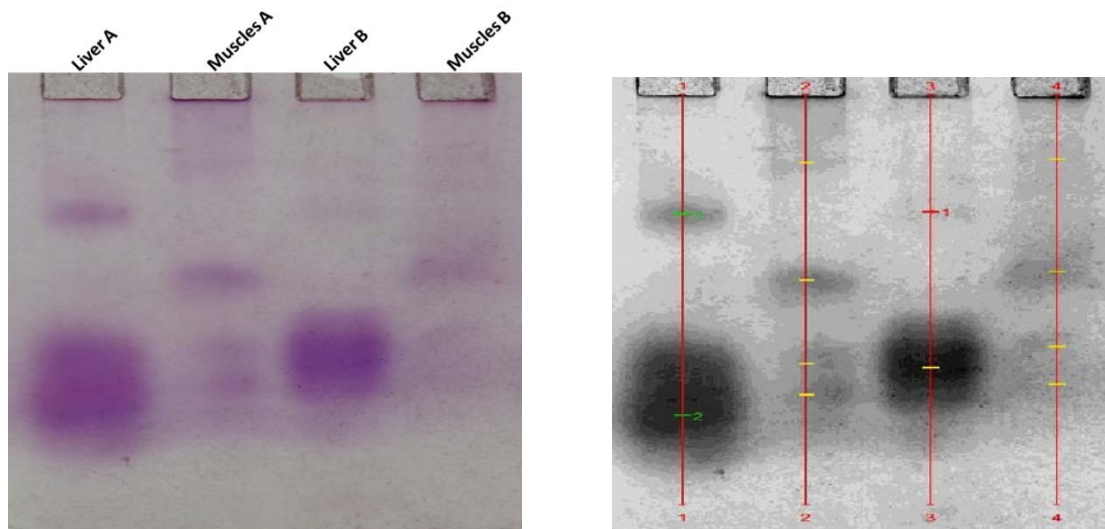
**Table 6a.** Data of the electrophoretic pattern of  $\beta$ -esterase in liver of fishes living in different contaminated areas with different environmental conditions.

El-Qanater				El-Qatta			
Rf	Band intensity	B, %	Qty	Rf	Band intensity	B, %	Qty
0.293	128.831	43.163	5.061	0.288	110.400	38.006	2.904
0.784	169.642	56.837	13.040	0.668	180.080	61.994	4.421

**Table 6b.** Data of the electrophoretic pattern of  $\beta$ -esterase in muscles of fishes living in different contaminated areas with different environmental conditions

El-Qanater				El-Qatta			
Rf	Band intensity	B %	Qty	Rf	Band intensity	B %	Qty
0.168	114.768	22.471	4.630	0.159	115.602	23.298	10.225
0.454	131.571	25.761	6.996	0.434	129.127	26.024	10.232
0.657	128.520	25.164	11.076	0.616	124.242	25.040	2.518
0.734	135.869	26.603	4.235	0.707	127.213	25.638	3.048

Rf = Relative Mobility, B, % = Band Percent, Qty = Band Quantity

**Figure 17.** Native electrophoretic  $\beta$ -esterase pattern showing the variations in number and arrangement of enzyme types in liver and kidney tissues isolated from two different locations (A and B).

Data of the similarity indices and genetic distances documented in Table 7, number and arrangement of the bands in liver tissues in fishes taken from both locations (A and B) are similar by 25.5 %, while those in the muscle tissues are similar by 29 %. The similarity indices, results showed a significant difference arrived to 74.5 % in the liver and 70.0 % in the muscle, there were similarity and physiological relationships among all the groups depending on the electrophoretic  $\beta$ -esterase pattern. Alterations were detected in the electrophoretic  $\beta$ -esterase pattern which may be ascribe to increasing of heavy metals of the Nile River water.

**Table 7.** Data of SI and GD showing number and arrangement of the pattern of  $\beta$ -esterase bands in liver and muscles tissues isolated from two different locations (A and B).

		Liver A	Muscles A	Liver B	Muscles B
		Similarity Index			
Liver A	Genetic Distance	100	0	25.5	0
Muscles A		100	100	36.1	29
Liver B		74.5	63.9	100	0
Muscles B		100	71	100	100

A = El-Qanater, B = El-Qatta

During the study, he found that the heavy metals accumulate in the muscles fish with different concentrations. The fish

muscle plays a key role in the metabolism and secretion of xenobiotic compound with morphological changes occurring in some toxic conditions.<sup>46</sup> During the study, electrophoretic alterations in the fish liver and muscles tissues were noticed. This might be attributed to ability of the metals to change activities of the hepatic enzymes leading to histopathological changes in the liver. Moreover, alterations were detected in the electrophoretic CAT and Gpx patterns. This might be caused due to presence of Cd that has the ability to alter the cell adhesion and the cellular antioxidant defence mechanisms.<sup>47</sup>

## REFERENCES

- <sup>1</sup>Helal, H. A., Studies on the Zooplankton of Dametta Branch of the River Nile North of El-Mansoura. Zoology Department, Mansoura University, **1981**, p. 462.
- <sup>2</sup>El Bouraie, M .M., Motawea, E. A., Mohamed, G. G., Yehia, M. M., Water quality of Rosetta branch in Nile delta, Egypt, *Suo*, **2011**, 62(1), 31–37.
- <sup>3</sup>Eiman, M., Zamzam, H., Effect of selenium-mercury interaction on *Clarias lazera* fish. *Proc. 3rd Congr. Toxicol. Developing Countries*, Cairo, Egypt, 19-23 November **1996**, p. 379-392.
- <sup>4</sup>Eisler, R., *Lead Hazards to Fish, Wildlife, and Invertebrates: A Synoptic Review*; US Fish and Wildlife Service, Patuxent Wildlife Research Center, **1988**.

- <sup>5</sup>Khalil, M. K. H., Radwan, A. M. and El-Moselhy, K. H. M. Distribution of phosphorus fractions and some of heavy metals in surface sediments of Burullus lagoon and adjacent Mediterranean Sea. *Egypt. J. Aquat. Res.*, **2007**, *33*(1), 277–289.
- <sup>6</sup>Ali, Z. Malik, R. N. and Qadir, A., Heavy metals distribution and risk assessment in soils affected by tannery effluents, *Chem. Ecol.*, **2013**, *29*, 676–692. <https://doi.org/10.1080/02757540.2013.810728>
- <sup>7</sup>Hogstrand, C. and Haux, C., Binding and detoxification of heavy metals in lower vertebrates with reference to metallothionein. Comparative, *Biochem. Physiol.*, **2001**, *100*, 137-141. [https://doi.org/10.1016/0742-8413\(91\)90140-0](https://doi.org/10.1016/0742-8413(91)90140-0)
- <sup>8</sup>Damek-Proprawa, M. and Sawicka-Kapusta, K., Damage to the liver, kidney and testis with reference to burden of heavy metals in yellownecked mice from areas around steel works and zinc smelters in Poland, *Toxicology*, **2003**, *186*, 1-10. [https://doi.org/10.1016/S0300-483X\(02\)00595-4](https://doi.org/10.1016/S0300-483X(02)00595-4)
- <sup>9</sup>Dautremepuits, C., Paris-Palacios, S., Betoulle, S., Vernet, G., Modulation in Hepatic and Head Kidney Parameters of Carp (Cyprinus Carpio L.) Induced by Copper and Chitosan. *Comp. Biochem. Physiol. Part C. Toxicol. Pharmacol.*, **2004**, *137*(4), 325–333. <https://doi.org/10.1016/j.cca.2004.03.005>
- <sup>10</sup>Ahmed, M. K., Shaheen, N., Islam, M. S., Al-Mamun, M. H., Islam, S., Mohiduzzaman, M. and Bhattacharjee, L., Dietary intake of trace elements from highly consumed cultured fish (*Labeorohita*, *Pangasius spangasius* and *Oreochromis mossambicus*) and human health risk implications in Bangladesh. *Chemosphere*, **2015**, *128*, 284–292. <https://doi.org/10.1016/j.chemosphere.2015.02.016>
- <sup>11</sup>Manusu, H. P. and Wrigley, C. W., Identification of species of fish by gradient-gel electrophoresis. *Aust. Vet. J.*, **1985**, *62*(11), 372-6. <https://doi.org/10.1111/j.1751-0813.1985.tb14212.x>
- <sup>12</sup>Valenzuela, M. A., Gamarra, N., Gómez, L., Kettlun, A. M., Sardon, M., Pérez, L. M., Vinagre, J., Guzman, N. A. A., Comparative Study of Fish Species Identification by Gel Isoelectrofocusing Two-Dimensional Gel Electrophoresis, and Capillary Zone Electrophoresis. *J. Capill. Electrophor. Microchip Technol.*, **1999**, *6*(3–4), 85–91.
- <sup>13</sup>APHA, AWWA, WEF *Standard Methods for examination of water and wastewater*, American Public Health Association, American Water Works Association (AWWA) and Water Environment Federation (WEF), 22<sup>nd</sup> ed., Washington. **2012**
- <sup>14</sup>Ghazaly, K. S., The Bioaccumulation of Potential Heavy Metals in the Tissues of the Egyptian Edible Marine Animals. 2.-Molluscs. *Bull. Natl. Inst. Oceanogr. Fish.*, **1988**, *14*(2), 79-86
- <sup>15</sup>Laemmli, U. K. Cleavage of structural proteins during the assembly of the head of Bacteriophage T4. *Nature*, **1970**, *227*, 680-685. <https://doi.org/10.1038/227680a0>
- <sup>16</sup>Darwesh, O. M., Moawad, H., Barakat, O. S. and Abd El-Rahim, W. M., Bioremediation of textile reactive blue azo dye residues using nanobiotechnology approaches. *Res. J. Pharm., Biol. Chem. Sci.*, **2015**, *6*(1), 1202-1211.
- <sup>17</sup>Subramaniam, H. N. and Chaubal, K. A., Evaluation of intracellular lipids by standardized staining with a Sudan black B fraction. *J. Biochem. Biophys. Methods*, **1990**, *21*(1), 9-16. [https://doi.org/10.1016/0165-022X\(90\)90040-J](https://doi.org/10.1016/0165-022X(90)90040-J)
- <sup>18</sup>Abulyazid, I., Abd Elhalim, S. A., Sharada, H. M., Aboulthana, W. M. and Abd Elhalim, S. T., Hepatoprotective effect of carob pods extract (*Ceratonia siliqua* L.) against cyclophosphamide induced alterations in rats. *Int. J. Curr. Pharm. Rev. Res.*, **2017**, *8*(2), 149-162. <https://doi.org/10.25258/ijcpr.v8i02.9199>
- <sup>19</sup>Rescigno, A., Sanjust, E., Montanari, L., Sollai, F., Soddu, G., Rinaldi, A. C., Oliva, S. and Rinaldi, A., Detection of laccase, peroxidase and polyphenol oxidase on a single polyacrylamide gel electrophoresis. *Anal. Lett.*, **1997**, *30*(12), 2211-2220. <https://doi.org/10.1080/00032719708001733>
- <sup>20</sup>Egyptian Organization for Standardization, *Egyptian standard, maximum levels for heavy metal concentrations in food*. ES 2360-1993, UDC: 546.19: 815, Egypt. **1993**.
- <sup>21</sup>Canli, M., Ay, Ö. and Kalay, M., Levels of heavy metals (Cd, Pb, Cu, Cr and Ni) in tissue of *Cyprinus Carpio*, *Barbus Capito* and *Chondrostoma Regium* from the Seyhan River. Turkey, *Turk. J. Zoology*, **1998**, *22*, 149-157.
- <sup>22</sup>Ghallab, M. H., *Some physical and chemical changes on the River Nile downstream of Delta barrage at El-Rahawy drain*. M.Sc. Thesis. Fac. Sci. Ain Shams Univ., Egypt. **2000**.
- <sup>23</sup>El-Sayed, M. and Salem, W. M., Hydrochemical assessments of surface Nile water and ground water in an industry area – South West Cairo, *Egypt. J. Petrol.*, **2015**, *24*, 277–288. <https://doi.org/10.1016/j.ejpe.2015.07.014>
- <sup>24</sup>Haggag, Y. H. M., *Environmental and chemical studies on the River Nile Pollutants and their relation to water quality at Rosetta branch*, Egypt. Ph. D. Thesis, Genetic Engineering & Biotechnology Institute, Sadat City University, **2017**.
- <sup>25</sup>Egyptian Governmental Law No. 48/1982- Decision 92 (2013) The implementer regulations for Law 48/1982, 92/2013 regarding the protection of the River Nile and water ways from pollution. *Map Periodical Bull.*, **1982**, 21-30.
- <sup>26</sup>Mantoura, R. F. C., Dickson, A. and Riley, J. P., The complexation of metals with humic materials in natural waters. *Estuarine Coastal Marine Sci.*, **1978**, *6*, 382-409. [https://doi.org/10.1016/0302-3524\(78\)90130-5](https://doi.org/10.1016/0302-3524(78)90130-5)
- <sup>27</sup>Moustafa, S. S., *Alterations in antioxidant defense system and biochemical metabolites in fish from Rosetta branch of the River Nile as a bio-indicator of environmental pollution*. Ph.D. Thesis, Fac. of science, Ain Shams University, **2017**.
- <sup>28</sup>WHO *Guidelines for drinking-water quality*. 2<sup>nd</sup>ed. Contents: V. I. Recommendations. WHO library cataloguing in publication date, Geneva. I-129, **1993**.
- <sup>29</sup>Abdel-Moati, M. A. R. and El-Sammak, A. A., Man-made impact on the geochemistry of the Nile delta lakes: a study of metals concentrations in sediments. *Water Air Soil Contam.*, **1997**, *97*, 413-429. <https://doi.org/10.1007/BF02407476>
- <sup>30</sup>Khalil, M., T.; Nahed, S. G., Nasr, A. M. A. and Sally, S. M., Antioxidant defense system alterations in fish as a bio-indicator of environmental pollution, *Egypt. J. Aquatic Biol. Fisheries*, **2017**, *21*(3), 11-28. <https://doi.org/10.21608/ejabf.2017.3536>
- <sup>31</sup>Tayel, S. I., Mahmoud, S. A., Ahmed, N. A. M. and Abdel Rahman A. A. S., Pathological impacts of environmental toxins on *Oreochromis niloticus* fish inhabiting the water of Damietta branch of the River Nile, Egypt. *Egypt. J. Aquatic Biol. Fisheries*, **2018**, *22*(5), 309-321. <https://doi.org/10.21608/ejabf.2018.25660>
- <sup>32</sup>WHO (World Health Organization), *Evaluation of Certain Food Additives and Contaminants* (Forty-first report of the joint FAO/ WHO Expert Committee on Food Additives). WHO, Geneva, Technical Report Series no. 837, **1993**.
- <sup>33</sup>Ahmed, N. A., Biochemical studies on pollution of the River Nile at different station of Delta barrage, Egypt. Ph.D. Thesis, Fac. of Agric. Benha Univ., Egypt, **2012**.
- <sup>34</sup>Sorensen, E. M. *Metal poisoning in fish*, Environmental and life sciences Associates. Austin. Texas. CRC Press Inc., Boston. **1991**.
- <sup>35</sup>Abu El-Ella, S. M., *Studies on the toxicity and bioconcentration of cadmium on grass carp Ctenopharyngo donidella*. M. Sc. Thesis, Faculty of Science, Helwan University, Egypt., **1996**.
- <sup>36</sup>Dimari, G. A., Abdulrahman, F. I., Akan, J. C. and Garba, S., Metals concentration in tissues of *Tilapia gallier*, *Crariaslazera* and *Osteoglossidae* Caught from Alau Dam, Maiduguri, Borno State, Nigeria. *Am. J. Environ. Sci.*, **2008**, *4*(4), 373-379. <https://doi.org/10.3844/ajessp.2008.373.379>
- <sup>37</sup>Goher, M. E., Abdo, M. H., Mangood, A. H., Hussein, M. M., Water quality and potential health risk assessment for consumption of *Oreochromis niloticus* from El-Bahr El-

- Pharaony Drain. Egypt., *Fresenius Environ. Bull.*, **2015**, 24(11), 3590–3602.
- <sup>38</sup>FAO *Report of fisheries and aquaculture markets in the Middle East.*, **2014**, <<http://www.thefishsite.com/articles/1870/fao-report-fisheries-and-aquaculture-markets-in-the-middle-east>>
- <sup>39</sup>USEPA (United States Environmental Protection Agency), Mid-Atlantic Risk Assessment. United States Environmental Protection Agency, Washington, **2013**, URL: <[http://www.epa.gov/reg3hwmd/risk/human/rb-concentration\\_table/users-guide.htm](http://www.epa.gov/reg3hwmd/risk/human/rb-concentration_table/users-guide.htm)> (Accessed 26.03.14).
- <sup>40</sup>Kumar, B., Virendra Kumar, V., Ashish Kumar, N., Paromita, C., Rita, S., Human health hazard due to metal uptake via fish consumption from coastal and fresh water waters in Eastern India along the Bay of Bengal. *J. Marine Biol. Oceanogr.*, **2013**, 2(3), 7. <https://doi.org/10.4172/2324-8661.1000115>
- <sup>41</sup>Ukoha, P. O., Ekere, N. R., Udeogu, U. V., Agbazue, V. E., Potential health risk assessment of heavy metals concentrations in some imported frozen fish species consumed in Nigeria. *Int. J. Chem. Sci.*, **2014**, 12(2), 366–374.
- <sup>42</sup>Adeyeye E. I., Akinyugha N. J., Fesobi M. E. and Tenabe V. O., Determination of some metals in *Clarias gariepinus* (Cuvier and Valenciennes), *Cyprinocarpio* (L) and *Oreochromis niloticus* (L.) fishes in a polyculture freshwater pond and their environments. *Aquaculture*, **1996**, 147, 205-214. [https://doi.org/10.1016/S0044-8486\(96\)01376-2](https://doi.org/10.1016/S0044-8486(96)01376-2)
- <sup>43</sup>Paris-Palacios, S., Biagianti-Risbourg, S. and Vernet, G., Biochemical and (ultra) structural hepatic perturbation of *Brachydaniorerio* (Teleostei, Cyprinidae) exposed to two sublethal concentrations of copper sulphate. *Aquat. Toxicol.*, **2000**, 50, 109-124. [https://doi.org/10.1016/S0166-445X\(99\)00090-9](https://doi.org/10.1016/S0166-445X(99)00090-9)
- <sup>44</sup>Hechtenberg, S. and Beyersmann, D., Inhibition of sarcoplasmic reticulum Ca<sup>2+</sup>-ATPase activity by cadmium, lead and mercury, *Enzyme*, **1991**, 45, 109-115. <https://doi.org/10.1159/000468875>
- <sup>45</sup>Pratap, H. B. and Wendelaar Bonga, S. E., Calcium homeostasis in low and high calcium water acclimatized *Oreochromismossambicus* exposed to ambient and dietary cadmium. *J. Environ. Biol.*, **2007**, 28, 385-393.
- <sup>46</sup>Rocha, E. and Monteiro, R. A. F., Histology and Cytology of Fish Liver: A Review. In: *Ichthyology: Recent Research Advances*, Saksena D.N. (Ed.). Science Publishers, Enfield, New Hampshire. ISBN: 1-57808-053-3, pp: 321-344, **1999**.
- <sup>47</sup>Yano, C. L. and Marcondes, M. C. C. G., Cadmium chloride-induced oxidative stress in skeletal muscle cells *in vitro*. *Free Radicals Biol. Med.*, **2005**, 39, 1378-1384. <https://doi.org/10.1016/j.freeradbiomed.2005.07.001>

Received: 22.12.2019.

Accepted: 16.02.2020.



# MOLECULAR STRUCTURE MODELS OF $Al_2Ti_3$ AND $Al_2V_3$ CLUSTERS ACCORDING TO DFT QUANTUM-CHEMICAL CALCULATIONS

Oleg V. Mikhailov<sup>[a]\*</sup> and Denis V. Chachkov<sup>[b]</sup>

**Keywords:** Metal cluster. aluminum; titanium; vanadium; molecular structure; DFT method.

Basic parameters of molecular structures of  $Al_2Ti_3$  and  $Al_2V_3$  metal clusters (bond lengths, bond angles, and torsion (dihedral) angles), have been calculated using DFT method at the OPBE/QZVP level. It has been shown that the  $Al_2Ti_3$  cluster may exist in 14 modifications and  $Al_2V_3$  in 11 ones, differing noticeably in their total energy. Besides, the molecular structures of these metal clusters differ significantly in terms of geometric parameters as well as in external form. Moreover, the most energetically stable modifications of  $Al_2Ti_3$  and  $Al_2V_3$  clusters differ each other considerably in geometric form also.

\* Corresponding Authors

E-Mail: olegmkhlv@gmail.com

[a] Kazan National Research Technological University, K. Marx Street 68, 420015 Kazan, Russia

[b] Kazan Department of Joint Supercomputer Center of Russian Academy of Sciences – Branch of Federal Scientific Center “Scientific Research Institute for System Analysis of the RAS”, Lobachevski Street 2/31, 420111 Kazan, Russia

## INTRODUCTION

Earlier quantum chemical calculations of a number of heterobimetallic metal clusters containing atoms of various *p*- and *d*-elements<sup>1–18</sup> has been carried out using the density functional theory (DFT) method. Some of such metal clusters have been applied in various fields of science and technology.<sup>10–14</sup> In the works cited above, the objects of study were the so-called (*dd*) heterobimetallic metal clusters, which included atoms of two different *d*-elements, namely (Cu, Fe),<sup>1</sup> (Pd, Fe),<sup>2</sup> (Pd, Ag),<sup>3–5</sup> (Pt, Cu),<sup>6</sup> (Au, Fe),<sup>7</sup> (Au, Pd)<sup>8</sup> and (Au, Ag).<sup>9</sup> However, of no less interesting are the (*pd*) heterobimetallic metal clusters that include atoms of different categories of metals, namely, *p*- and *d*-elements, since theoretically it can be expected that they will demonstrate such new properties that are not inherent of metal clusters containing metal atoms of only one category.

Among the most important *p*-elements is aluminum, which has a very wide industrial application. Nevertheless, only a few (*pd*) metal clusters containing this *p*-element and any of *d*-metals are described in the literature.<sup>15–18</sup> On the one hand, such metal clusters can serve as efficient catalysts for a number of sol–gel technology processes that occur in inorganic as well as in organic silicate media. On the other hand, they can play the role of specific “precursors” for the production of micro- and nano-particles of metal oxides and metal chalcogenides, that, in turn, are very convenient starting materials for the creation of various composite materials. Previously<sup>16–21</sup> we have carried out quantum chemical calculations, using the DFT method, of molecular structures of four different (*pd*) metal clusters with the  $Al_2M_3$  composition ( $M = Cr, Mn, Fe, Co, Ni, Cu, Zn$ ) and showed that each of them exists in various modifications. Besides, the number of such modifications varies from 8 in

the case of  $Fe^{17,19}$  and  $Cu^{19,20}$  to 25 in the case of  $Mn^{21}$ . On the other hand, it seems reasonable to see how, with the same formal stoichiometric composition of  $Al_2M_3$ , the nature of another *3d*-metal affects the number of possible modifications of the corresponding metal cluster and their relative stability. Taking into account this circumstance, as well as the fact that the  $Al_2M_3$  metal clusters for  $M = Cr, Mn, Fe, Co, Ni, Cu, Zn$  have already been studied by us,<sup>16–21</sup> metal clusters having the same stoichiometric composition  $Al_2M_3$  but containing Ti and V as a *3d*-metal, were selected as the objects of this study. These two elements are the first two members of a group of *3d*-elements (electronic configurations are  $4s^23d^1$  and  $4s^23d^2$ , respectively), and calculations of metal clusters of the  $Al_2M_3$  type by DFT method has not yet been carried out for them. In view of this, this investigation is devoted to the identification of possible modifications of metal clusters of  $Al_2Ti_3$  and  $Al_2V_3$  composition, the calculation of the basic parameters of their structures [metal-metal bond lengths, bond and torsion (dihedral) angles] and relative stability of these modifications from an energy point of view.

## CALCULATION METHODS

The quantum-chemical calculations of  $Al_2Ti_3$  and  $Al_2V_3$  metal clusters were carried out using the density functional method (DFT) combining the standard extended split-valence QZVP basis<sup>22,23</sup> and the OPBE functional.<sup>24,25</sup> The data of previous works<sup>26–29</sup> give us reason to assert that the given method allows to obtain the most accurate estimation of ratio between energies of the high-spin state and low-spin state and, at the same time, rather reliably predicts the key geometric parameters of molecular structures for various compounds of *3p*- and *3d*-elements. To build quantum chemical models of the molecular structures of the metal clusters under examination, GAUSSIAN09 software was used.<sup>30</sup> As before,<sup>16–21</sup> the accordance of the found stationary points to the energy minima was confirmed by calculation of the second derivatives with respect to the atomic coordinates. Besides, all equilibrium structures corresponding to the minima at the potential energy surface revealed only real positive frequency values. Parameters of the molecular structures for spin multiplicities ( $M_s$ ) more than 1, were

determined using the so-called unrestricted method (UOPBE) and for  $M_S = 1$ , using the so-called restricted method (ROPBE). Along with this, the unrestricted method in conjunction with the GUESS = Mix option was used for the cases when  $M_S$  was equal to 1. The data, obtained as a result of such a procedure, are similar to those obtained using ROPBE method.

## RESULTS AND DISCUSSION

According to results of DFT quantum-chemical calculation of  $Al_2Ti_3$  and  $Al_2V_3$  metal clusters, 14 forms of cluster  $Al_2Ti_3$  and 11 forms of cluster  $Al_2V_3$  are capable to autonomous existence. Molecular structures of  $Al_2Ti_3$  cluster are presented in **Figure 1**. Relative total energies of these structures are given in table 1. As may be seen from these data, only half of the 14 modifications of  $Al_2Ti_3$ , namely  $Al_2Ti_3$ (I),  $Al_2Ti_3$ (II),  $Al_2Ti_3$ (IV),  $Al_2Ti_3$ (V),  $Al_2Ti_3$ (VII),  $Al_2Ti_3$ (VIII) and  $Al_2Ti_3$ (X), contain a covalent Al–Al bond, in the other seven  $Al_2Ti_3$  structures, there are only the Ti–Ti and Ti–Al bonds.

**Table 1.** Relative total energies of different structures of the  $Al_2Ti_3$  clusters.

Structure symbol	Spin multiplicity of ground state	Relative total energy, $\text{kJ mol}^{-1}$	Number of chemical bonds in the structure		
			Al–Al	Al–Ti	Ti–Ti
$Al_2Ti_3$ (I)	3	80.9	1	6	2
$Al_2Ti_3$ (II)	1	24.1	1	6	2
$Al_2Ti_3$ (III)	1	93.0	0	6	2
$Al_2Ti_3$ (IV)	5	60.7	1	6	1
$Al_2Ti_3$ (V)	5	19.7	1	5	2
$Al_2Ti_3$ (VI)	3	37.2	0	5	3
$Al_2Ti_3$ (VII)	1	44.8	1	5	3
$Al_2Ti_3$ (VIII)	1	77.5	1	5	3
$Al_2Ti_3$ (IX)	5	73.0	0	6	1
$Al_2Ti_3$ (X)	3	37.0	1	6	2
$Al_2Ti_3$ (XI)	5	0.0	0	6	3
$Al_2Ti_3$ (XII)	3	12.6	0	6	3
$Al_2Ti_3$ (XIII)	1	21.5	0	6	3
$Al_2Ti_3$ (XIV)	1	51.1	0	6	3

From the information contained in it clearly follows that the most stable in total energy is the modification of  $Al_2Ti_3$  (XI), having a geometry of a trigonal bipyramid, in the “equatorial flatness” of which there are three titanium atoms, the atoms of aluminium are located at its vertices. The modification showing the next higher total energy, namely  $Al_2Ti_3$  (XII), has a similar structure (Figure 1). It is interesting to note in this connection that in both these most stable modifications, Al–Al bond is absent. In most of the  $Al_2Ti_3$  modifications, 10 out of 14, there are six Ti–Al bonds, and only in four of them, namely in  $Al_2Ti_3$  (V)- $Al_2Ti_3$  (VIII), there are five. Complete set of Ti–Ti bonds, that is 3, occurs in seven structures,  $Al_2Ti_3$  (VI)- $Al_2Ti_3$  (VIII),  $Al_2Ti_3$  (XI)- $Al_2Ti_3$  (XIV); two such bonds are present in five modifications,  $Al_2Ti_3$  (I)-  $Al_2Ti_3$  (III),  $Al_2Ti_3$  (V) and  $Al_2Ti_3$  (X). Finally, in two modifications,  $Al_2Ti_3$  (IV) and  $Al_2Ti_3$  (IX) have one.

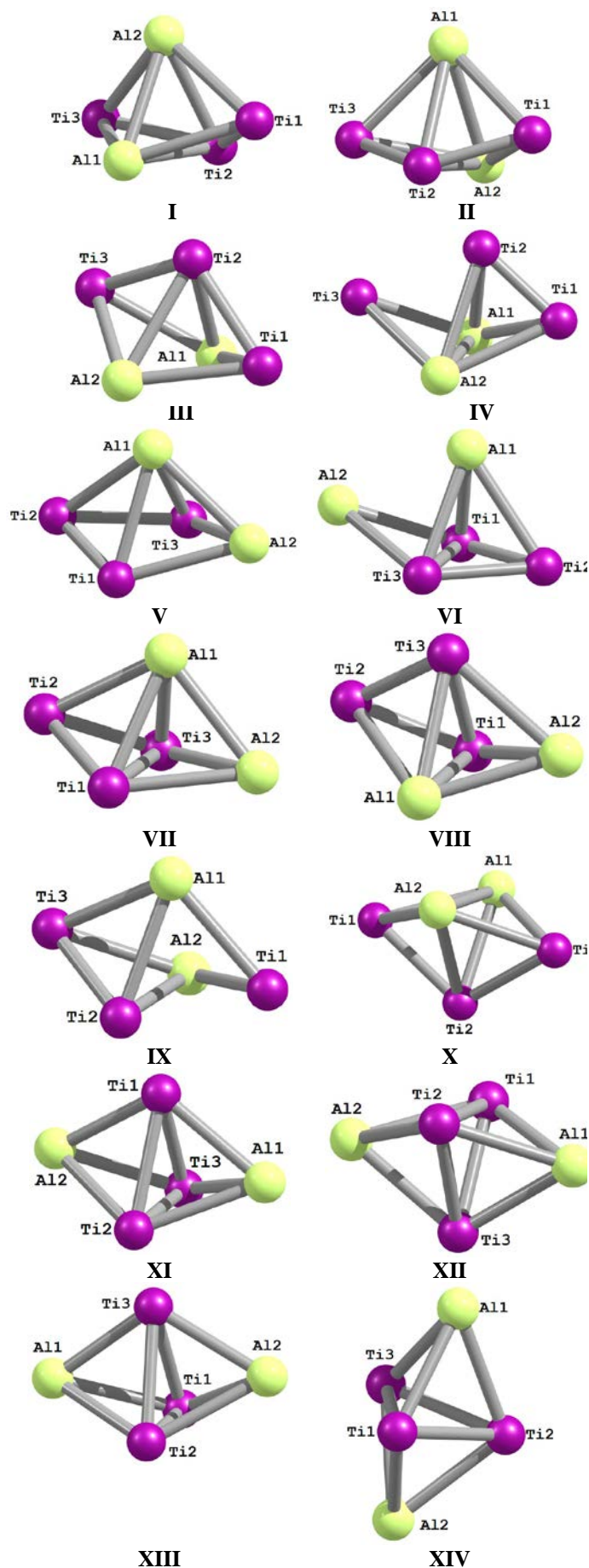


**Figure 1.** Molecular structures of  $Al_2Ti_3$  clusters.

The most energetically favorable  $Al_2Ti_3$  (XI) modification contains maximal possible number of Al–Ti and Ti–Ti bonds (6 and 3, respectively). On the whole, it can be stated that most of the modifications of the given metal cluster have the structure of a trigonal bipyramid or close to it. The exceptions are only  $Al_2Ti_3$  (V) with a structure close to the tetragonal pyramid and also  $Al_2Ti_3$  (IV),  $Al_2Ti_3$  (VI) and  $Al_2Ti_3$  (IX), which have the structure of a “cap” tetrahedron (Figure 1). The Ti–Ti bond lengths in  $Al_2Ti_3$  metal clusters are in the ranges of 210–260 pm, and the lengths of the Al–Ti and Al–Al bonds are in the ranges of 252–270 nm and 255–280 nm, respectively, that taking into account the atomic radii of these elements, 143 pm for Al and 132 pm for Ti, seems quite natural and predictable.

Among all modifications of cluster under examination, four modifications, namely  $Al_2Ti_3$  (IV),  $Al_2Ti_3$  (V),  $Al_2Ti_3$  (IX), and  $Al_2Ti_3$  (XI), have  $M_S = 5$ , four,  $Al_2Ti_3$  (I),  $Al_2Ti_3$  (VI),  $Al_2Ti_3$  (X), and  $Al_2Ti_3$  (XII) have  $M_S = 3$  and the other six have  $M_S = 1$  (Table 1). It is noticed from these data that the last spin state for the given metal cluster is predominant. Nevertheless, in fairness, it should be noticed that the nearest in energy to the conformation  $Al_2Ti_3$ (XI),  $Al_2Ti_3$  (XII), and  $Al_2Ti_3$ (V), with relative total energies 12.6 and 19.7 kJ mol<sup>-1</sup>, respectively, have in the ground state  $M_S = 3$  and  $M_S = 5$ , respectively (Table 1). The most high-energetic modification of the considered metal cluster, and namely  $Al_2Ti_3$  (III), has relative total energy 93.0 kJ mol<sup>-1</sup> and  $M_S = 1$ . It should be noted in this connection that the most stable modification of  $Al_2Ti_3$  with  $M_S = 1$ , is  $Al_2Ti_3$  (XIII) having relative total energy 21.5 kJ mol<sup>-1</sup> (Table 1).

Nine oscillations, active in IR spectrum, should appear in a nonlinear five-atom molecule (to number of which belongs  $Al_2Ti_3$ ) according to theoretical expectations. This quantity turns out to be correct in  $Al_2Ti_3$  (XI) metal cluster according to our calculation (Table 2).

**Table 2.** The oscillation frequencies in most stable modification of  $Al_2Ti_3$  (XI) cluster.

Oscillation frequency, cm <sup>-1</sup>	Assignment of oscillation frequency
121	Wagging for Al1 and Al2 atoms relatively Ti1–Ti3 bond
154	Wagging for Al1 and Al2 atoms relatively Ti1–Ti2 bond
203	Scissoring for Ti1, Ti2, and Ti3 atoms
217	Stretching ( <i>asym.</i> ) for Al1 and Al2 atoms relatively Ti1 atom
237	Stretching ( <i>asym.</i> ) for Al1 and Al2 atoms relatively Ti1–Ti2 bond
250	Scissoring for Al1, Ti3, and Al2 atoms
263	Stretching ( <i>sym.</i> ) for Al1 and Al2 atoms relatively Ti3 atom
345	Stretching ( <i>sym.</i> ) for Al1, Ti3 and Al2, Ti3 atom pairs
350	Stretching ( <i>sym.</i> ) with participation of all atoms in $Al_2Ti_3$ metal cluster

Molecular structures of the various  $Al_2V_3$  metal clusters are shown in Figure 2 and the relative total energies of them are given in the table 3. As may be seen from these data in six of 11 of these structures, the direct valence bond of Al–Al occurs, the exceptions are the structures of  $Al_2V_3$  (VII)– $Al_2V_3$

(XI). Also, in most of the modifications of metal cluster under the study, excluding only  $Al_2V_3$  (VIII) and  $Al_2V_3$  (IX), there are at least one V–V bond. Nevertheless, in each of the modifications of  $Al_2V_3$ , there are at least five Al–V bonds. It is noteworthy that in  $Al_2V_3$  (VIII) and  $Al_2V_3$  (IX) modifications mentioned above, there are only Al–V bonds (6 in the each of them). Besides, the most stable modification of this metal cluster, namely  $Al_2V_3$ (V), contains 7 metal–metal bonds (Table 3).

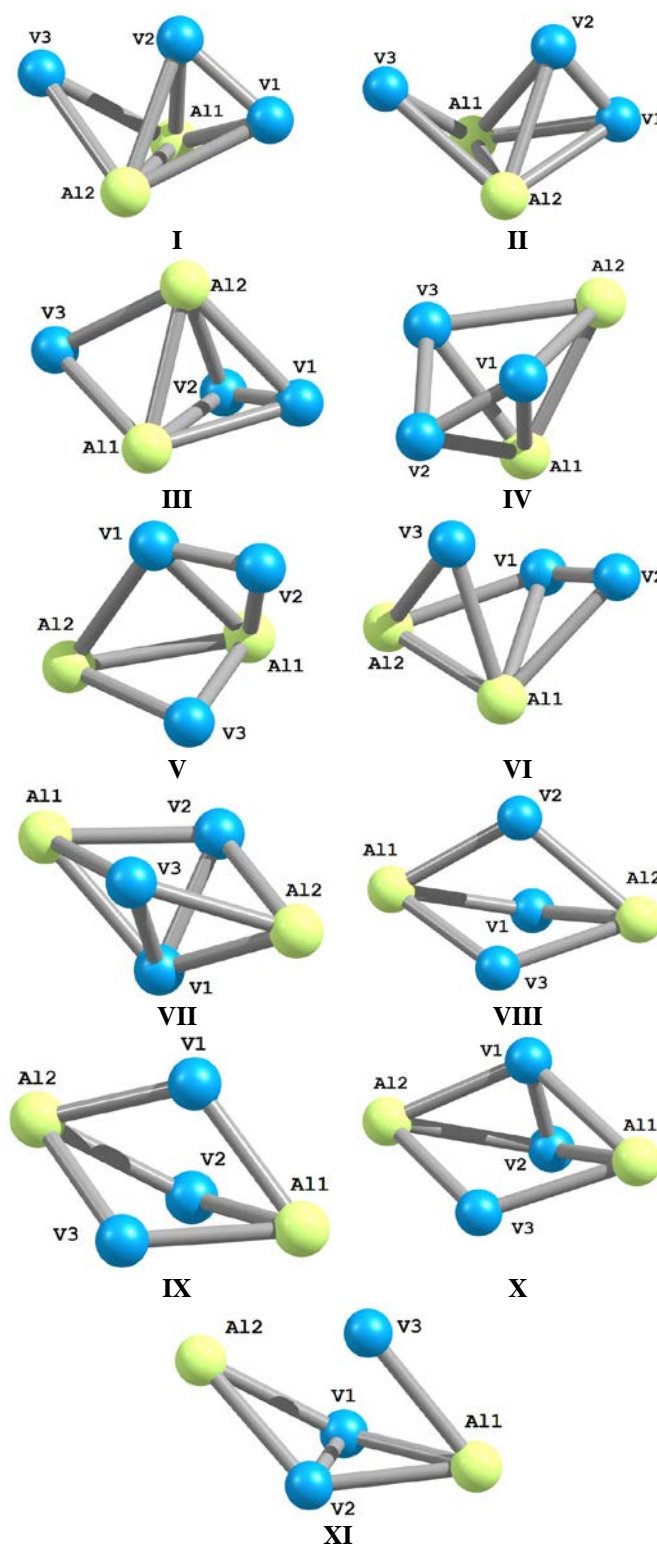


**Figure 2.** Molecular structures of  $Al_2V_3$  clusters.

It should be noted especially that, on the whole, molecular structures of Al<sub>2</sub>V<sub>3</sub> differ substantially from molecular structures of Al<sub>2</sub>Ti<sub>3</sub>, at that, not only by the number of metal-metal bonds, but, also, by its geometrical form (Figures 1 and 2).

As can be seen from the data of Table 3, the most stable modification, namely Al<sub>2</sub>V<sub>3</sub> (V), has not the highest spin multiplicity (6), but a lower one (4). Besides, which is characteristic, the structures with the highest M<sub>S</sub> = 6 generally have noticeably larger values of the total energies than those with multiplicities M<sub>S</sub> = 2 and M<sub>S</sub> = 4. It is characteristic that the Al<sub>2</sub>V<sub>3</sub> (II) structure nearest to Al<sub>2</sub>V<sub>3</sub> (V) in energy has the same spin multiplicity as Al<sub>2</sub>V<sub>3</sub>(V), and its molecular structure, at least in general terms, resembles Al<sub>2</sub>V<sub>3</sub> (V). At the same time, the following three structures with increasing energy, namely Al<sub>2</sub>V<sub>3</sub>(III), Al<sub>2</sub>V<sub>3</sub> (I) and Al<sub>2</sub>V<sub>3</sub> (IV), have different M<sub>S</sub> values, namely, 6, 2, and 2, respectively. The least stable in terms of energy is the modification of Al<sub>2</sub>V<sub>3</sub> (IX), the total energy of which is not only much higher (by almost 150 kJ mol<sup>-1</sup>) than that of Al<sub>2</sub>V<sub>3</sub>(V), but also of all the other modifications of the metal cluster under study. Remarkably, it has the highest spin multiplicity (6). The V–V bond lengths in the Al<sub>2</sub>V<sub>3</sub> metal cluster considered here are in the 170–275 pm range, while the Al–V and Al–Al bond lengths are in the 250–270 nm and 255–270 nm ranges, respectively (Table 3). Taking into account the radii of the atoms of these elements, 143 pm for Al and 134 pm for V, it seems quite natural.

**Table 3.** Relative total energies of different structures of the Al<sub>2</sub>V<sub>3</sub> clusters.

Structure symbol	Spin multiplicity of ground state	Relative total energy, kJ mol <sup>-1</sup>	Number of chemical bonds in the structure		
			Al–Al	Al–V	V–V
Al <sub>2</sub> V <sub>3</sub> (I)	2	25.9	1	6	1
Al <sub>2</sub> V <sub>3</sub> (II)	4	2.4	1	6	1
Al <sub>2</sub> V <sub>3</sub> (III)	6	18.8	1	6	1
Al <sub>2</sub> V <sub>3</sub> (IV)	2	26.7	1	5	2
Al <sub>2</sub> V <sub>3</sub> (V)	<b>4</b>	<b>0.0</b>	<b>1</b>	<b>5</b>	<b>1</b>
Al <sub>2</sub> V <sub>3</sub> (VI)	6	26.8	1	5	1
Al <sub>2</sub> V <sub>3</sub> (VII)	2	30.2	0	6	2
Al <sub>2</sub> V <sub>3</sub> (VIII)	4	71.3	0	6	0
Al <sub>2</sub> V <sub>3</sub> (IX)	6	141.0	0	6	0
Al <sub>2</sub> V <sub>3</sub> (X)	4	59.6	0	6	1
Al <sub>2</sub> V <sub>3</sub> (XI)	6	74.6	0	5	1

As in Al<sub>2</sub>Ti<sub>3</sub> metal clusters, nine oscillations active in IR spectrum developed in Al<sub>2</sub>V<sub>3</sub> ones also, according to our calculation. Frequencies of such oscillation for most stable modification of Al<sub>2</sub>V<sub>3</sub>, namely Al<sub>2</sub>V<sub>3</sub> (V), are presented in table 4. It should be noted in this connection that, despite the same the total number of oscillations active in the IR spectra of the Al<sub>2</sub>Ti<sub>3</sub> (XI) and Al<sub>2</sub>V<sub>3</sub> (V) clusters, their characteristics differ very strongly from each other. It is enough to compare the range of frequencies that are active in the IR spectrum. In the case Al<sub>2</sub>Ti<sub>3</sub> (XI), it is less than 250 cm<sup>-1</sup> (from 121 to 350 cm<sup>-1</sup>), while in the case of Al<sub>2</sub>V<sub>3</sub> (V) is almost 500 cm<sup>-1</sup> (from 96 to 586 cm<sup>-1</sup>) i.e., almost twice as large. The values of these frequencies are also considerably different among themselves. At the same time, which is noteworthy, there are dissimilarities not only in

terms of the frequencies of these oscillations, but also in their nature. No close similarity between the frequencies of the metal clusters considered here and the composition of the metal clusters described previously,<sup>16–21</sup> is found.

The general structural feature of both Al<sub>2</sub>Ti<sub>3</sub> and Al<sub>2</sub>V<sub>3</sub> metal clusters under examination, is the presence of several M–M bonds (M= Ti, V) formed by the same atom with its "neighbors" (Figures 1 and 2). On the average, the number of Al–Al, Al–M and M–M bonds in Al<sub>2</sub>Ti<sub>3</sub> metal clusters, as can see by comparing figures 1 and 2, is somewhat more than in Al<sub>2</sub>V<sub>3</sub> ones. At the same time, here, as well as in the metal clusters described earlier,<sup>16–21</sup> the values of most of the bond angles and, also, torsion (dihedral) angles, are significantly lower than 90° (see Tables 1 and 3).

**Table 4.** The oscillation frequencies in most stable modification of Al<sub>2</sub>V<sub>3</sub> (V) cluster.

Oscillation frequency, cm <sup>-1</sup>	Assignment of oscillation frequency
96	Scissoring for Al2 and V2 atoms relatively V1–V3 bond
175	Scissoring for Al2 and Al2 atoms relatively V1–V3 bond
189	Scissoring for V1, Al2 and V3 atoms
201	Superposition of scissoring oscillations of atoms V1, V2, V3 and atoms V1, V3, Al2
216	Stretching ( <i>asym.</i> ) for Al1–Al2 and Al1–V2 bonds
241	Stretching ( <i>sym.</i> ) for Al1–V1 and Al1–V2 bonds
271	Stretching ( <i>asym.</i> ) for Al1–V3 and Al2–V3 bonds
330	Stretching ( <i>sym.</i> ) for Al1–Al2, Al1–V3, and Al2–V3 bonds
586	Stretching for V1–V2 bond

There are many common features of the both Al<sub>2</sub>Ti<sub>3</sub> and Al<sub>2</sub>V<sub>3</sub> metal clusters studied by us. The most typical structure according to theoretical expectations, is a trigonal bipyramid. This is especially pronounced for Al<sub>2</sub>Ti<sub>3</sub>. At the same time, as is apparent from figures 1 and 2. A greater structural diversity is noted among Al<sub>2</sub>V<sub>3</sub> metal clusters, although the total number of their modifications is less than the number of such modifications for Al<sub>2</sub>Ti<sub>3</sub> metal clusters. All of them are also characterized by relatively high values of the lengths of these Al–Al, Al–M and M–M bonds, which, as a rule, exceed 200 pm almost in every case. The few exceptions to this rule are only V1–V2 bond lengths in the Al<sub>2</sub>V<sub>3</sub> (I)–Al<sub>2</sub>V<sub>3</sub>(VI), Al<sub>2</sub>V<sub>3</sub>(X) and Al<sub>2</sub>V<sub>3</sub>(XI) structures, which lie in the range from 171.7 pm, in the Al<sub>2</sub>V<sub>3</sub> (VI) to 188.1 pm, in the Al<sub>2</sub>V<sub>3</sub> (I) (see Supporting Information). Curiously enough in the structures of Al<sub>2</sub>Ti<sub>3</sub> metal clusters there is no such examples, although the radius of the Ti atom (132 pm) is even slightly smaller than the radius of the V atom (134 pm). The overwhelming majority of the aluminum-titanium and aluminum-vanadium metal clusters considered here, either has no symmetry elements at all, or has only one plane of symmetry. The only exception is the Al<sub>2</sub>V<sub>3</sub> (IX) metal cluster, which has one axis of symmetry of the third order, three axes of symmetry of the second order, and, also, three planes of symmetry (Figure 2). The Al<sub>2</sub>Mn<sub>3</sub> (XVIII) and Al<sub>2</sub>Zn<sub>3</sub> (XIV) metal clusters described in our previous article<sup>21</sup> have similar structures, but each of them

has three M–M bonds, which are absent in Al<sub>2</sub>V<sub>3</sub> (**IX**). In this connection, we would like to note that this cluster has the highest energy among all the Al<sub>2</sub>V<sub>3</sub> metal clusters.

The key structural parameters of most stable Al<sub>2</sub>Ti<sub>3</sub> and Al<sub>2</sub>V<sub>3</sub> metal clusters, and namely Al<sub>2</sub>Ti<sub>3</sub> (**XI**) and Al<sub>2</sub>V<sub>3</sub> (**V**), are presented in the table 5. As can be seen from it, the longest are Al–Al bonds, the shortest are Ti–Ti bonds. Similar situation, in average, occurs for both types of metal clusters under examination.

**Table 5.** Metal–metal bond lengths, bond and torsion angles in the molecular structures of most stable modifications of Al<sub>2</sub>Ti<sub>3</sub> (**XI**) and Al<sub>2</sub>V<sub>3</sub> (**V**) metal clusters.

Al <sub>2</sub> Ti <sub>3</sub> ( <b>XI</b> )		Al <sub>2</sub> V <sub>3</sub> ( <b>V</b> )	
Metal-metal bond lengths, pm*			
Al1Al2	(422.7)	Al1Al2	270.2
Al1Ti1	254.4	Al1V1	263.7
Al1Ti2	258.2	Al1V2	265.7
Al1Ti3	258.2	Al1V3	252.2
Al2Ti1	254.4	Al2V1	261.0
Al2Ti2	258.2	Al2V2	(378.8)
Al2Ti3	258.2	Al2V3	254.4
Ti1Ti3	258.7	V1V3	(265.4)
Ti2Ti3	239.0	V2V3	(253.3)
Ti1Ti2	258.8	V1V2	171.7
Bond angles, deg **			
Ti1Al1Ti2	60.6	V1Al1V2	37.8
Ti1Al2Ti2	60.6	V1Al2V2	(22.9)
Ti1Al1Al2	(33.8)	V1Al1Al2	58.5
Ti1Al2Al1	(33.8)	V1Al2Al1	59.5
Ti2Al1Al2	(35.6)	V2Al1Al2	90.0
Ti2Al2Al1	(35.0)	V2Al2Al1	(44.5)
Al1Ti1Al2	112.3	Al1V1Al2	62.0
Al1Ti2Al2	109.9	Al1V2Al2	(45.5)
Al1Ti3Al2	109.9	Al1V3Al2	64.5
Ti1Al1Ti3	60.6	V1Al1V3	(61.9)
Ti1Al2Ti3	60.6	V1Al2V3	62.0
Ti1Ti3Ti2	62.5	V1V3V2	(38.6)
Ti2Al1Ti3	55.1	V2Al1V3	58.5
Ti2Al2Ti3	55.1	V2Al2V3	(41.6)
Ti1Ti2Ti3	62.5	V1V2V3	(74.5)
Torsion (dihedral) angles, deg ***			
Ti1Al2Al1Ti3	(-126.2)	V1Al2Al1V3	74.3
Ti2Al2Al1Ti3	(107.4)	V2Al2Al1V3	(52.1)
Ti1Ti3Ti2Al1	-67.4	V1V3V2Al1	(-76.3)
Ti1Ti3Ti2Al2	-67.4	V1V3V2Al2	(-19.1)
Ti1Al1Al2Ti2	(-126.4)	V1Al1Al2V2	(-22.3)
Ti1Ti2Al1Al2	(-31.0)	V1V2Al1Al2	-31.8
Ti1Ti2Al2Al1	(31.0)	V1V2Al2Al1	-31.8
Ti2Ti3Al2Al1	(41.9)	V2V3Al2Al1	(56.4)

In this table in brackets are shown \* = distances between two atoms not involved in chemical bonds, \*\* = angles formed by three atoms among which at least two atoms do not form chemical bonds, and \*\*\* = dihedral angles formed by four atoms among which at least two atoms do not form chemical bonds are parenthesized.

Taking into account the atomic radii of the chemical elements contained in Al<sub>2</sub>M<sub>3</sub> metal clusters considered here, Al 143 pm, Ti 132 pm and V 134 pm, the indicated ratio between these bond lengths seems quite normal. Since the radii of titanium and vanadium atoms differ among themselves only slightly, one would expect that, in average, M–M bonds in the metal clusters considered here, should be close to each other. The data of our calculation, in general, are in accordance with this expectation (see Supporting Information).

When characterizing the spin multiplicity of the ground state of the most stable modifications of each of these metal clusters, we would like to stress the following. Despite the fact that the low-spin state for both of them as a whole, judging by the data of tables 2 and 4, is less characteristic compared to high-spin, the latter is realized only in the case of the most stable aluminum-titanium metal cluster of Al<sub>2</sub>Ti<sub>3</sub> (**XI**). At the same time, for the most stable aluminum-vanadium metal cluster of Al<sub>2</sub>V<sub>3</sub> (**V**), the ground state has spin multiplicity which is an intermediate between the minimum and the maximum value of the spin multiplicity. By taking into consideration the electron configurations of the titanium and vanadium atoms (3d<sup>2</sup>4s<sup>2</sup> and 3d<sup>3</sup>4s<sup>2</sup>, respectively), this tendency is quite expected.

## CONCLUSION

As can be seen from the calculated data presented above, the five-atomic metal clusters Al<sub>2</sub>Ti<sub>3</sub> and Al<sub>2</sub>V<sub>3</sub> under study, form a fairly significant number of structural modifications, that differ significantly from one another in their structural geometrical parameters and in terms of total energies. In addition, the number of modifications of both the one and the other metal cluster (14 and 11, respectively) exceeds the number of modifications of the Al<sub>2</sub>Fe<sub>3</sub> metal cluster<sup>20</sup> (of which there are only 8), but turns out to be much smaller than the number of modifications of Al<sub>2</sub>Mn<sub>3</sub>, 25.<sup>21</sup> Most of the modifications of these metal clusters, both Al<sub>2</sub>Ti<sub>3</sub> and Al<sub>2</sub>V<sub>3</sub>, either have no symmetry elements at all, or have only one plane of symmetry. Moreover, in the modifications of Al<sub>2</sub>Ti<sub>3</sub> metal cluster, as a rule, each of the aluminum and titanium atoms in their composition, has been connected through chemical bonds to its three neighbors, whereas in the modifications of Al<sub>2</sub>V<sub>3</sub> one, this is manifested to a considerably lesser degree. It is noteworthy that the lowest-energetic modification in the case of Al<sub>2</sub>Ti<sub>3</sub> has a spin multiplicity of the ground state 5, in the case of Al<sub>2</sub>V<sub>3</sub> it is 4, although judging by the electronic configurations of the atoms in them (3s<sup>2</sup>3p<sup>1</sup>, 4s<sup>2</sup>3d<sup>1</sup> and 4s<sup>2</sup>3d<sup>2</sup>, respectively), the total number of unpaired electrons in Al<sub>2</sub>Ti<sub>3</sub> should be less than in Al<sub>2</sub>V<sub>3</sub>. Besides, the difference between the energies of the lowest-energy and the highest-energy modifications in the case of Al<sub>2</sub>V<sub>3</sub> (141.0 kJ mol<sup>-1</sup>) was significantly larger than in the case of Al<sub>2</sub>Ti<sub>3</sub> (93.0 kJ mol<sup>-1</sup>), although much less than in the case of a metal cluster Al<sub>2</sub>Fe<sub>3</sub>, where it exceeds 300 kJ mol<sup>-1</sup>.<sup>20</sup>

## ACKNOWLEDGEMENT

The present study was carried out with financial support in the framework of draft No. 4.5784.2017/8.9 to the

competitive part of the state task of the Russian Federation on the 2017–2019 years. All quantum-chemical calculations were performed at the Kazan Department of Joint Supercomputer Center of Russian Academy of Sciences – Branch of Federal Scientific Center “Scientific Research Institute for System Analysis of the RAS”. Contribution of author Chachkov D.V. was funded by the state assignment to the Federal State Institution “Scientific Research Institute for System Analysis of the Russian Academy of Sciences” for scientific research.

## REFERENCES

- Ling, W., Dong, D., Shi-Jian, W., Zheng-Quan, Z., Geometrical, electronic, and magnetic properties of Cu<sub>n</sub>Fe (n=1–12) clusters: A density functional study, *J. Phys. Chem. Solids*, **2015**, *76*, 10–16. <https://doi.org/10.1016/j.jpcs.2014.07.022>
- Ma, L., Wang, J., Hao, Y., Wang, G., Density functional theory study of FePd<sub>n</sub> (n = 2–14) clusters and interactions with small molecules, *Comput. Mater. Sci.* **2013**, *68*, 166–173. <https://doi.org/10.1016/j.commatsci.2012.10.014>
- Kilimis, D. A., Papageorgiou, D. G., Density functional study of small bimetallic Ag–Pd clusters *J. Mol. Struct. (TheoChem)*, **2010**, *939*, 112–117. <https://doi.org/10.1016/j.theochem.2009.09.048>
- Zhao, S., Y. Ren, Y., J. Wang, J., W. Yin, W., Density functional study of NO binding on small Ag<sub>n</sub>Pd<sub>m</sub> (n + m ≤ 5) clusters *Comput. Theor. Chem.* **2011**, *964*, 298–303. <https://doi.org/10.1016/j.comptc.2011.01.009>
- Al-Odail, F., Mazher, J., Abuelela, A. M., A density functional theory study of structural, electronic and magnetic properties of small Pd<sub>n</sub>Ag (n=1–8) clusters, *Comput. Theor. Chem.* **2018**, *1125*, 103–111. <https://doi.org/10.1016/j.comptc.2018.01.005>
- Chaves, A. S., Rondina, G. G., Piotrowski, M. J., Da Silva, J. L. F., Structural formation of binary PtCu clusters: A density functional theory investigation, *Comput. Mater. Sci.* **2015**, *98*, 278–286. <https://doi.org/10.1016/j.commatsci.2014.11.022>
- Dong, D., Xiao-Yu, K., Jian-Jun, G., Ben-Xia, Z., First-principle study of Au<sub>n</sub>Fe (n = 1–7) clusters, *J. Mol. Struct.* **2009**, *902*, 54–58. DOI: 10.1016/j.theochem.2009.02.009
- Liu, X., Tian, D., Meng, C., DFT study on stability and H<sub>2</sub> adsorption activity of bimetallic Au<sub>79-n</sub>Pd<sub>n</sub> (n = 1–55) clusters, *Chem. Phys.*, **2013**, *415*, 179–185. <https://doi.org/10.1016/j.chemphys.2013.01.014>
- Hong, L., Wang, H., Cheng, J., Huang, X., Sai, L., Zhao, J., Atomic structures and electronic properties of small Au–Ag binary clusters: Effects of size and composition, *Comput. Theor. Chem.*, **2012**, *993*, 36–44. <https://doi.org/10.1016/j.comptc.2012.05.027>
- Maroun, F., Ozanam, F., Magnussen, O. M., Behm, R. J., The Role of Atomic Ensembles in the Reactivity of Bimetallic Electrocatalysts, *Science*, **2001**, *293*, 1811–1814.
- Eberhardt, W., Clusters as new materials, *Surf. Sci.* **2002**, *500*, 242–270. [https://doi.org/10.1016/S0039-6028\(01\)01564-3](https://doi.org/10.1016/S0039-6028(01)01564-3)
- Yang, J. X., Guo, J. J., Die, D., Ab initio study of Au<sub>n</sub>Ir (n = 1–8) clusters, *Comput. Theor. Chem.* **2011**, *963*, 435–438. <https://doi.org/10.1016/j.comptc.2010.11.013>
- Singh, N. B., Sarkar, U., A density functional study of chemical, magnetic and thermodynamic properties of small palladium clusters, *Mol. Simul.* **2014**, *40*, 1255–1264. <https://doi.org/10.1080/08927022.2013.861903>
- Bouderbala, W., Boudjahem, A. G., Soltani, A., Geometries, stabilities, electronic and magnetic properties of small Pd<sub>n</sub>Ir (n=1–8) clusters from first-principles calculations, *Mol. Phys.*, **2014**, *112*, 1789–1798. <https://doi.org/10.1080/00268976.2013.865089>
- Wen, J. Q., Xia, T., Zhou, H., Wang, J. F., A density functional theory study of small bimetallic Pd<sub>n</sub>Al (n=1–8) clusters, *J. Phys. Chem. Solids*, **2014**, *75*, 528–534. <https://doi.org/10.1016/j.jpcs.2013.12.018>
- Mikhailov, O. V., Chachkov, D. V., Models of molecular structure of heteronuclear clusters Al<sub>2</sub>Fe<sub>3</sub>, Al<sub>2</sub>Co<sub>3</sub>, and Al<sub>2</sub>Ni<sub>3</sub> according to the data of quantum-chemical density functional simulation, *Russ. J. Gen. Chem.*, **2016**, *86*, 1991–1999. <https://doi.org/10.1134/S1070363216090036>
- Mikhailov, O. V., Chachkov, D. V., Models of molecular structures of aluminum–iron clusters AlFe<sub>3</sub>, Al<sub>2</sub>Fe<sub>3</sub>, and Al<sub>2</sub>Fe<sub>4</sub> according to quantum-chemical DFT calculations, *Russ. J. Inorg. Chem.* **2017**, *62*, 336–343. <https://doi.org/10.1134/S0036023617030135>
- Mikhailov, O. V., Chachkov, D. V., Models of Molecular Structures of Al<sub>2</sub>Cr<sub>3</sub> and Al<sub>2</sub>Mo<sub>3</sub> Metal Clusters according to Density Functional Theory Calculations, *Russ. J. Inorg. Chem.*, **2018**, *63*, 786–799. <https://doi.org/10.1134/S0036023618060177>
- Mikhailov, O. V., Chachkov, D. V., DFT calculation of molecular structures of Al<sub>2</sub>Fe<sub>3</sub> and Al<sub>2</sub>Cu<sub>3</sub> heterobinuclear clusters, *Struct. Chem.*, **2018**, *29*, 1543–1549. <https://doi.org/10.1007/s11224-018-1146-9>
- Chachkov, D. V., Mikhailov, O. V., DFT Quantum Chemical Calculation of the Molecular Structures of the Metal Clusters Al<sub>2</sub>Cu<sub>3</sub> and Al<sub>2</sub>Ag<sub>3</sub>, *Russ. J. Inorg. Chem.*, **2019**, *64*, 79–87. <https://doi.org/10.1134/S0036023619010030>
- Mikhailov, O. V., Chachkov, D. V., Quantum-chemical calculation of molecular structures of Al<sub>2</sub>Mn<sub>3</sub> and Al<sub>2</sub>Zn<sub>3</sub> clusters by using DFT method, *Struct. Chem.* **2019**, *30*, 1289–1299. <https://doi.org/10.1007/s11224-019-1283-9>
- Schaefer, A., Horn, H., Ahlrichs, R., Fully optimized contracted Gaussian basis sets for atoms Li to Kr, *J. Chem. Phys.*, **1992**, *97*, 2571–2577. <https://doi.org/10.1063/1.463096>
- Weigend, F., Ahlrichs, R., Balanced basis sets of split valence, triple zeta valence and quadruple zeta valence quality for H to Rn: Design and assessment of accuracy, *Phys. Chem. Chem. Phys.* **2005**, *7*, 3297–3305. <https://doi.org/10.1039/b508541a>
- Hoe, W.-M., Cohen, A., Handy, N. C., Assessment of a new local exchange functional OPTX, *Chem. Phys. Lett.*, **2001**, *341*, 319–328. [https://doi.org/10.1016/S0009-2614\(01\)00581-4](https://doi.org/10.1016/S0009-2614(01)00581-4)
- Perdew, J. P., Burke, K., Ernzerhof, M., Generalized Gradient Approximation Made Simple, *Phys. Rev. Lett.*, **1996**, *77*, 3865–3868. <https://doi.org/10.1103/PhysRevLett.77.3865>
- Paulsen, H., Duelund, L., Winkler, H., Toftlund, H., Trautwein, A. X., Free Energy of Spin-Crossover Complexes Calculated with Density Functional Methods, *Inorg. Chem.*, **2001**, *40*, 2201–2203. <https://doi.org/10.1021/ic000954q>
- Swart, M., Groenhof, A. R., Ehlers, A. W., Lammertsma, K., Validation of Exchange–Correlation Functionals for Spin States of Iron Complexes, *J. Phys. Chem. A.*, **2004**, *108*, 5479–5483. <https://doi.org/10.1021/jp049043i>
- Swart, M., Ehlers, A.W., Lammertsma, K., Performance of the OPBE exchange-correlation functional, *Mol. Phys.*, **2004**, *102*, 2467–2474. <https://doi.org/10.1080/0026897042000275017>
- Swart, M., Metal–ligand bonding in metallocenes: Differentiation between spin state, electrostatic and covalent bonding, *Inorg. Chim. Acta*, **2007**, *360*, 179–189. <https://doi.org/10.1016/j.ica.2006.07.073>
- Gaussian 09, Revision A.01, Frisch, M. J.; Trucks, G. W., Schlegel, H. B., Scuseria, G. E., Robb, M. A., Cheeseman, J. R., Scalmani, G., Barone, V., Mennucci, B., Petersson, G. A., Nakatsuji, H., Caricato, M., Li, H., Hratchian, H. P., Izmaylov, A. F., Bloino, J., Zheng, G., Sonnenberg, J. L., Hada, M., Ehara, M., Toyota, K., Fukuda, R., Hasegawa, J., Ishida, M., Nakajima, T., Honda, Y., Kitao, O., Nakai, H., Vreven, T., Montgomery, J. A. Jr., Peralta, J. E., Ogliaro, F., Bearpark, M., Heyd, J. J., Brothers, E., Kudin, K. N.,

Staroverov, V. N., Kobayashi, R., Normand, J., Raghavachari, K., Rendell, A., Burant, J. C., Iyengar, S. S., Tomasi, J., Cossi, M., Rega, N., Millam, J. M., Klene, M., Knox, J. E., Cross, J. B., Bakken, V., Adamo, C., Jaramillo, J., Gomperts, R., Stratmann, R. E., Yazyev, O., Austin, A. J., Cammi, R., Pomelli, C., Ochterski, J. W., Martin, R.L., Morokuma, K., Zakrzewski, V. G., Voth, G.A., Salvador, P., Dannenberg, J. J., Dapprich, S., Daniels, A. D., Farkas, O., Foresman, J. B., Ortiz, J. V., Cioslowski, J., and Fox, D. J. Gaussian, Inc., Wallingford CT, 2009.

Received: 05.01.2020.

Accepted: 02.02.2020.



# CORROSION BEHAVIOUR OF 18 CARAT GOLD IN RINGER SOLUTIONS IN THE PRESENCE OF SODIUM CHLORIDE AND GLUCOSE

S. Agiladevi<sup>[a,b]\*</sup> and S. Rajendran<sup>[b,c]</sup>

**Keywords:** 18 Carat gold; electrochemical studies; Ringer solutions; corrosion;

This work aims at studying the electrochemical behaviour of metals like 18 carat gold in presence of Simulated Ringer's Solution and Lactated Ringer's Solution in presence of 100 ppm of NaCl and also 100 ppm of glucose are used to simulate the body fluids. The behaviour of the metal was monitored by polarization study and electrochemical impedance spectroscopy (EIS). All the experiments were carried out at a constant temperature of 37 °C. From these studies, it was concluded that the avoid of excess of NaCl and also glucose in both Ringer solutions in medicinal uses.

## \* Corresponding Authors

E-Mail: agilakarmega@gmail.com

- [a] Department of Chemistry, K S R Institute for Engineering and Technology, Tiruchengode 637 215, India  
[b] Research and Development Center, Bharathiar University, Coimbatore, India  
[c] Corrosion Research Centre, Department of Chemistry, St. Antony's College for Arts and Science for Women, Thamarapadi, Dindigul 624005, India

## INTRODUCTION

Surface properties and anti-corrosion characteristics are the most important material characteristics determining the biofunctionality of all implant materials. 18 Carat gold has been a valuable biomaterial for manufacturing implants due to its unique properties such as shape memory effect, super elasticity and good mechanical properties.<sup>1-4</sup> Many devices such as stent, orthodontic wires and root canal files have been used clinically.<sup>2-5</sup>

Ringer's analysis of the influence of blood constituents on contraction of the frog heart (1882-1885) pioneered general development of artificial extracellular media for maintenance of living material during in vitro physiological studies. "Ringer's solutions" are thus defined here as those designed to substitute for the blood plasma, hemolymph, or other extracellular fluids of any species with respect to variables such as ionic concentrations, pH, and osmotic pressure. Media described in the literature as "physiological salines" and "balanced salt solutions" are included here under the general Ringer's heading. Mimicry of native conditions is achieved in varying degrees by the many different Ringer's formulations. Ringer's solutions are typically intended for relatively short-term maintenance of living material, not for its growth or extended culture. In this respect they differ from cell, tissue, and organ culture media, which are more complex and beyond the scope of this Compendium.

Since Na<sup>+</sup> is normally the principal extracellular ion, sodium chloride is the major component of most Ringer's solutions. Some formulations have relatively few additional

ingredients but are nevertheless more complex than most "buffered salines", consisting principally of sodium chloride and a pH buffer, presented Ions such as Na<sup>+</sup>, K<sup>+</sup>, Ca<sup>2+</sup>, and Mg<sup>2+</sup> are critical for many functions. Researchers initiating work are urged to select physiological solutions carefully for the particular species to be studied, and to consider developing new ones based on analysis of the natural extracellular medium. Many Ringer's solutions,<sup>6-8</sup> are the product of empirical testing for retention of the activity being studied. Thus, in addition to being used directly, recipes provided here can serve as a starting point for improved formulations.

The Electrochemical impedance spectroscopy (EIS) is a relatively modern technique widely extended in several scientific fields. The EIS consists on a non-destructive technique when working under equilibrium conditions (free corrosion potential or open circuit potential), particularly sensible to small changes in the system that allows to characterize material properties and electrochemical systems even in low conductive media.

The impedance method consists in measuring the response of an electrode to a sinusoidal potential modulation of small amplitude (typically 5-10 mV) at different frequencies. The alternative current (AC) modulation is superimposed either onto an applied anodic potential or cathodic potential or onto the corrosion potential.<sup>9,10</sup>

## EXPERIMENTAL

### Materials and methods

Corrosion resistance of 18 Carat Gold in Ringer's Solution and lactated Ringer solution has been investigated by polarization study and AC impedance measurements. All measurements were performed at 37±1 °C. Ringer's Solution was composed of 6.0 g L<sup>-1</sup> NaCl, 0.075 g L<sup>-1</sup> KCl, 0.1 g L<sup>-1</sup> CaCl<sub>2</sub> and 0.1 g L<sup>-1</sup> NaHCO<sub>3</sub>. The lactated Ringer solution comprised of 6.0 g L<sup>-1</sup> NaCl, 0.3 g L<sup>-1</sup> KCl, 0.2 g L<sup>-1</sup> CaCl<sub>2</sub> and 3.1 g L<sup>-1</sup> sodium lactate.<sup>6-8,11</sup>

The 18 carat gold was composed of 75 % gold and 25 % copper.

### AC impedance measurements

H and CH electrochemical workstation impedance analyzer model CHI 660 was used to record AC impedance measurements. A three-electrode cell assembly was used. The working electrode was the studied metal. A saturated calomel electrode (SCE) was the reference electrode and platinum the counter electrode.<sup>13,14</sup> The real part ( $Z'$ ) of the cell impedance was measured in ohms for various frequencies. The charge transfer resistance ( $R_t$ ) and double layer capacitance ( $C_{dl}$ ) values were calculated

$$R_t = (R_s + R_i) - R_s \quad (1)$$

where  $R_s$  = solution resistance, and

$$C_{dl} = 1/2\pi R_t f_{max},$$

where  $f_{max}$  = maximum frequency.

The equivalent circuit diagram for such system is shown in Figure 1.

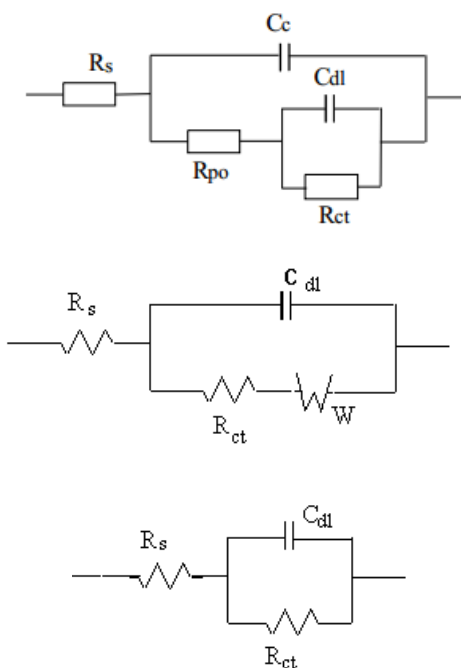


**Figure 1.** Equivalent circuit for a failed coating.  $C_c$  - The capacitance of the intact coating,  $R_{po}$  - pore resistance,  $R_{ct}$  - charge transfer resistance,  $R_s$  - solution resistance,  $C_{dl}$  - double layer capacitance,  $W$  - Warburg diffusion resistance.

## RESULTS AND DISCUSSION

Corrosion resistance of 18 carat gold in simulated Ringer's solution and lactated Ringer's solution has been measured by polarization study and AC impedance spectra<sup>13,15-33</sup>

An increase in corrosion resistance results in increase in  $LPR$  value, decrease in corrosion current, increase in charge transfer resistance, increase in impedance value and decrease in  $C_{dl}$  value.

### Polarization study

In the polarization study, shown in Figure 2 to 7, the corrosion parameters like corrosion potential ( $E_{corr}$ ), Tafel slopes ( $b_c$ =cathodic,  $b_a$ =anodic),  $LPR$  (linear polarization resistance) value and corrosion current were measured. They are given in Table 1.

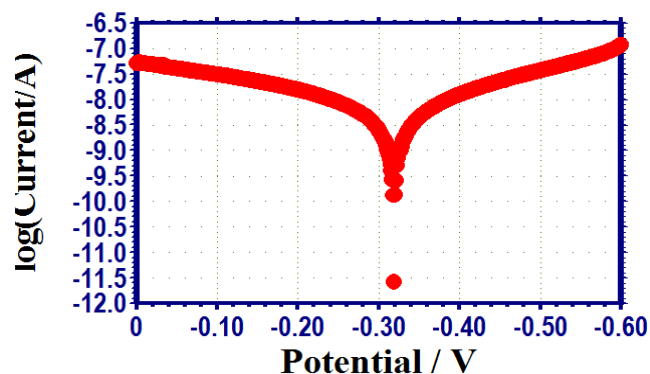


**Figure 2.** Polarisation curve of 18 carat gold immersed in Simulated Ringer's Solution.

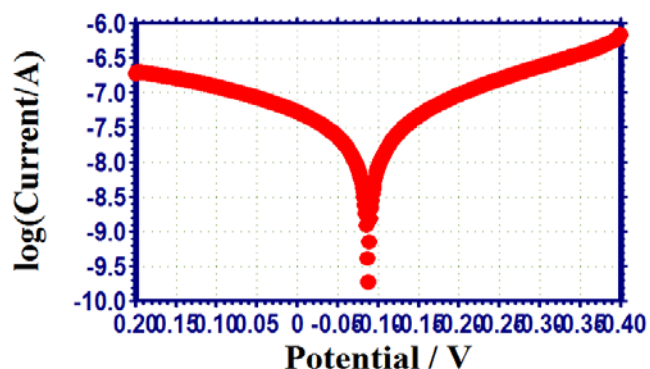


**Figure 3.** Polarisation curve of 18 carat gold immersed in Simulated Ringer's Solution + 100 ppm of NaCl.

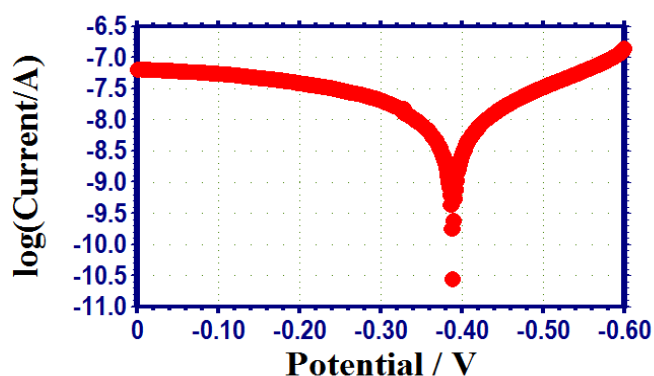


**Figure 4.** Polarisation curve of 18 carat gold immersed in Simulated Ringer's Solution + 100 ppm of glucose.

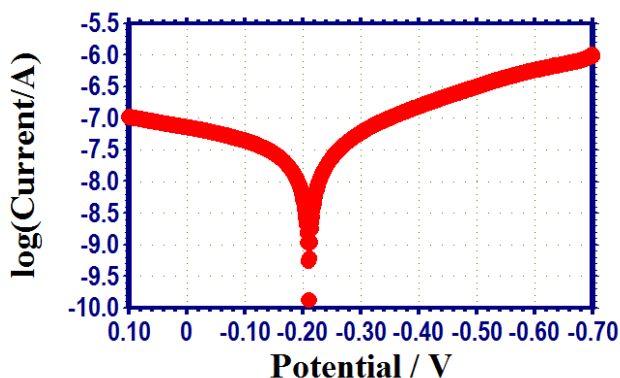


Figure 5. Polarisation curve of 18 carat gold immersed in Lactated Ringer's Solution.

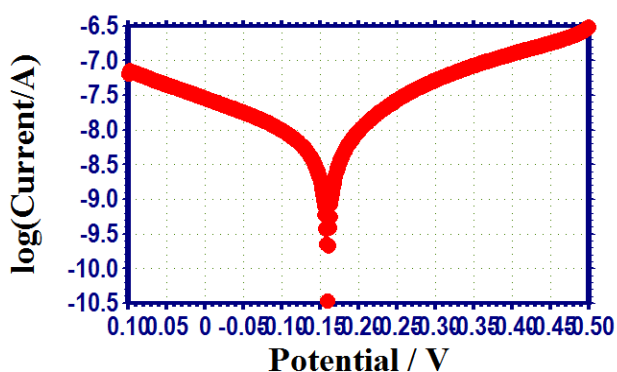


Figure 6. Polarisation curve of 18 carat gold immersed in Lactated Ringer's Solution + 100 ppm NaCl.

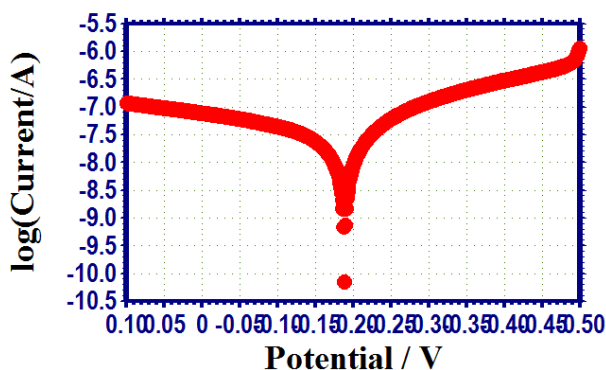


Figure 7. Polarisation curve of 18 carat gold immersed in Lactated Ringer's Solution + 100 ppm glucose.

### Ringer's Solution

#### Influence of 100 ppm of NaCl

It can be seen from the Table 1, that the corrosion resistance of 18 carat gold decreases in presence of 100 ppm of NaCl. In the presence of NaCl,  $LPR$  value decreases from 7361238 to 4472869 ohm  $\text{cm}^2$ . The corrosion current increases from  $5.44 \times 10^{-9}$  to  $2.657 \times 10^{-8}$  A  $\text{cm}^{-2}$ .

#### Influence of 100 ppm of glucose

Similarly, the corrosion resistance of 18 carat gold decreases in presence of 100 ppm of glucose. In the presence of glucose,  $LPR$  value decreases from 7361238 to 1540062 ohm  $\text{cm}^2$ . The corrosion current increases from  $9.584 \times 10^{-9}$  to  $2.657 \times 10^{-8}$  A  $\text{cm}^{-2}$ .

### Lactated Ringer's Solution

#### Influence of 100 ppm of NaCl

It is observed from the Table 1, that the corrosion resistance of 18 carat gold decreases in presence of 100 ppm of NaCl, the corrosion resistance decreases. In the presence of NaCl,  $LPR$  value decreases from 5028338 ohm  $\text{cm}^2$  to 1873424 ohm  $\text{cm}^2$ . The corrosion current increases from  $3.605 \times 10^{-9}$  A  $\text{cm}^{-2}$  to  $2.467 \times 10^{-8}$  A  $\text{cm}^{-2}$ .

#### Influence of 100 ppm of glucose

Similarly, the corrosion resistance of 18 carat gold decreases in presence of 100 ppm of glucose. In the presence of glucose,  $LPR$  value decreases from 5028338 to 1403355 ohm  $\text{cm}^2$ . The corrosion current increases from  $7.625 \times 10^{-9}$  to  $2.467 \times 10^{-8}$  A  $\text{cm}^{-2}$ .

### AC impedance spectra

The instrument polarization study was used to record AC impedance spectra also are shown in Figure 8 to 13. Corrosion parameters such as charge transfer resistance ( $R_t$ ), double layer capacitance ( $C_{dl}$ ), Impedance are measured. They are given in Table 2.

### Ringer's solution

#### Influence of 100 ppm of NaCl

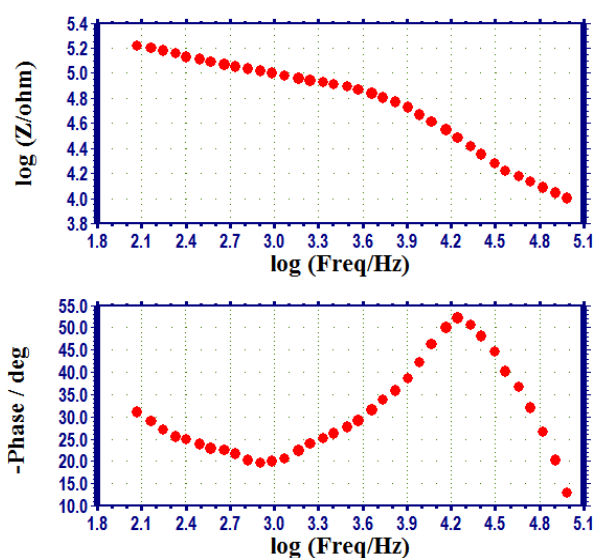
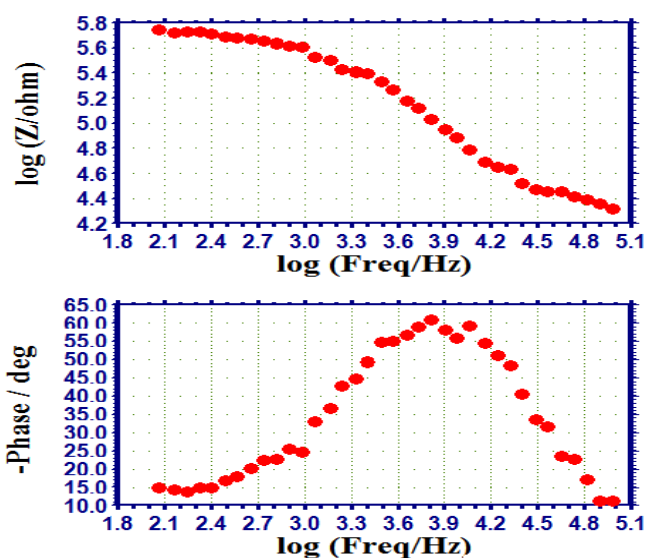
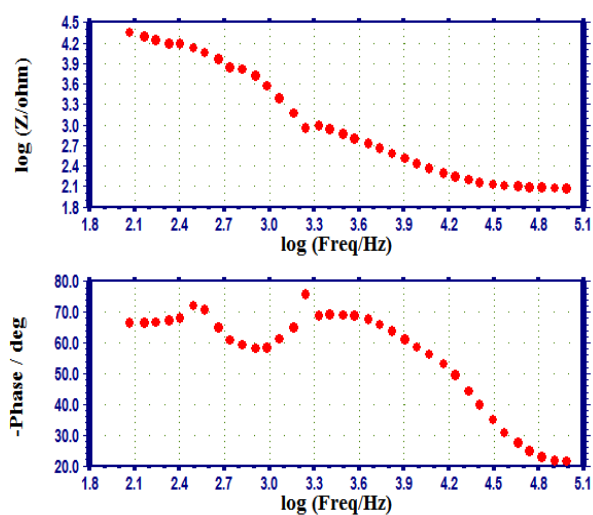
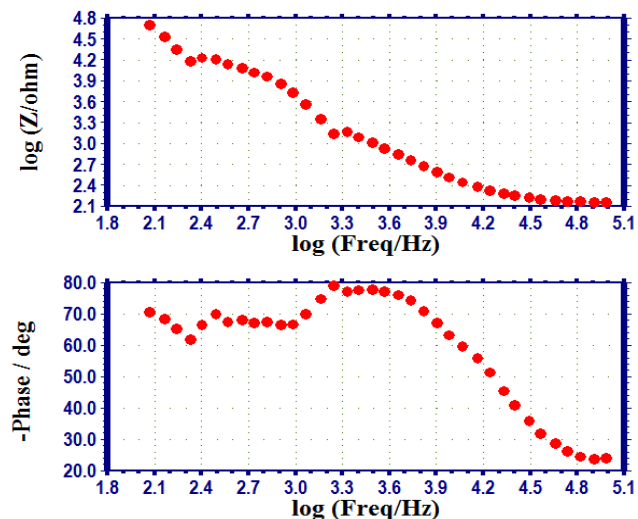
It is noted from the Table 2, that the corrosion resistance of 18 carat gold decreases in the presence of 100 ppm of NaCl, the  $R_t$  value decreases from 537220 to 139115 ohm  $\text{cm}^2$ .  $C_{dl}$  value increases from  $9.493 \times 10^{-12}$  to  $3.666 \times 10^{-11}$  F  $\text{cm}^{-2}$ . The impedance value decreases from 5.775 to 5.247.

#### Influence of 100 ppm of glucose

Similarly, the corrosion resistance of 18 carat gold decreases in the presence of 100 ppm of glucose, the  $R_t$  value decreases from 537220 to 9430 ohm  $\text{cm}^2$ .  $C_{dl}$  value increases from  $9.493 \times 10^{-12}$  to  $5.408 \times 10^{-10}$  F  $\text{cm}^{-2}$ . The impedance value decreases from 5.775 to 4.430. From this, it is inferred that the corrosion resistance of 18 carat gold in Ringer's solution decreases in the presence of 100 ppm of NaCl and also 100 ppm of glucose.

**Table 1.** Polarization study of the study of corrosion of 18-carat gold.

System	$E_{\text{corr}}$ , mV vs SCE	$b_c$ , mV decade <sup>-1</sup>	$b_a$ , mV decade <sup>-1</sup>	LPR, $\Omega \text{ cm}^2$	$I_{\text{corr}}$ , A cm <sup>-2</sup>
Ringer's solution	-319	169	202	7361238	2.657X10 <sup>-8</sup>
Ringer's solution+100 ppm NaCl	-389	179	220	4472869	5.442X10 <sup>-9</sup>
Ringer's solution+100 ppm Glucose	-88	167	215	1540062	9.584 X10 <sup>-9</sup>
Lactate Ringer's solution	-160	141	235	5028338	2.467 X10 <sup>-8</sup>
Lactate Ringer's solution+100 ppm NaCl	-211	171	279	1873424	3.605 X10 <sup>-9</sup>
Lactate Ringer's solution+100 ppm Glucose	-189	165	394	1403355	7.625 X10 <sup>-9</sup>

**Figure 8.** AC impedance spectra of 18 carat gold immersed in simulated Ringer's solution.**Figure 10.** AC impedance spectra of 18 carat gold immersed in simulated Ringer's solution +100 ppm of glucose.**Figure 9.** AC impedance spectra of 18 carat gold immersed in simulated Ringer's solution +100 ppm of NaCl.**Figure 11.** AC impedance spectra of 18 carat gold immersed in Lactated Ringer's Solution.

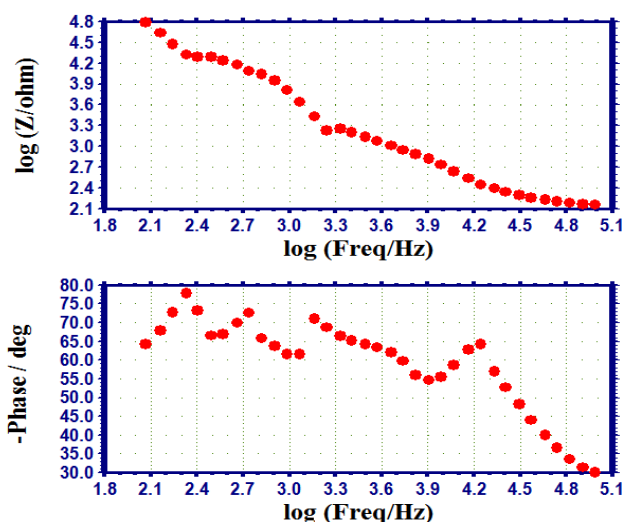


Figure 12. AC impedance spectra of 18 carat gold immersed in Lactated Ringer's Solution + 100 ppm of NaCl.

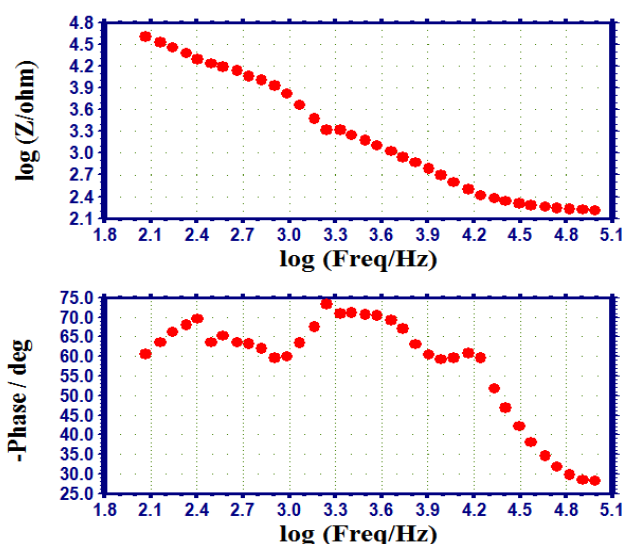


Figure 13. AC impedance spectra of 18 carat gold immersed in Lactated Ringer's Solution + 100 ppm of glucose.

### Lactated Ringer's Solution

#### Influence of 100 ppm of NaCl

It is observed from the Table 2, that the corrosion resistance of 18 carat gold decreases in the presence of 100 ppm of NaCl, the  $R_t$  value decreases from 27920 to 19990 ohm  $\text{cm}^2$ .  $C_{dl}$  value increases from  $1.827 \times 10^{-11}$  to  $2.551 \times 10^{-10}$  F  $\text{cm}^2$ . The impedance value decreases from 4.792 to 4.769.

#### Influence of 100 ppm of glucose

Similarly, the corrosion resistance of 18 carat gold decreases in the presence of 100 ppm of glucose, the  $R_t$  value decreases from 27920 to 17550 ohm  $\text{cm}^2$ .  $C_{dl}$  value increases from  $1.827 \times 10^{-11}$  to  $5.569 \times 10^{-9}$  F  $\text{cm}^2$ . The impedance value decreases from 4.792 to 4.679.

From this, it is inferred that the corrosion resistance of 18 carat gold in Lactated Ringer's solution decreases in presences of 100 ppm of NaCl and also 100 ppm of glucose.

Table 2. Corrosion parameters as determined by AC Impedance.

System	$R_t$	$C_{dl}$	Impedance
Ringer's solution	537220	$9.493 \times 10^{-12}$	5.775
Ringer's solution +100 ppm NaCl	139115	$3.666 \times 10^{-11}$	5.247
Ringer's solution +100 ppm glucose	9430	$5.408 \times 10^{-10}$	4.430
Lactate Ringer's solution	27920	$1.827 \times 10^{-11}$	4.792
Lactate Ringer's solution +100 ppm NaCl	19990	$2.551 \times 10^{-10}$	4.769
Lactate Ringer's solution +100 ppm glucose	17550	$5.569 \times 10^{-9}$	4.679

## CONCLUSION

The corrosion resistance of 18 carat gold in Ringer's solution and in lactated Ringer's solution has been evaluated by polarization study and AC impedance spectra. The influence of 100 ppm of NaCl and also of 100 ppm of glucose on the corrosion resistance of 18 carat gold has also been investigated. This study leads to the following conclusions.

Corrosion resistance of 18 carat gold in Ringer's and lactated Ringer's solutions decreases in presence of 100 ppm of NaCl and also of 100 ppm of glucose. This is confirmed by polarization study and AC impedance spectra. It implies, care must be taken to avoid excess of NaCl and also glucose in Ringer's and also in lactated Ringer's solution.

## ACKNOWLEDGEMENT

The authors are thankful to the Managements of their institutions and to St, Joseph's Research and Community Development Trust, Dindigul for their help and encouragement.

## REFERENCES

- <sup>1</sup>Kamachimudali, U., Sridhar, T. M., Raj, B., Corrosion of bioimplants, *Sadhana*, **2001**, 28, 601. <https://doi.org/10.1007/BF02706450>
- <sup>2</sup>Duerig, T. W., The Use of Superelasticity in Modern Medicine, *MRS Bull.*, **2002**, 27,101. <https://doi.org/10.1557/mrs2002.44>
- <sup>3</sup>Shabalovskaya, S. A., Surface, corrosion and biocompatibility aspects of Nitinol as an implant material, *Int. Mater. Rev.*, **2001**, 46, 233. <https://doi.org/10.1006/plas.2001.1555>
- <sup>4</sup>Duerig, T. W., Pelton, A., Stockel, D., An overview of nitinol medical applications, *Mater. Sci. Eng.*, **1999**, 149, 273-275. [https://doi.org/10.1016/S0921-5093\(99\)00294-4](https://doi.org/10.1016/S0921-5093(99)00294-4)

- <sup>5</sup>Duerig, T. W., Tolomeo, D. E., Wholey, M., An overview of superelastic stent design, *Min. Invas. Therap. Allied Technol.*, **2000**, 9, 235. <https://doi.org/10.3109/13645700009169654>
- <sup>6</sup>Kumar, S., Narayanan, T. S. N. S., Electrochemical characterization of  $\beta$ -Ti alloy in Ringer's solution for implant application, *J. Alloy Compd.*, **2009**, 479, 699. <https://doi.org/10.1016/j.jallcom.2009.01.036>
- <sup>7</sup>Kumar, S., Narayanan, T. S. N. S., Raman, S. G. S., Seshadri, S. K., Fretting corrosion behaviour of thermally oxidized CP-Ti in Ringer's solution, *Corros. Sci.*, **2012**, 52, 711. <https://doi.org/10.1016/j.corsci.2009.10.029>
- <sup>8</sup>Kumar, S. K., Narayanan, T. S. N., S., Raman, S. G. S., Seshadri, S. K., Thermal oxidation of Ti6Al4V alloy: Microstructural and electrochemical characterization, *Mater. Chem. Phys.*, **2010**, 119, 327. <https://doi.org/10.1016/j.matchemphys.2009.09.007>
- <sup>9</sup>Carlos, C. V., Munoz, A. I., Electrochemical Aspects in Biomedical Alloy Characterization, *Trends Mater. Sci.*, **2011**, 13, 307-513.
- <sup>10</sup>Conway, B. E., Bockris, J., White, R. E., Edts, *Modern Aspects of Electrochemistry*, Kluwer Academic/Plenum Press Publishers, New York, **1999**, 32, 143-248.
- <sup>11</sup><https://www.bbroun.ph/>
- <sup>12</sup>Raykhtsaum, G., Agarwal, D. P., The color of gold, *Gold Technol.*, **1997**, 10, 26.
- <sup>13</sup>Shyamala Devi, B., Rajendran, S., Corrosion inhibition by trisodium citrate (TSC) -  $Zn^{2+}$  system, *Eur. Chem. Bull.*, **2012**, 1, 150-157. <http://dx.doi.org/10.17628/ecb.2012.1.150-157>.
- <sup>14</sup>Rajendran, S., Uma, V., Krishnaveni, A., Jeyasundari, J., Shyamaladevi, B., Manivannan, M., Corrosion behavior of metals in artificial saliva in presence of D-Glucose, *Arab. J. Sci. Eng.*, **2009**, 34, 147-158.
- <sup>15</sup>Florence, J. F., Rajendran, S., Srinivasan, K. N., Effect of henna (*Lawsonia inermis*) extract on electrodeposition of nickel from Watt's bath, *Electroplating Finish.*, **2012**, 31, 1-4.
- <sup>16</sup>Sribharathy, V., Rajendran, S., Corrosion inhibition by green inhibitor: sodium metavanadate-spirulina system, *Chem. Sci. Rev. Lett.*, **2012**, 1, 25-29.
- <sup>17</sup>Tamilselvi, S., Murugaraj, R., Rajendran, N., Electrochemical impedance spectroscopic studies of titanium and its alloys in saline medium, *Mater. Corros.*, **2007**, 58, 113-120. <https://doi.org/10.1002/maco.200603979>
- <sup>18</sup>Rajendran, S., Anuradha, K., Kavipriya, K., Krishnaveni, A., Thangakani, J. A., Inhibition of corrosion of carbon steel in sea water by sodium molybdate- $Zn^{2+}$  system, *Eur. Chem. Bull.*, **2012**, 1, 503-510. <http://dx.doi.org/10.17628/ecb.2012.1.503-510>.
- <sup>19</sup>Anbarasi, C. M., Rajendran, S., Investigation of the inhibitive effect of octanesulfonic acid - zinc-ion system on corrosion of carbon steel, *Chem. Eng. Commun.*, **2012**, 199, 1596-1609. <https://doi.org/10.1080/00986445.2012.672498>
- <sup>20</sup>Sribharathy, V. G., Rajendran, S., Corrosion inhibition of carbon steel by sodium metavanadate, *J. Electrochem. Sci. Eng.*, **2012**, 2, 121-131. doi: 10.5599/jese.2012.0014.
- <sup>21</sup>Rajendran, S., Sribharathy, V., Krishnaveni, A., Jeyasundari, J., Sathiyabama, J., Muthumegala, T. S., Manivannan, M., Inhibition effect of self assembled films formed by adipic acid molecules on carbon steel surface, *Zastita Materijala*, **2011**, 52, 163-172.
- <sup>22</sup>Liu, K. M., Wu, S. L., Chu., P. K., Chung, C. Y., Chu, C. L., Yeung, K. W. K., Lu, W. W., Cheung, K. M. C., Luk, K. D. K., Effects of water plasma immersion ion implantation on surface electrochemical behavior of NiTi shape memory alloys in simulated body fluids, *Appl. Surf. Sci.*, **2007**, 253, 3154-3159. <https://doi.org/10.1016/j.apsusc.2006.07.008>
- <sup>23</sup>Wan, P., Ren, Y., Zhang, B., Yang, K., Effect of nitrogen on biocorrosion behavior of high nitrogen nickel-free stainless steel in different simulated body fluids, *Mater. Sci. Eng. C*, **2012**, 32, 510-516. <https://doi.org/10.1016/j.msec.2011.12.002>
- <sup>24</sup>Thangam, Y. Y., Kalanithi, M., Anbarasi, C. M., Rajendran, S., Inhibition of corrosion of carbon steel in a dam water by sodium molybdate -  $Zn^{2+}$  system, *Arab. J. Sci. Eng.*, **2009**, 34, 49-60.
- <sup>25</sup>Kanimozhi, S. A., Rajendran, S., Inhibitive properties of sodium tungstate- $Zn^{2+}$  system and its synergism with HEDP, *Int. J. Electrochem. Sci.*, **2009**, 4, 353-368.
- <sup>26</sup>Sathiyabama, J., S. Rajendran, S., Jeyasundari, J., Shyamaladevi, B., The effect of  $Zn^{2+}$  ion in promoting inhibitive property of phenolphthalein, *J. Eng. Sci. Tech.*, **2010**, 3, 27-31. <https://doi.org/10.25103/jestr.031.05>
- <sup>27</sup>Johnsirani, V., Rajendran, S., Sathiyabama, J., Muthumegala, T. S., Krishnaveni, A., Beevi, N. H., *Bulg. Chem. Commun.*, **2012**, 44, 41-51.
- <sup>28</sup>Nithya, A., Rajendran, S., Corrosion Inhibition Effect of Carbon Steel in Sea Water by L-Arginine- $Zn^{2+}$  System, *Bulg. Chem. Commun.*, **2010**, 42, 119-125.
- <sup>29</sup>Anthony, N., Sherine, H. B., Rajendran, S., Investigation of the inhibiting effect of CMC -  $Zn^{2+}$  system in the corrosion of carbon steel in neutral chloride solution, *Arab. J. Sci. Eng.*, **2010**, 35, 41-53.
- <sup>30</sup>Johnsirani, V., Sathiyabama, J., Rajendran, S., Prabha, A. S., Inhibitory Mechanism of Carbon Steel Corrosion in Sea Water by an Aqueous Extract of Henna Leaves, *Int. Scholar. Res. Notices*, **2012**, 10, 1-9. <https://doi.org/10.5402/2012/574321>
- <sup>31</sup>Tamilselvi, S., Rajendran, N., Electrochemical studies on the stability and corrosion resistance of Ti-5Al-2Nb-1Ta alloy for biomedical applications, *Trends Biomater. Artificial Organs*, **2006**, 20, 1-5.
- <sup>32</sup>Sangeetha, M., Rajendran, S., Sathiyabama, J., Prabhakar, P., Eco friendly extract of banana peel as corrosion inhibitor for carbon steel in sea water, *J. Nat. Prod. Plant Resour.*, **2012**, 2, 601-610.
- <sup>33</sup>Rajendran, S., Thangavelu, C., Venkatesh, T., Study of Synergistic effect of diethylene triamine penta (methylene phosphonic acid) and adipic acid on the inhibition of corrosion of alkaline aluminium, *Der Chemica Sinica.*, **2012**, 3, 1475-1485.

Received: 29.12.2019.

Accepted: 23.02.2020.



## ACTIVITY OF Pd-MnO<sub>x</sub>/CORDIERITE (Mg,Fe)<sub>2</sub>Al<sub>4</sub>Si<sub>5</sub>O<sub>18</sub>) CATALYST FOR CARBON MONOXIDE OXIDATION

V. Bakhtadze,<sup>\*[a]</sup> V. Mosidze,<sup>[a]</sup> T. Machaladze,<sup>[a]</sup> N. Kharabadze,<sup>[a]</sup>  
D. Lochoshvili,<sup>[a]</sup> M. Pajishvili,<sup>[a]</sup> R. Janjgava,<sup>[a]</sup> and N. Mdivani<sup>[a]</sup>

**Keywords:** CO oxidation; manganese oxides; aluminosilicate blocks, promoting, active surface.

Physical-chemical characteristics and activity of the Pd-MnO<sub>x</sub>-catalyst, deposited on cordierite carrier, was studied in the CO oxidation reaction. The results obtained on the catalyst Pd-MnO<sub>x</sub>/Al-Si showed the similar activity in the CO oxidation reaction as in the case of the Pd-MnO<sub>x</sub>/CaO.2Al<sub>2</sub>O<sub>3</sub> catalyst.

\*Corresponding Authors

Fax: +995 32 2301430

E-Mail: vbakhtkat@yahoo.com

[a] Iv. Javakhishvili Tbilisi State University, R. Agladze Institute of Inorganic Chemistry and Electrochemistry, Georgia, 0186, Tbilisi, Mindeli str. 11.

### INTRODUCTION

Manganese oxides are well-known as the highly efficient catalysts of deep oxidation. The catalysts, prepared on their basis, are used in the processes of gas purification and other important chemical-technological processes.<sup>1-3</sup> Manganese oxides, together with copper and cobalt oxides, are considered as possible replacement of platinum metals in automobile catalysts for purification of exhaust gases from CO, CH<sub>x</sub>, NO<sub>x</sub>.<sup>4,5</sup> The catalysts, obtained by their combination with the oxides of some metals of variable valency and with the metals of platinum group (Pt, Pd) or Ag, exhibit the mutual-promoting effect in the oxidation reaction.<sup>6,7</sup> Simultaneously they retain the high activity after calcination over prolonged period at high temperatures. By the use, in the technology of the catalysts of aluminium oxide, of the carrier, preliminary modified by calcium oxide, the Mn-Pd catalyst was elaborated available for oxidation of CO and hydrocarbons of spent gases of the motor transport.<sup>8,9</sup> The mixed Mn-Pd catalysts (MPC-1), containing the minimum amount of palladium (up to 0.05 wt. %), was successfully tested in the systems for purification of spent gases of petrol engines and diesel locomotives operating on diesel fuel.<sup>10</sup>

Comparison of texture characteristics and activity of the Mn-Pd catalysts on calcium aluminate carrier (CaO.2Al<sub>2</sub>O<sub>3</sub>, CA<sub>2</sub>) of ShN-2M mark in the reaction of CO oxidation, the sample with 4.0÷5.0 wt. % of Mn+0.05 wt. % of Pd content was proved to be the most active.<sup>9</sup> On the carrier, apart from the phase of β-MnO<sub>2</sub>, the formation of the phase β-Mn<sub>2</sub>O<sub>3</sub> is observed in nearly equal proportion. The addition of palladium to the oxide-manganese catalyst leads to the formation of new centers on the surface which are active in the reaction of CO oxidation. The particles of palladium are dispersed in the matrix of MnO<sub>2</sub>, they don't penetrate into the depth of the pores.<sup>11,12</sup> In accordance with Ref.<sup>13</sup> the

addition of palladium and manganese to γ-Al<sub>2</sub>O<sub>3</sub>, hydrothermally treated even at the stage of impregnation and calcination of the catalyst, leads to the interaction between active components and carrier. As a result the variation of valence state of the part of Mn<sup>2+</sup> and formation of palladium complexes with γ-Al<sub>2</sub>O<sub>3</sub> takes place. Moreover, the active components interact with each other which leads to the shift of the equilibrium Mn<sup>3+</sup>+e<sup>-</sup>↔Mn<sup>2+</sup> on the surface in the direction of the formation of the ions of divalent manganese and to the growth of palladium dispersity.

For preparation of automobile catalysts, the aluminosilicate blocks with cellular structure<sup>14</sup> are intensively developed. Their specific surfaces, as a rule, don't exceed 1-2 m<sup>2</sup> g<sup>-1</sup>. The results of manganese and palladium deposition on the cordierite aluminosilicate blocks (Mg,Fe)<sub>2</sub>Al<sub>4</sub>Si<sub>5</sub>O<sub>18</sub>) are presented and the results of the study of their activity and physical-chemical properties in the reaction of CO-oxidation are given.

### EXPERIMENTAL PART

For laboratory testing, the manganese oxides used were deposited on plates and ground particles (Ø1,5–2.0 mm) of cordierite blocks via impregnation with aqueous solution of manganese(II) nitrate at various concentration of impregnating solution, changing the temperature and duration of impregnation. The Pd-MnO<sub>x</sub>/cordierite catalysts were prepared by impregnation of the carriers prepared with aqueous PdCl<sub>2</sub> solution. The samples prepared in this way were dried at 80-100 °C then calcined in an electric furnace at 350-450 °C for 2 h. The formed composites were treated by 4-5 % solution of aqueous NH<sub>4</sub>OH, then dried and calcined at 400 °C for 2 h.

Activity of the catalyst samples in the CO oxidation reaction was determined in a flowing plant at laboratory scale. Thermal analysis was performed on a STA-2500 device. ISM 65 LV scanning electron microscope was used to study the morphology of the catalyst surface. Specific surfaces of the samples were determined by application of the automated system ASAP 2020.

## RESULTS AND DISCUSSION

SEM pictures of the surface components of catalyst Pd-MnO<sub>x</sub>/cordierite at 1 μm of the layer depth could be seen in Fig. 1. The oxides of Mn and Pd are distributed uniformly on the cordierite surface. The dispersity of manganese oxide particles comprises nearly 100 nm. X-Ray phase and thermal analyses of the catalyst showed the presence of β-MnO<sub>2</sub> and β-Mn<sub>2</sub>O<sub>3</sub>. Specific surface area of the Pd-MnO<sub>x</sub>/cordierite comprises 3.0–5.0 m<sup>2</sup> g<sup>-1</sup> while the specific surface of initial cordierite doesn't exceed the value of 0.5–0.7 m<sup>2</sup> g<sup>-1</sup>. The activities of the catalyst samples before and after their treatment with aqueous ammonia in the CO oxidation reaction are showed in Fig. 2.

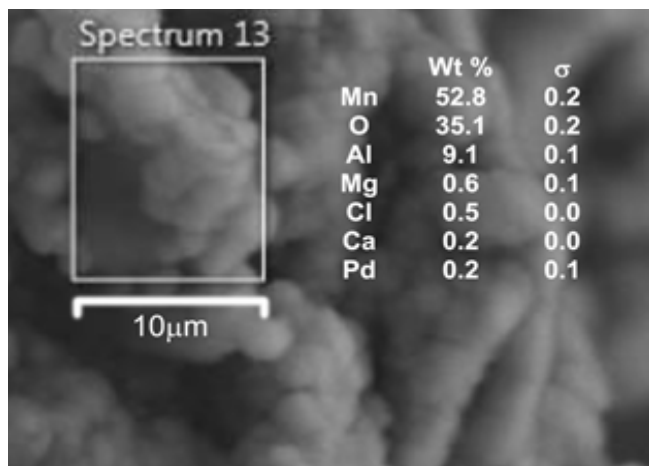


**Figure 1.** Surface distribution of active components in the catalyst Pd-MnO<sub>x</sub>/cordierite.

Before treatment by aqueous ammonia, the CO oxidation reaction on the catalyst comprised 98-100% in the temperature range from 205 °C to 210 °C. After treatment by aqueous ammonia, the same degree of CO-oxidation could be attained even at 175-180 °C. Similar promotion effect of aqueous ammonia treatment of Pd/CA<sub>2</sub> was observed.<sup>15</sup>

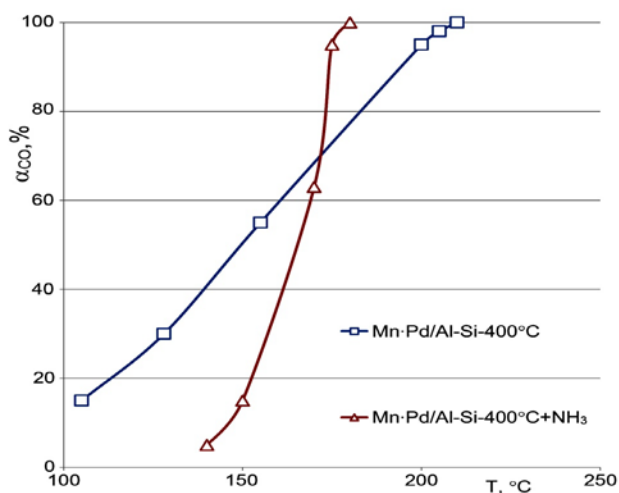
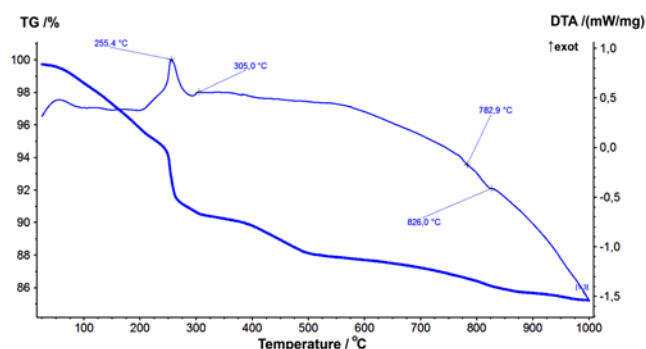
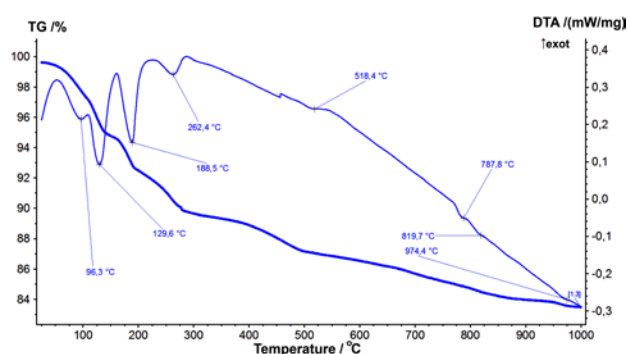


**Figure 2.** Dependence of Pd-MnO<sub>x</sub>/cordierite catalyst activity with and without aqueous ammonia treatment on the temperature in the CO oxidation ( $G_{\text{cat}} = 1.0$  g, composition of reaction mixture: 1.0 vol. % of CO+air, volume rate of the gas  $W = 15 \cdot 10^3$  h<sup>-1</sup>).

The treatment of the catalyst by ammonia water can lead to the formation of ammine-palladium complexes which can decompose with formation of catalytically active palladium black.<sup>16,17</sup>



a)



b)

**Figure 3.** Curves of thermal analyses (DTA and TG) of the catalyst Pd-MnO<sub>x</sub>/cordierite treated with aqueous ammonia (a) and without treatment of aqueous ammonia (b)

Comparison of the decomposition curves of Pd-MnO<sub>x</sub>/cordierite catalyst with and without treatment by aqueous ammonia, shows the exoeffect on the DTA curve at the temperatures: 255 and 305 °C which is indicative of the phase decomposition. This can only be observed in the aqueous ammonia treated sample.

## CONCLUSIONS

Activity of the Pd-MnO<sub>x</sub>/cordierite catalyst is similar with the activity of Pd-MnO<sub>x</sub>/CaO.2Al<sub>2</sub>O<sub>3</sub> catalyts in the CO oxidation reaction. Treatment of catalyst with aqueous ammonia has positive influence on the completion of the active surface species of the catalyst and reduces the temperature needs for total oxidation of carbon monoxide.

## ACKNOWLEDGEMENTS

This work was supported by Shota Rustaveli National Science Foundation of Georgia (SRNSFG) (Grant № 18-750)

## REFERENCES

- <sup>1</sup>Ioseliani, D., Bakhtadze, V., Investigation in the field of heterogenic catalysis, *Khim. Khim. Technol. Akad. Nauk. Gruzii, Sbornik Trudov*, Metsniereba, Tbilisi, **2001**, 120-133.
- <sup>2</sup>Bakhtadze, V., Mosidze, V., Janjgava, R., Chochishvili, N., Dzanashvili, D., Kharabadze, N., Pajishvili, M. Preparation of efficient catalysts – adsorbents for cleaning gases from sulfur compounds, *Eur. Chem. Bull.*, **2014**, *3(1)*, 46-49. DOI: <http://dx.doi.org/10.17628/ecb.2014.3.46-49>
- <sup>3</sup>Popova, N., Dosumov, K., Zheksenbaeva, Z., Komashko, L., Grigor'eva, V., Sass, A., and Salakova, R., Thermally stable multicomponent manganese catalyst for the deep oxidation of methane to CO<sub>2</sub>, *Kinet. Catal.*, **2006**, *47(6)*, 935-944. <https://doi.org/10.1134/S0023158406060140>
- <sup>4</sup>Tsikoza, L., Ismagilov, Z., Ushakov, V., Spojakina, V., and Ovsyanikova, I., Fuel Combustion Reactions and Catalysts: XXI. Synthesis and Characterization of Modified Mn-Al-O Catalysts for High-Temperature Oxidation, *Kinet. Catal.*, **2003**, *44(6)*, 806-812. <https://doi.org/10.1023/B:KICA.0000009058.43038.94>
- <sup>5</sup>Decarne, C., Bokova, M., Abi-Aad, E., Pryakhin, A., Lunin, V., and Aboukais, A., Effects of Ozone on Catalytic and Physicochemical Properties of Cu-Ce-Al-O Catalysts for Soot Combustion, *Kinet. Catal.*, **2003**, *44(5)*, 677-681. <https://doi.org/10.1023/A:1026102408243>
- <sup>6</sup>Shigapov, A., Dubkov, A., Ukropec, R., Carberry, B., Graham, G., Chun, W., and McCabe, R., Development of PGM-Free Catalysts for Automotive Applications, *Kinet. Catal.*, **2008**, *49(5)*, 756-764. <https://doi.org/10.1134/S0023158408050224>
- <sup>7</sup>Bakhtadze, V., Mosidze, V., ICESI 2019 International Conference on Engineering, Science and Industrial Applications. Proc., 22-24 August, 2019, Tokyo University of Science, Tokyo, Japan.
- <sup>8</sup>Bakhtadze, V., Mosidze, V., Kartvelishvili, D., Janjgava, R., Kharabadze, N., *Katal. Promysl.*, Modification of  $\gamma$ -,  $\chi$ -Al<sub>2</sub>O<sub>3</sub> alumina support by calcium oxide for the preparation of oxidation of CO and hydrocarbons commercial catalysts, *Katal. Promysl.*, **2012**, *2*, 56-63.
- <sup>9</sup>Bakhtadze, V., Kharabadze, N., Moroz, E., Supported Modified Mn-Pd Catalysts of the MPK-1 Series for CO Oxidation *Katal. Promysl.*, **2007**, *3*, 115-120
- <sup>10</sup>Bakhtadze, V., Mosidze, V., Kharabadze, N., Chochishvili, N., Fajishvili, M., Janjgava, R., Effect of SO<sub>2</sub> on the activity and physical-chemical properties of Mn-Pd catalyst for CO oxidation, *Slovak Int. Sci. J.*, **2017**, *1(7)*, 14-17. <https://doi.org/10.5089/9781475587937.002>
- <sup>11</sup>Bakhtadze, V., Mosidze, V., Kharabadze, N., Dzanashvili, D., Janjgava, R., Fajishvili, M., Chochishvili, N., Dispersity and activity of palladium in CO oxidation catalysts, *Khim. Zh. Gruzii*, **2014**, *14(1)*, 100-103.
- <sup>12</sup>Ivanova, A., Slavinskaya, E., Stonkus, O., Zaikovskii, V., Danilova, I., Gulyaev, R., Bulavchenko, O., Tsibulya, S., Boronin, A., Low-Temperature Oxidation of Carbon Monoxide over (Mn<sub>1-x</sub>M<sub>x</sub>)O<sub>2</sub> (M=Co, Pd) Catalysts, *Kinet. Catal.*, **2013**, *54(1)*, 81-94. <https://doi.org/10.1134/S0023158413010084>
- <sup>13</sup>Savonkina, M., Kupcha, L., Yegizarov, Yu., Potapovich, A., Zhizhenko, G., Zaretsky, M., Physico-chemical study of palladium-manganese catalysts based on aluminum oxide, *Vestnik Akad. Navuk BSSR, ser. Khim.*, **1986**(3), 58-62.
- <sup>14</sup>Farrauto, R., Heck, R., Honeycomb Catalysts: Present and Future, *Kinet. Catal.*, **1998**, *39(5)*, 646-652..
- <sup>15</sup>Bakhtadze, V., Mosidze, V., Kharabadze, N., Dzanashvili, D., Janjgava, R., Fajishvili, M., Chochishvili, N. Effect of Pd concentration and reductants on the activity of CO oxidation catalysts, *Khim. Zh. Gruzii*, **2015**, *15(1)*, 66-68.
- <sup>16</sup>Platinum metals., *A Guide to Preparative Inorganic Chemistry*, Edited by G. Brauer., Izdatinlit, **1956**, 723-726.
- <sup>17</sup>Chernyaev, I., About diamminitrochloropalladium [Pd(NH<sub>3</sub>)<sub>2</sub>NO<sub>2</sub>Cl], *Complex compounds of transition metals, Selected Works*, Moscow, Science, **1973**, 177-184.

Received: 01.12.2019.

Accepted: 04.03.2020.